January 2015

Evaluating Sedimentary Basins For Geothermal Power Production Potential And Bottom-Hole Temperature Corrections

Anna Marguerite Crowell

EVALUATING SEDIMENTARY BASINS FOR GEOTHERMAL POWER PRODUCTION POTENTIAL AND BOTTOM-HOLE TEMPERATURE CORRECTIONS

by

Anna M. Crowell
Bachelor of Science, Management/Computer Information Systems, Park University, 2003
Master of Science, Geology, University of North Dakota, 2011

A Dissertation

Submitted to the Graduate Faculty

of the

University of North Dakota

in partial fulfillment of the requirements

for the degree of

Doctor of Philosophy

Grand Forks, North Dakota
August
2015

This Dissertation, submitted by Anna M. Crowell in partial fulfillment of the requirements for the Degree of Doctor of Philosophy from the University of North Dakota, has been read by the Faculty Advisory Committee under whom the work has been done and is hereby approved.

Chairperson

This dissertation meets the standards for appearance, conforms to the style and format requirements of the Graduate School of the University of North Dakota, and is hereby approved.

Dean of the Graduate School

July 27, 2015
Date

PERMISSION

Title	Evaluating Sedimentary Basins for Geothermal Power Production Potential and Bottom-Hole Temperature Corrections
Department	Geology and Geological Engineering
Degree	Doctor of Philosophy

In presenting this dissertation in partial fulfillment of the requirements for a graduate degree from the University of North Dakota, I agree that the library of this University shall make it freely available for inspection. I further agree that permission for extensive copying for scholarly purposes may be granted by the professor who supervised my thesis work or, in his absence, by the chairperson of the department or the dean of the Graduate School. It is understood that any copying or publication or other use of this thesis or part thereof for financial gain shall not be allowed without my written permission. It is also understood that due recognition shall be given to me and to the University of North Dakota in any scholarly use which may be made of any material in my dissertation.

Anna M. Crowell
July 17, 2015

TABLE OF CONTENTS

LIST OF FIGURES v

ACKNOWLEDGEMENTS vi

ABSTRACT vii

CHAPTER

I. INTRODUCTION 1

Statement of Hypothesis 1

Previous Work 1

Geothermal Energy: The Only Sustainable Base Load Power Source 3

Evaluating Geothermal Potential in Select Basins 6

II. GEOSTATISTICAL ANALYSIS OF BOTTOM-HOLE TEMPERATURES 8

III. EVALUATING BOTTOM-HOLE TEMPERATURE CORRECTION SCHEMES 19

IV. ENERGY-IN-PLACE ESTIMATE FOR THE DENVER BASIN 41

V. ENERGY-IN-PLACE ESTIMATES FOR THE ILLINOIS AND MICHIGAN BASINS 55

VI. PLAY FAIRWAY ANALYSIS 69

VII. CONCLUSIONS 104

APPENDICES 106

Appendix A. List of Acronyms 107

SOURCES CITED 109

LIST OF FIGURES

Figure		Page
1	A temperature/depth plot for well 5086 in the Williston Basin along with bottom-hole temperatures	2
2	Areas where feasible solar collection may occur in the United States	4
3	Average wind speed for the United States.	4
4	Heat flow map created by Anna Crowell and modified by the Department of Energy to show current geothermal power activities in the United States	5
5	Total Percentage Energy by source (TPES) for the world, comparing 1973 to 2012	5
6	Comparison of CO2 emissions from 1973 to 2012	6
7	Graph of Energy in Place for the Williston Basin	105

ACKNOWLEDGEMENTS

The author wishes to thank Dr. William Gosnold, Dr. Gregory Vandeberg, Dr. Michael Mann, Dr. Dexter Perkins, Dr. Stephan Nordeng, and Dr. James “Josh” Crowell, James Crowell II, and Dr. Randi Clow. This work could not have been completed without your kindness, understanding, love, and guidance.

ABSTRACT

At present, the risks and costs associated with geothermal energy wildcat exploration are prohibitive. With improved technology, the future may be brighter, and a play fairway analysis, for geothermal exploration can guide development. Comparing geophysical data with geothermal gradient allows identification of potentially economic areas of interest. The play fairway analysis is a common tool used by the petroleum industry to identify areas for potential exploration. The analysis identifies areas in the Denver, Illinois, Michigan, and Williston Basins with the highest development potential. A great deal of data have potential for a play fairway analysis, but data quality is problematic due to systematic errors in bottom-hole temperatures (BHTs). Corrections to bottom-hole temperatures are necessary due to the perturbation of temperature caused by the drilling mud, and can range from 5 to 30 °C. Correction schemes for bottom-hole temperatures can be applied to both the energy-in-place estimates and play fairway analyses. The Harrison equation is the most accurate for basins less than 4.5 km deep. The Kehle correction is the most accurate for basins deeper than 4.5 km.

Chapter II explains why BHTs grouped by depth are more statistically robust than those grouped by geochronological unit. Chapter III demonstrates why the Harrison Equation is the best correction method to use for BHTs. Chapters IV and V give the volumetric energy-in-place for the Denver, Illinois, and Michigan Basins for discrete temperature ranges, and Chapter 6 provides the final Play Fairway Favorability maps.

CHAPTER I

INTRODUCTION

Statement of Hypothesis

The Environmental Protection Agency created the DRASTIC model in 1971 to identify areas of potential water contamination. We have now used that model for geothermal play fairway analysis and hypothesize that we will be able to complete initial evaluation of a target area for geothermal feasibility without the cost of drilling. If the model is successful, it will identify areas for geothermal energy production by highlighting areas with high geothermal gradient, low magnetic intensity, low bouger gravity anomaly, and low slope.

Previous Work

The Department of Energy initiated the State Coupled Geothermal Program in the mid-70s to identify areas in the United States with high geothermal potential. Several organizations contributed, but in most cases the energy estimated was based on only one or aquifers per basin. The initiative resulted in three USGS Circulars that were published: Circular 726 in 1975, Circular 790 in 1978, and Circular 892 in 1980 (USGS, 1975; USGS, 1978; USGS, 1980).

Soon after Circular 892 was published, funding ended for the project, and the industry lay stagnant until the mid-2000s when the Recovery Act was

introduced and funded. New work was completed by the University of North Dakota, including methods of examining bottom-hole temperature (BHT) correction, and a method for predicting temperature at depth for a well using thermal conductivity and heat flow data. The model to predict temperature at depth is called TSTRAT (Gosnold et al., 2012), an example of which is shown in Figure 1.

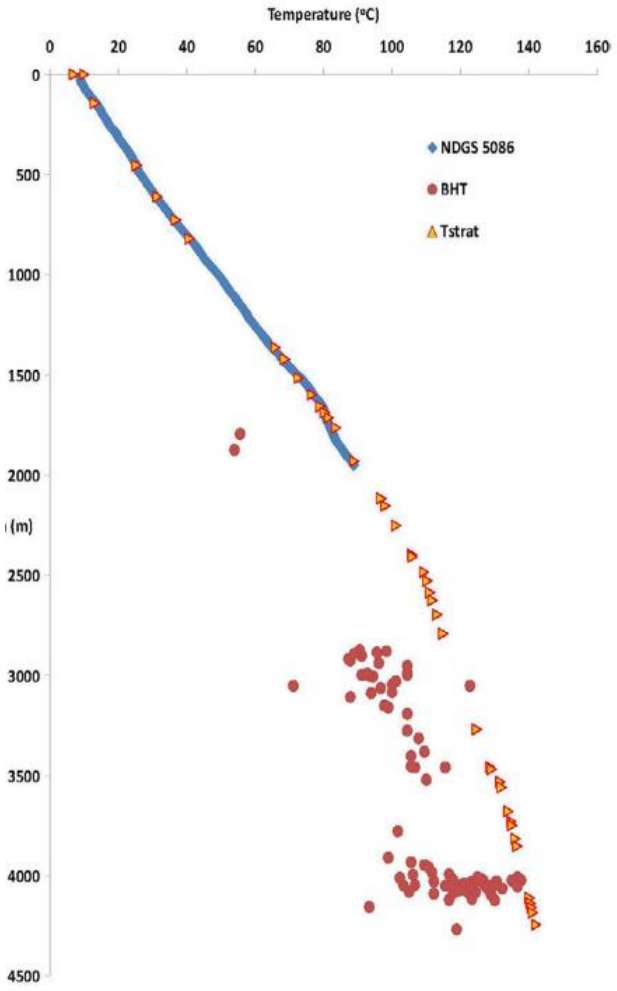

Figure 1. A temperature/depth plot for well 5086 in the Williston Basin along with bottom-hole temperatures. The continuous line represents true formation temperature, and is plotted against measured local bottom-hole temperatures to show the wide margin of error.

Geothermal Energy: The Only Sustainable Base Load Power Source

Wind (Figure 2), solar (Figure 3), and geothermal (Figure 4) sources only provide only 1.1% of the world's energy (Figure 5) (IEA, 2014).Wind and Solar sources cannot provide energy at all times, so they are called 'intermittent' sources. Geothermal energy, however, can also be turned on or off as needed, and is therefore considered a 'base load' source (GRC, 2014).

It is essential that engineers and scientists research sustainable energy sources if we are to diversify our nation's energy portfolio. The increased threat of climate change means the reduction of CO_2 emissions is crucial. A 1,000 MW (Megawatt) pulverized coal-fired power plant emits between six and eight Mt/yr (megaton per year) of CO_2 (Herzog and Golomb, 2004). In 2012, the United States (OECD, or Organization for Economic Co-operation and Development) was responsible for 38.3% of CO_2 emissions worldwide (Figure 6).

It was once thought that only places in the western U.S., like The Geysers in Northern California, or the Dixie Valley Geothermal Field in Nevada, contained economically extractable geothermal energy. These are two regions where subsurface water is hot enough to reach the surface at its boiling point. With current technology, such as Organic Rankin Cycle binary power plants (ORCs), district heating, direct use, and ground source heat pumps, geothermal energy use is no longer restricted to the far western reaches of the United States (Figure 4) (GRC, 2014).

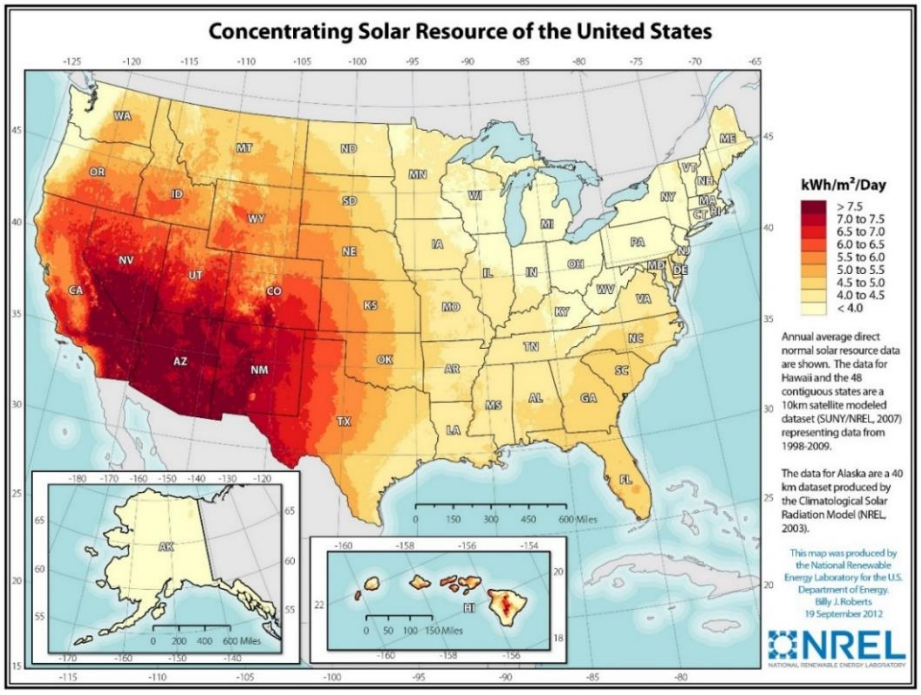

Figure 2. Areas where feasible solar collection may occur in the United States. (Roberts, 2012).

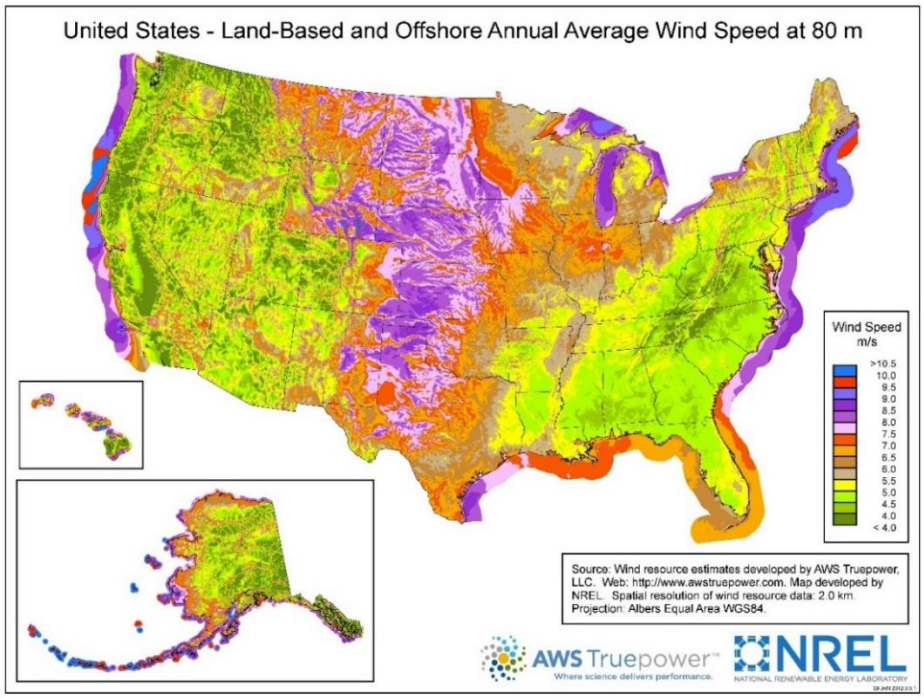

Figure 3. Average wind speed for the United States. (AWS/NREL, 2012).

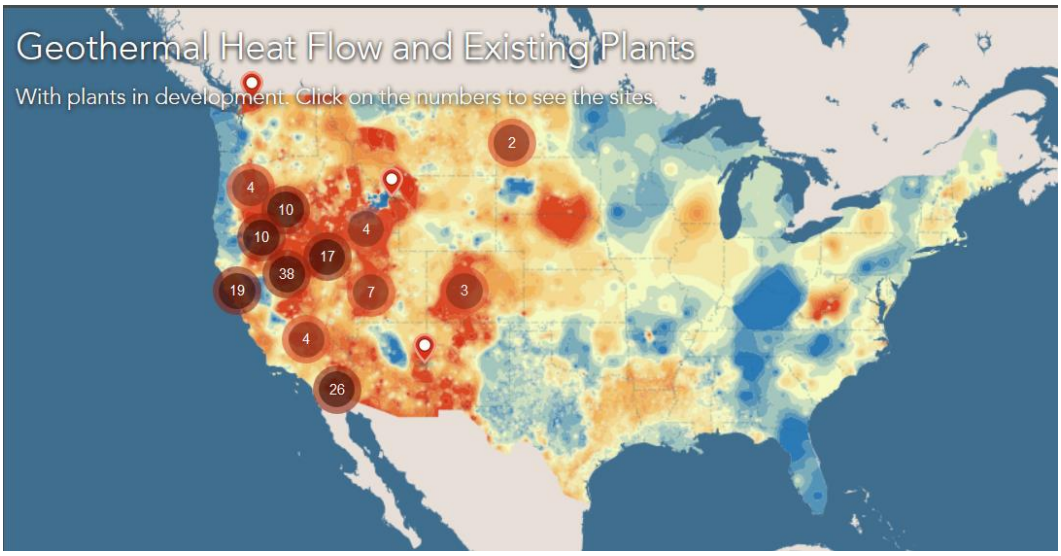

Figure 4. Heat flow map created by Anna Crowell and modified by the Department of Energy to show current geothermal power activities in the United States. (DOE, 2014)

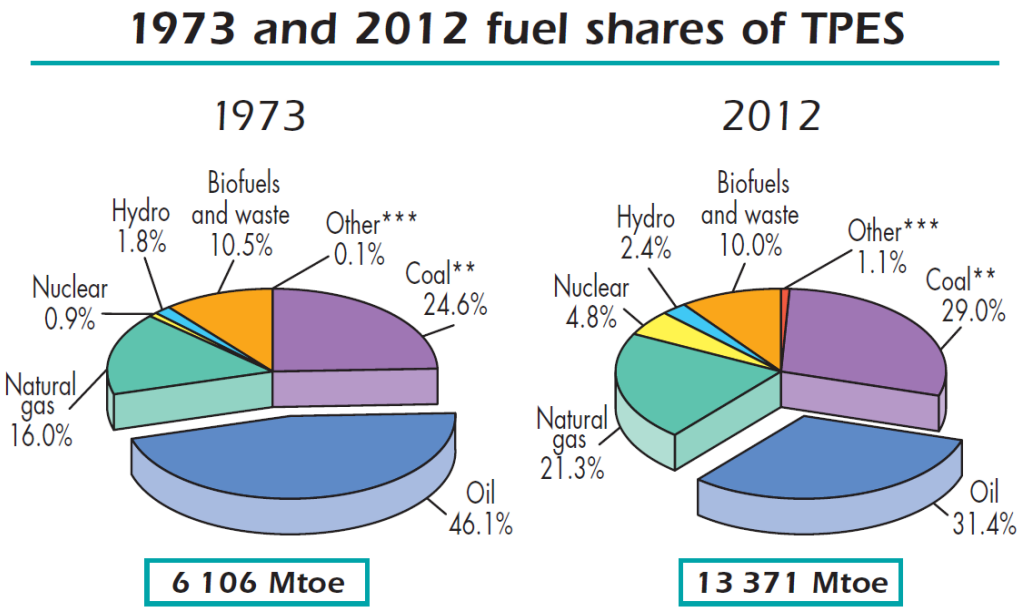

Figure 5. Total percentage energy by source (TPES) for the world, comparing 1973 to 2012. (IEA, 2014)

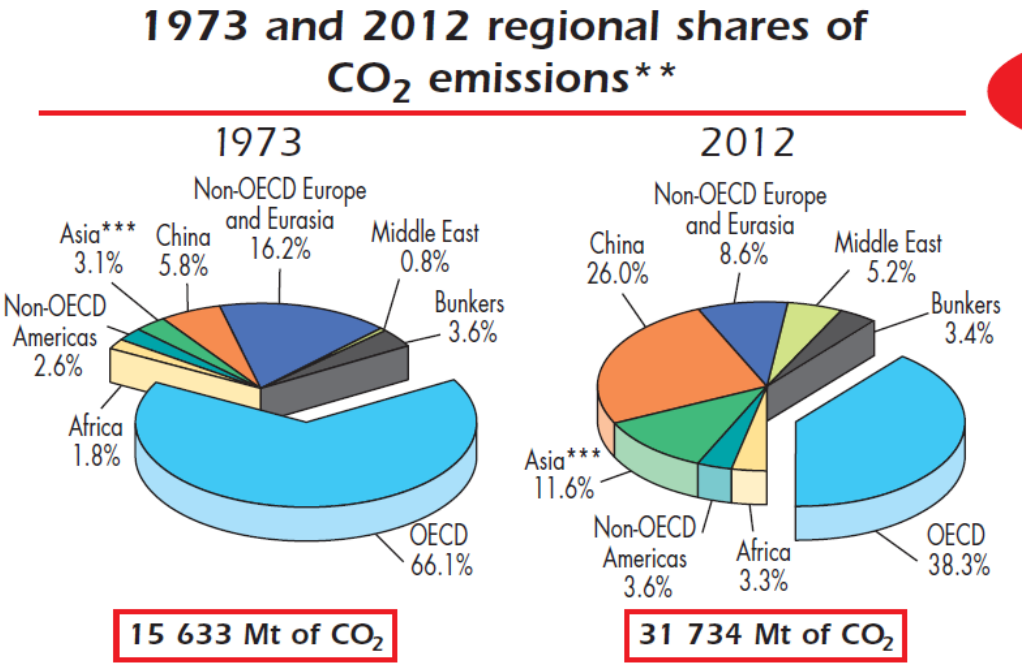

Figure 6. Comparison of CO_2 emissions from 1973 to 2012. (IEA, 2014)

Evaluating Geothermal Potential in Select Basins

This dissertation contains five papers all focused on one overarching theme: identifying areas that have the best potential for geothermal development. Chapter II presents a geostatistical analysis of bottom-hole temperatures. Chapter III gives an evaluation of the bottom-hole temperature correction methods. Chapters IV and V present estimation of the energy in place for the Denver, Illinois, and Michigan Basins. Chapter VI combines the generated information from the first four papers with other geophysical data to create final play fairway maps. Because BHT data from Montana and South Dakota did not have any temperatures greater than 90℃, the point at which geothermal power production becomes economic, an alternative approach was necessary for the Williston

Basin. Work from Crowell 2011, in which a previous energy-in-place estimation was made, was used for further evaluation of the Williston Basin.

Each publication (Chapters II - VI) contains its own literature review. I have not renumbered figures in publications to preserve the flow of the articles.

CHAPTER II

GEOSTATISTICAL ANALYSIS OF BOTTOM-HOLE TEMPERATURES

Table of Contents

List of Figures 9

Introduction 10

Geostatistical Analysis of Bottom-hole Temperatures in the Denver and Williston Basins: North America 12

- Abstract 12
- Methods 13
- Results 15
  - Denver Basin 15
  - Williston Basin 16
- Discussion 17
- Conclusions 17
- Sources Cited 18

List of Figures

Figure		Page
1	Spatial Representation of the 10,766 wells with bottom-hole temperature data in the Williston Basin.	14
2	Spatial representation of the 49,222 wells with bottom-hole temperature data in the Denver Basin.	14
3	Moran's I analysis for the Denver Basin. Non-correlated units are denoted in red.	15
4	Results of the Getis-Ord analysis for the Denver Basin. Non-correlated units are shown in red, while weakly correlated units are shown in yellow.	15
5	Results of the Moran's I analysis for the Williston Basin. Non-correlated units are denoted in red.	16
6	Results of the Getis-Ord analysis for the Williston Basin. Non-correlated units are shown in red, while weakly correlated units are shown in yellow.	16

Introduction

The following publication, Crowell 2015, has been accepted for publication in the Transactions of the Geothermal Resources Council, Volume 39, available in October 2015. It is presented here as it was accepted for publication.

BHTs may be used to complete an energy-in-place analysis for a sedimentary basin. To do this, the data must be divided into subsets. Because BHTs are often measured shortly after the well is drilled, the temperature of the borehole has been disturbed by the drilling mud circulation, so the measured temperatures must be corrected.

Some BHT datasets are robust, but others are problematic. Although the Denver Basin and Williston Basin data included formation of measurement information as well as the depth of the temperature measurement, the Michigan and Illinois Basins did not provide formation information. Consequently, geostatistical analysis of the Denver and Williston Basins determined if creating subsets of the data by depth was an acceptable alternative to creating subsets of data by formation. If the subsets are strongly correlated by depth, a correction by depth is possible.

The Moran's I and Getis-Ord GI* tests evaluate different properties of a dataset. Moran's I is a test of Spatial Autocorrelation that determines if members of a dataset are related using a statistically calculated standard deviation (z-score) and probability (p-score) to show if clustering exists (Paradis, 2009; Esri, 2013). This statistical test relates data using Tobler's first law of Geography, "All things are related, but nearby things are more related than distant things (Tobler, 1970; Anselin, 1999)."

The Getis-Ord test also uses the z-score. If the score is exceptionally high or exceptionally low when compared with a random sample, it is "hot spot," meaning a higher than average standard deviation suggesting possible anomalous values (Esri, 2013).

The combination of the Moran's I and Getis-Ord GI* tests found that not only is it acceptable to separate temperatures out by depth, it is more statistically accurate than separating by formation. We also found the systematic distribution in the analysis showing that correction based on depth is feasible.

Geostatistical Analysis of Bottom-Hole Temperatures in the Denver and Williston Basins: North America

Anna Crowell
Harold Hamm School of Geology and Geological Engineering

University of North Dakota

Keywords: Geostatistics, GIS, Williston Basin, Denver Basin, Bottom-Hole Temperatures

Abstract

Bottom-hole temperatures (BHTs) obtained from oil and gas wells have never been completely reliable due to the formation temperature disturbance caused by the influence of the drilling mud on the formation rock during drilling. A correction method must be applied before any BHT data can be used. The source and method of the correction, however, has been a topic of dissention since the early 70s, when BHTs began to be used for estimates of temperature at depth to determine such things as hydrocarbon maturity, thermal history, and geothermal energy assessment.

Several correction methods are currently used: the Harrison (Harrison et.al., 1983), Kehle (Kehle et al., 1970), and Förster (Förster et al., 1996) are among the most prevalent. None of these methods yield a correction that represents a statistically accurate distribution of BHTs, although the Harrison and Kehle have been found to be a much better approximation (Crowell and Gosnold, 2013). All of these methods were developed using a top-down approach, where an equilibrium temperature profile has been obtained and a correction equation was developed to attempt to shift the best fit line of the data points to the best fit line of the data obtained at equilibrium.

In addition, formation data are not always included with the bottom-hole temperature data. This makes resource assessment based on formation difficult, if not impossible. We therefore hypothesize that by using two geostatistical methods, Moran's I and Getis-Ord, we will be able to evaluate if a better correlation exists between a depth-interval well parsing versus a geochronological unit well parsing, and if a correlation exists, is it strong enough to indicate that a correction factor is possible.

Methods

We used geostatistical methods to examine the BHT datasets for the Williston basin (Figure 1) in North Dakota, and the Denver basin (Figure 2) in Colorado and Nebraska. The first geostatistical method we used was a spatial autocorrelation method called Global Moran's I. Global Moran's I is a geostatistical method that examines the frequency distribution of a dataset and compares it to an expected or random dataset. A Z-value is generated that can then be used to determine if the data is clustered (correlated) or random (non-correlated). We also wanted to determine the degree of clustering with a dataset if it is spatially correlated. We used the Getis-Ord Hot Spot analysis, which determines a Z-value and returns whether the data sets are random (non-correlated), low clustering (weakly correlated) or high clustered (strongly correlated). The datasets were then split up into 500 meter depth interval units as well as geo-chronological units, and analyzed the using both geostatistical methods. Once Z-values were calculated, we were able to determine if the data were spatially auto-correlated based on BHT, and therefore correctable. We were also be able to tell if parsing out wells using the depth interval method, or by the geochronological unit method, was statistically best for resource assessment.

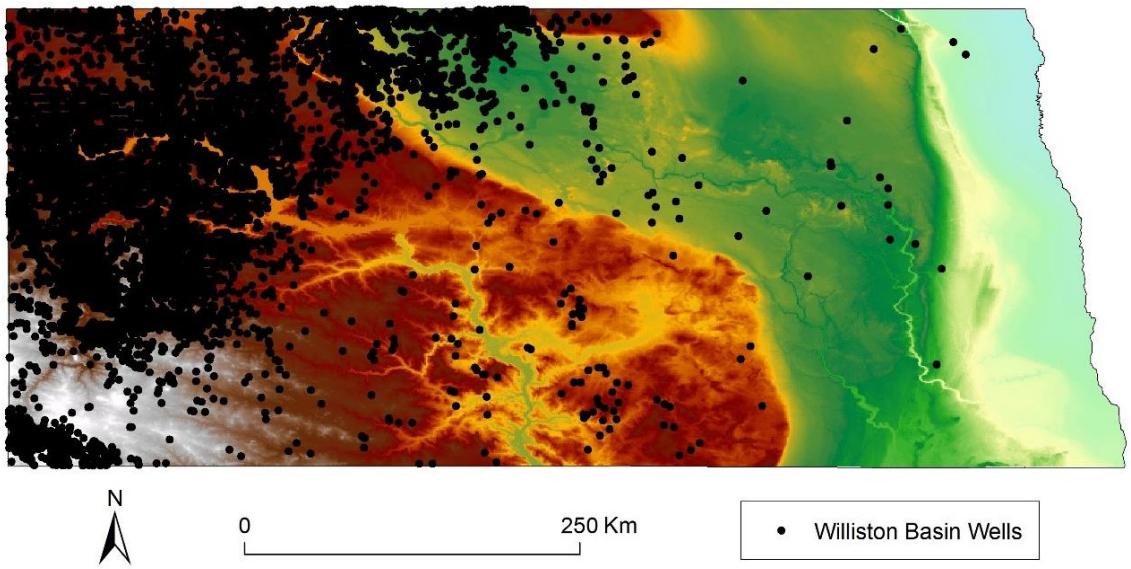

Figure 2. Spatial Representation of the 10,766 wells with bottom-hole temperature data in the Williston Basin.

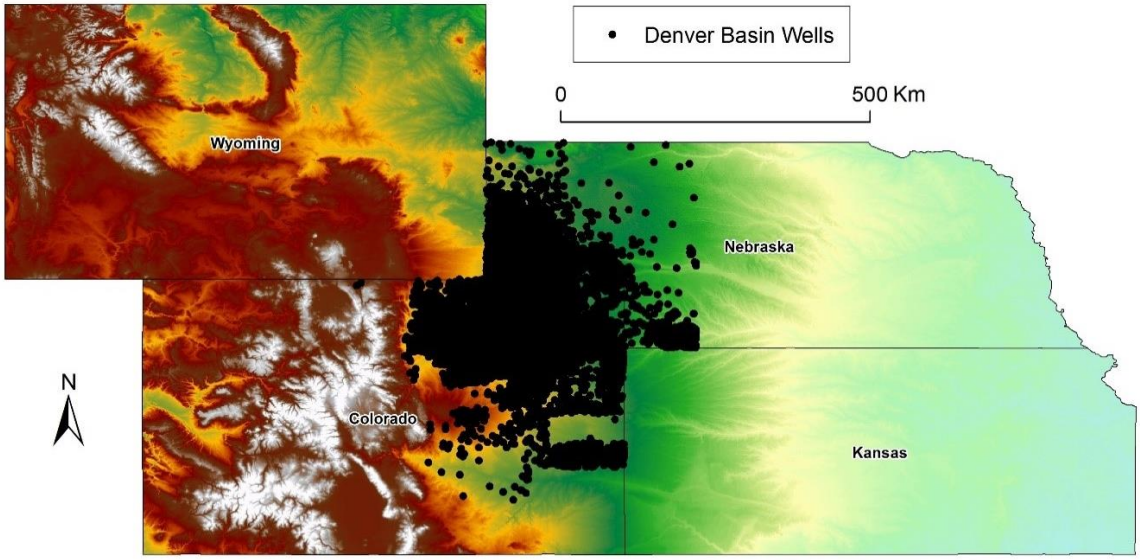

Figure 3. Spatial representation of the 49,222 wells with bottom-hole temperature data in the Denver Basin**.**

Results

Denver Basin

The Moran's I (Figure 3) analysis indicates that BHTs are correlated stronger by depth interval unit than by geochronological unit, since the z-values indicate clustering within the dataset for every interval, whereas only five of the eight geochronological units were spatially correlated. The Getis-Ord Analysis (Figure 4) indicates that four of the five depth intervals were highly clustered, indicating a high spatial correlation. The geochronological units were only highly clustered (high spatial correlation) in two instances, and either random or low clustering (non-correlated or low-correlation) for the other six units.

Denver Basin

Interval	Z-score	Distribution	p-value	# wells	Interval	Z-score	Distribution	p-value	# wells
500-1000m	21.42	Clustered	0	1,414	Upper Cretaceous	46.05	Clustered	0	12,739
1000-1500m	30.93	Clustered	0	8,772	Lower Cretaceous	113.85	Clustered	0	33,148
1500-2000m	67.62	Clustered	0	17,924	Jurassic	0.77	Random	0.44	480
2000-2500m	115.6	Clustered	0	19,524	Permian	2.22	Clustered	0.026	331
2500-3000m	8.68	Clustered	0	1,542	Pennsylvanian	7.76	Clustered	0	1,478
					Mississippian	31.5	Clustered	0	845
					Ordovician	0.207	Random	0.836	132
					Cambrian	4.34	Clustered	0.000014	54
All Wells	182.12	Clustered	0	49,222					

Figure 4. Moran's I analysis for the Denver Basin. Non-correlated units are denoted in red.

Denver Basin

Interval	Z-score	Distribution	p-value	# wells	Interval	Z-score	Distribution	p-value	# wells
500-1000m	0.99	Random	0.32	1414	Upper Cretaceous	67.25	High Cluster	0	12739
1000-1500m	8.73	High Cluster	0	8772	Lower Cretaceous	68.56	High Cluster	0	33148
1500-2000m	13.69	High Cluster	0	17924	Jurassic	-0.01	Random	0	480
2000-2500m	8.88	High Cluster	0	19524	Permian	0.79	Random	0.43	331
2500-3000m	64.32	High Cluster	0	1542	Pennsylvanian	-6.84	Low Cluster	0	1478
					Mississippian	-10.58	Low Cluster	0	845
					Ordovician	-0.57	Random	0.57	132
					Cambrian	-2.92	Low Cluster	0.0035	54
All Wells	158	High Cluster	0	49222					

Figure 5. Results of the Getis-Ord analysis for the Denver Basin. Non-correlated units are shown in red, while weakly correlated units are shown in yellow.

Williston Basin

The results of the Moran's I analysis for the Williston Basin (Figure 5) were not nearly as polarized as the results for the Denver Basin. All eight depth interval units were clustered showing spatial autocorrelation, and eight of the nine geochronological units were clustered. The results of the Getis-Ord analysis for the Williston Basin are shown in Figure 6. Six of the eight depth interval units were highly clustered, one was weakly clustered, and one was random. Of the nine geochronological units, six were highly clustered and three were random.

Williston Basin

Interval	Z-score	Distribution	p-value	# wells	Interval	Z-score	Distribution	p-value	# wells
500-1000m	8.97	Clustered	0	253	Cretaceous	8.89	Clustered	0	261
1000-1500m	40.3	Clustered	0	905	Jurassic	7.05	Clustered	0	50
1500-2000m	24.93	Clustered	0	990	Pennsylvanian	5.18	Clustered	0	216
2000-2500m	48.63	Clustered	0	846	Mississippian	134	Clustered	0	7,285
2500-3000m	23.6	Clustered	0	2,773	Devonian	21.24	Clustered	0	914
3000-3500m	23.86	Clustered	0	3,532	Silurian	32.34	Clustered	0	372
3500-4000m	10.86	Clustered	0	705	Ordovician	4.49	Clustered	7E-07	1,487
4000-4500m	2.32	Clustered	0.0199	707	CambroOrd	7.62	Clustered	0	100
					Precambrian	1.3	Random	0.195	51

All Wells	130	Clustered	0	10,766

Figure 6. Results of the Moran's I analysis for the Williston Basin. Non-correlated units are denoted in red.

Williston Basin

Interval	Z-score	Distribution	p-value	# wells	Interval	Z-score	Distribution	p-value	# wells
500-1000m	4.77	High Cluster	0.000002	253	Cretaceous	2.2	High Cluster	0.027576	261
1000-1500m	3.2898	High Cluster	0.001003	905	Jurassic	1.36	Random	0.173	50
1500-2000m	-0.489	Random	0	990	Pennsylvanian	0.573	Random	0.567	216
2000-2500m	-10.12	Low Cluster	0	846	Mississippian	50.8	High Cluster	0	7285
2500-3000m	9.96	High Cluster	0	2773	Devonian	16.66	High Cluster	0	914
3000-3500m	17.88	High Cluster	0	3532	Silurian	8.039	High Cluster	0	372
3500-4000m	8.747	High Cluster	0	705	Ordovician	2.12	High Cluster	0.033849	1487
4000-4500m	3.788	High Cluster	0.000152	707	CambroOrd	6.39	High Cluster	0	100
					Precambrian	1.5	Random	0.132209	51

All Wells	65.78	High Cluster	0

Figure 7. Results of the Getis-Ord analysis for the Williston Basin. Non-correlated units are shown in red, while weakly correlated units are shown in yellow.

Discussion

The geostatistical analyses for both basins, completed by using depth interval units, yields better spatial autocorrelation results than intervals defined by geochronological units; therefore, it is still possible to do a layer-by-layer geothermal resource assessment using data that is missing formation information. Since the bottom-hole temperatures are statistically clustered in relation to depth, the temperatures appear to be correctable with the commonly-used depth-variable correction methods, such as the Harrison and Kehle

Conclusions

Both the Moran's I and the Getis-Ord analyses showed a clustered distribution of bottom-hole temperatures for the Williston and Denver basins, indicating that a systematic correction based on depth is possible. Further work must be done to determine the parameters needed in order to create the best possible correction equation.

We have debated whether grouping bottom-hole temperatures by formation, or by 500 meter depth intervals is the statistically best method for geothermal resource assessments. With the results of this analysis we can state, with confidence, that the depth interval unit method is the most statistically accurate grouping of bottom-hole temperatures.

Sources Cited

Crowell, A., and W. Gosnold, 2013, GIS-Based Resource Assessment of the Denver Basin: Colorado and Nebraska, Geothermal Resources Council Transactions, v. 37.

Esri, Inc., 2013. ArcGIS 10.2 Helpfiles. Environmental Systems Research Institute, Redmond, CA. www.esri.com.

Förster, A., Merriam, D.F., and Davis, J.C., 1996, Statistical analysis of some bottom-hole temperature (BHT) correction factors for the Cherokee Basin, southeastern Kansas: Tulsa Geol. Soc. Trans., pp. 3-9.

Harrison W.E., K.V. Luza, M.L Prater, and P.K. Chueng, 1983, Geothermal resource assessment of Oklahoma, Oklahoma Geological Survey, Special Publication 83-1.

Kehle, R. O., R. J. Schoeppel, and R. K. Deford, 1970, The AAPG Geothermal Survey of North America, Geothermics, vol. 2, no. PART 1, p. 358-367.

CHAPTER III

EVALUATING BOTTOM-HOLE TEMPERATURE CORRECTION SCHEMES

Table of Contents

List of Figures 20

Introduction 21

Correcting Bottom-hole Temperatures in the Denver Basin: Colorado and Nebraska 22

- Abstract 22
- Introduction 23
- Existing Bottom-hole Temperature Correction Schemes 29
- Method 32
- Conclusion 35
- Acknowledgments 37
- Sources Cited 38

List of Figures

Figure		Page
1	Locations of wells logged at equilibrium	23
2	Spatial extent of the Denver Basin BHT data	24
3	Cross sectional view of the Denver Basin	25
4	Stratigraphic column of the Denver Basin for the Colorado Piedmont	26
5	Plot of uncorrected bottom-hole temperatures with the equation from Harrison-corrected data	30
6	Plot of uncorrected bottom-hole temperatures with the equation from Kehle-corrected data	31
7	Plot of uncorrected bottom-hole temperatures with the equation from Förster-corrected data	32
8	Plot of BHTs from wells at equilibrium	33
9	Graphical representation of an integration	34
10	Plot of uncorrected bottom-hole temperatures with the equation from equilibrium-corrected data	35
11	Comparison of correction equations	36

Introduction

The publication, Crowell et al., 2012, is presented as it was published in the Transactions of the Geothermal Resources Council, Volume 36, pages 201-206.

If BHTs are to be used for energy-in-place estimates, they must be corrected. Oil companies typically measure BHTs shortly after drilling, which means the drilling mud has disturbed the temperature of rock surrounding the borehole. This can result in borehole temperature measurement inaccuracies of as much as ± 30 °C.

We evaluated the Harrison, Kehle, and Förster correction schemes, and a method for quantifying how well each scheme corrected the data was developed. Equilibrium data from the Denver Basin was compared to BHT corrections to create a customized correction equation.

Correcting Bottom-Hole Temperatures in the Denver Basin: Colorado and Nebraska

Anna M. Crowell, Aaron T. Ochsner, Will Gosnold
UND Geothermal Laboratory
Department of Geology and Geological Engineering
University of North Dakota

Keywords: Geothermal, Bottom-Hole Temperatures, Bottom-Hole Temperature Corrections, Denver Basin, Colorado, Nebraska, BHT, Harrison, Kehle, Förster

Abstract

We have examined the problem of bottom-hole temperatures (BHTs) in the Colorado and Nebraska portions of the Denver Basin with the use of three existing correction schemes; the Förster Correction, the Harrison Correction, and the Kehle Correction. We integrated the results of these three equations with the results of equilibrium temperatures to quantify which existing correction works best with Denver Basin stratigraphy. Of the three existing corrections, we determined that the Förster Correction has the least amount of area between curves for the integration, thus it is the best correction. Since we had the equilibrium data, we created a tailored correction scheme for the Denver Basin: Temperature Correction Factor (Tcf) = 0.0124x + 7.8825.

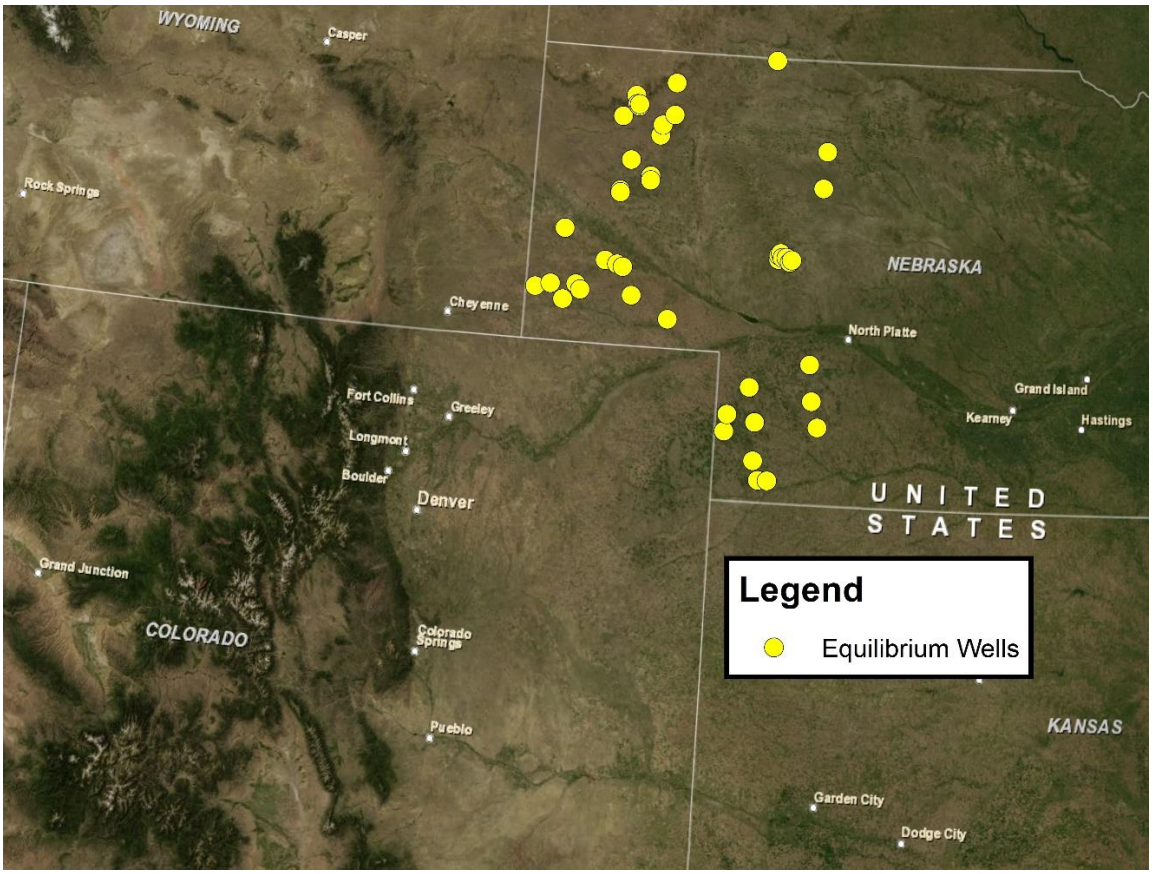

Figure 1. Locations of wells logged at equilibrium.

Introduction

The Denver Basin (Figure 2) is an asymmetric syncline with an axis that trends north-south, parallel to the Rocky Mountains, and has a surface area of approximately 155,000 km^2 (Curtis, 1988; Martin, 1965). The western flanks of the basin dip downward to the east to a maximum depth of about 4,000 m and grade into a westward-dipping surface that continues into Nebraska and Kansas. A north-south-trending transect along the eastern edge of the Front Range reveals a similar asymmetrical geometry with respect to the basin's east-west asymmetry. The point of maximum depth, centered beneath El Paso county (Irwin, 1976), is much closer to the basin's southern boundary in central Colorado than to its terminus in southeastern Wyoming.

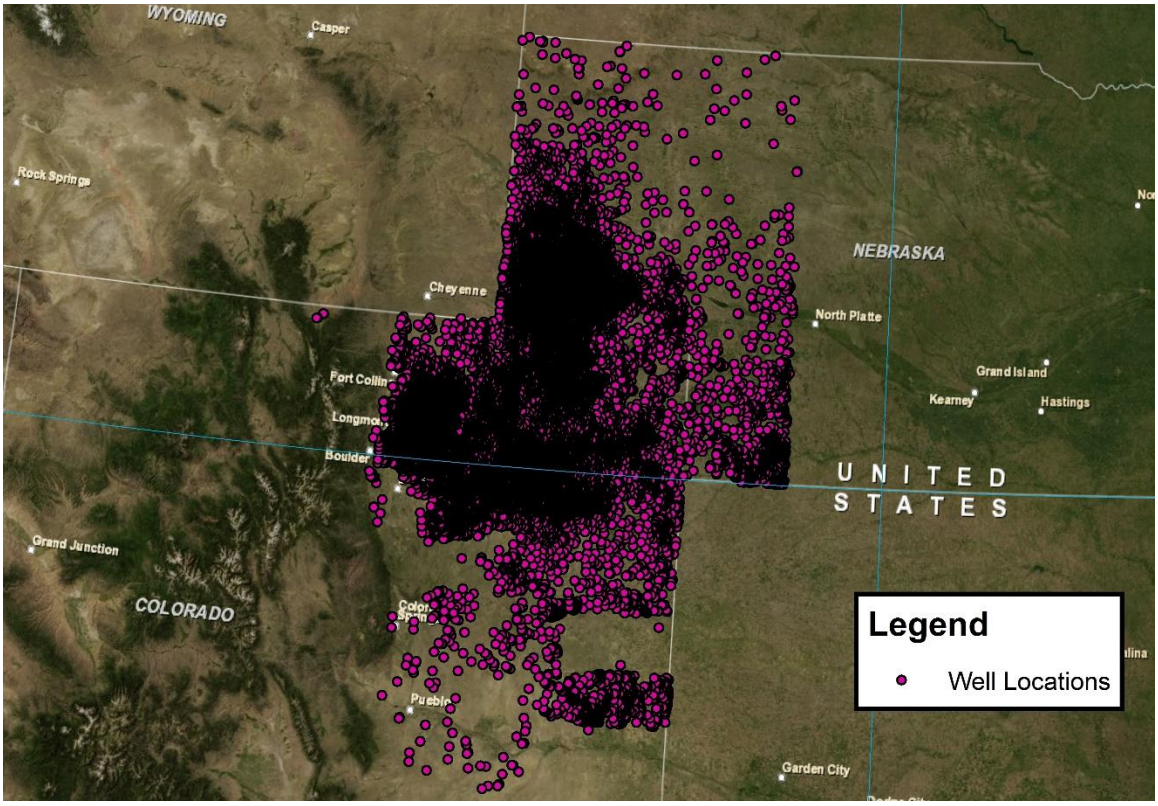

Figure 2. Spatial extent of the Denver Basin BHT data.

The Wet Mountain range near Pueblo, which is the brink of the southernmost extent of the Denver Basin, trends west/northwest and is characterized by a zone of westward-dipping reverse faults of varying angles (Curtis, 1988). A series of diverse fold and fault geometries (some exposed, some buried by Tertiary sediments) follow along the western border of the basin (Figure 3); including the entirety of the Front Range from the Wet Mountains in the south to the Laramie Range of southeastern Wyoming. The most prominent bounding features from the northwestern to northern edges of the basin are the Hartville and Black Hills Uplift features, both of which expose Late Archean and Early Proterozoic granites and metamorphic rocks (Sims et al., 1997). The northeastern, eastern and southeastern flanks of the Denver Basin are embodied by a semi-continuous, curvilinear series of structural arches. In Nebraska, the Chadron and Cambridge structural

arches trend northeast-southwest and north-south, respectively, and constitute an Ouachita-induced upwelling of Precambrian and early Paleozoic rocks (Curtis, 1988; Carlson, 1993; Martin, 1965; Reed, 1958). The north-northeasterly-trending Las Animas arch is structurally similar to the Chadron and Cambridge Arches, and trends from the Wet Mountains in Colorado, cutting through the northwestern corner of Kansas, and merging with the southern portion of the Cambridge Arch (Merewether, 1987).

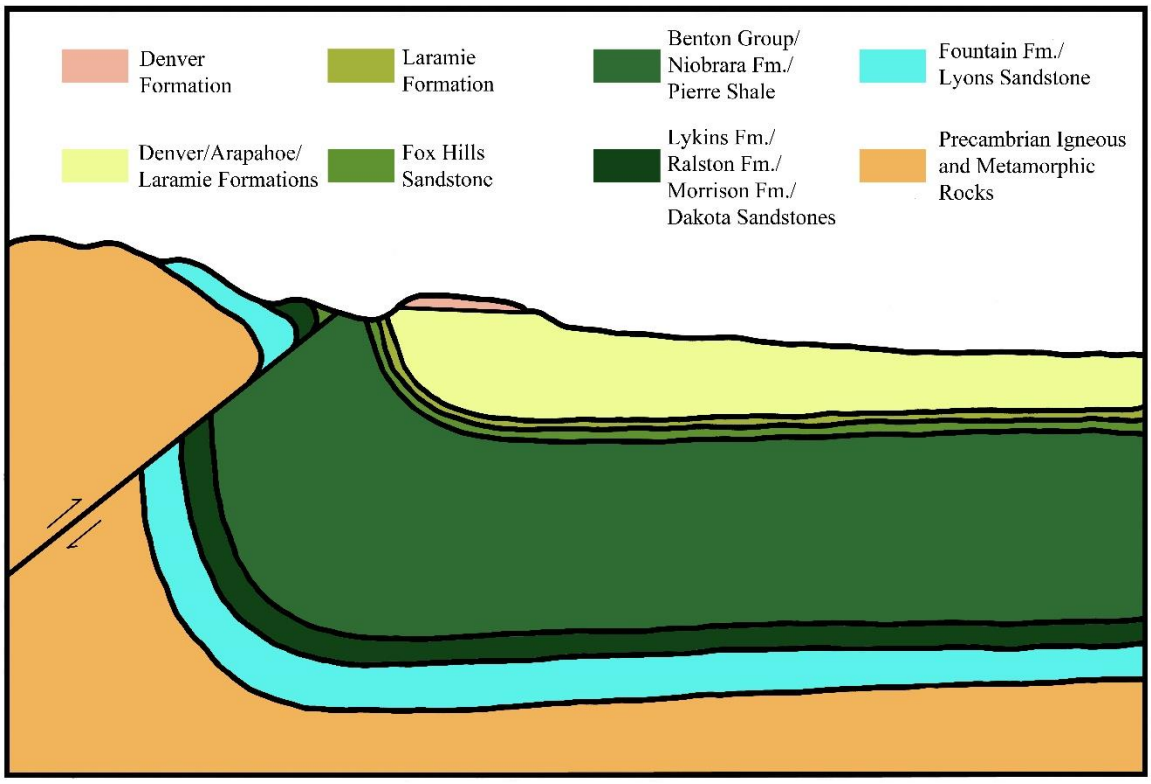

Figure 3. Cross sectional view of the Denver Basin. (Modified from Noe et al., 1999)

The sedimentary stratigraphic record (Figure 4) of the Denver Basin begins with the Upper Cambrian (Reagan Sandstone and equivalent Sawatch Sandstone) sandstones at the base. Upper Cambrian sandstones are thin and discontinuously present, existing primarily in the northernmost portion of the basin, in outcrops in the southern Front Range, and in much of the central and western subsurface (Curtis, 1988). The Reagan Sandstone is present in Nebraska, and thins westward (Condra and Reed, 1959).

Eon	Era	Period	Epoch	Formation		Rock Type	Thickness (m)
Phanerozoic	Cenozoic	Paleogene	Paleocene	Green Mountain Conglomerate		Conglomerate, Sandstone, Shale	198
	Mesozoic	Cretaceous	Upper	Denver Formation		Claystone, Siltstone, Sandstone, and Conglomerate	290
				Araphahoe Formation		Claystone, Siltstone, Sandstone, and Conglomerate	121
				Laramie Formation		Siltstone, Claystone, and Sandstone	168
				Fox Hills Sandstone		Shale and Sandstone	55
				Pierre Shale		Shale, some Sandstone beds	1890
				Niobrara Formation	Smoky Hill Shale	Shale and Limestone	43
					Fort Hayes Limestone	Limestone	43
				Carlisle Shale		Claystone, Siltstone, Calcarenite and Hard Limestone Beds	162
				Greenhorn Limestone			
				Graneros Shale			
			Lower	Dakota Group	South Platte Formation	Sandstone and Shale	91
					Lytle Formation	Sandstone and Conglomerate	
		Jurassic	Upper	Morrison Formation		Siltstone and Claystone	91
				Ralston Creek Formation		Sandstone and Siltstone	27
		Triassic	?	Lykins Formation		Shale, Limestone, and Siltstone	137
	Paleozoic	Permian		Lyons Formation		Sanstone and Conglomerate	58
		Carbon.	Penn.	Fountain Formation		Sandstone and Conglomerate	502
Precambrian				Precambrian		Igneous and Metamorphic Rocks	

Figure 4. Stratigraphic column of the Denver Basin for the Colorado Piedmont. (Modified from Abbot and Noe, 2002)

The limestones and dolomites of the lower Ordovician Arbuckle Group (equivalent Manitou Limestone) thin westward and northward from considerable thicknesses in eastern Colorado and western Nebraska portions of the basin, and appear to be present in the deepest part of the basin's trough (Irwin, 1976), although they are absent from the hinge of the Cambridge Arch (Condra and Reed, 1959).

Silurian rocks appear to be absent from the entire basin according to Curtis (1988), and from the Nebraska portion specifically according to Carlson (1993) and Condra and Reed (1959). Martin (1965) asserts that Early, Middle, and Late Silurian fossiliferous

limestones are present at two localities in the Front Range on the Colorado-Wyoming border.

The Devonian system is unrepresented in the Denver Basin (Condra and Reed, 1959); however, the deposition of the limestone units of the Guernsey Formation began during the late Devonian and continued through the middle Mississippian. According to Curtis (1988), the Guernsey Formation is present in the northern extremity of the basin. Mississippian limestone units of variable thickness are observed to be present throughout the central part of the basin (almost exclusively in Colorado), and although they are often assumed to be part of the Madison Limestone, their equivalence to the formally-accepted Madison Limestone type-lithology has not been verified (Curtis, 1988). Other Mississippian units, including the Williams Canyon, Gilmore City and St. Genevieve Limestones, the Harrison Shale, and Warsaw Formation carbonates and mudstones are present in the southeastern Denver Basin along the Las Animas Arch (Kirkham and Ladwig, 1979; Merewether, 1987).

The Pennsylvanian and Permian systems have a complex lithology, and constitute a significant portion of the stratigraphic section throughout the entire basin. The Pennsylvanian system is characterized by the Fountain Formation, which extends throughout the central and southern Denver Basin and includes an array of reddish-brown arkosic conglomerates, yellow-gray arkosic sandstones, and light green and reddish-brown shales (Kirkham and Ladwig, 1979). These lithologies dominate the western region of the basin's Pennsylvanian system and grade eastward into fine clastics and carbonates (Curtis, 1988). The Permian system is also well represented (in part by the Lyons sandstone), and consists primarily of red shales and sandstones, gypsum, salt

deposits, and limestones. Pennsylvanian and Permian sections generally thicken toward the west and south, and reach a maximum combined thickness of more than 1,300 m in the southern part of the basin trough (Curtis, 1988; Irwin, 1976).

Triassic rocks are virtually non-existent in the Nebraska portion of the Denver Basin, but are present in the northwestern part of the basin, thickening into Wyoming and pinching out toward the east and south. These lithologies are mostly Chugwater and Lykins red sandstones and siltstones (Curtis, 1988; Irwin, 1976).

The Jurassic system is represented throughout the entire basin, particularly by the interbedded mudstones, limestones, sandstones, and conglomerates of the upper Jurassic Morrison Formation (Kirkham and Ladwig, 1979). Evaporites and limy siltstones and shales of the middle Jurassic Sundance, Ralston Creek, and Entrada formations underlie the Morrison and unconformably overlie Triassic and Permian units in various localities (Curtis, 1988).

Cretaceous units of the Denver Basin are historically important petroleum-source and reservoir rocks. The "D" and "J" sandstones of the Dakota Group, which consists of Cretaceous conglomeratic sandstones and gray shales (Kirkham and Ladwig, 1979), are particularly noteworthy petroleum-production units. Along with the Dakota Group, the dark shales, calcareous shales, and limestones of the overlying Graneros, Greenhorn, Carlile, and Niobrara formations extend throughout the basin. The Pierre Shale, composed of gray silty and sandy shales and interbedded sandstones, also exists throughout the basin, and is the thickest stratigraphic unit of the Denver Basin with a thickness of 900 m (3,000 ft) in western Nebraska (Condra and Reed, 1959) and 2,500 m (8,000 ft) in the central part of the basin (Curtis, 1988; Irwin, 1976). Overlying Fox Hills

silty sandstones contain iron-rich concretions and thin coal beds (Kirkham and Ladwig, 1979). The Lance Formation, (equivalent Laramie) consists of coal-bearing siltstones and sandstones and caps the Denver Basin's Mesozoic stratigraphic system beneath an unconformity with overlying Tertiary sediments (Raynolds, 2002).

Tertiary rocks in the Denver basin are tectonically unperturbed, and are perhaps the most diverse of any single geologic period for the basin. They include Paleocene arkosic sandstones and conglomerates, Oligocene fluvial siltstone and sandstone of the White River Group and Wall Mountain tuffstone, and conglomerates, gravels and sands of the overlying Miocene Arikaree and Ogallala Formations. Quaternary cover throughout the basin is characterized by fluvial, alluvial, and eolian sands, silts, and loess (Burchett, 1969; Condra and Reed, 1959; Curtis, 1988; Kirkham and Ladwig, 1979).

Existing Bottom-Hole Temperature Correction Schemes

The Harrison, Kehle, and Förster equations were created with a specific region or dataset in mind. This makes the application of these corrections to other basins inappropriate since all basins have different lithologies and thermal histories (Crowell and Gosnold, 2011). The Harrison Correction, created by Harrison (1983) and subsequently re-defined by Blackwell and Richards (2004), was determined using equilibrium and disequilibrium data from the Anadarko and Arkoma basins in Oklahoma. The practice was appropriate since the lithologies of both basins are very similar. The Harrison Correction equation (Figure 5), as defined by the Southern Methodist University Geothermal Laboratory (Blackwell and Richards, 2004; Blackwell et al., 2010), is:

$$\boldsymbol{Tcf}\ (℃) = \mathbf{-16.512 + 0.0183\,x - 0.00000234\,x^2}$$

where x is depth in meters.

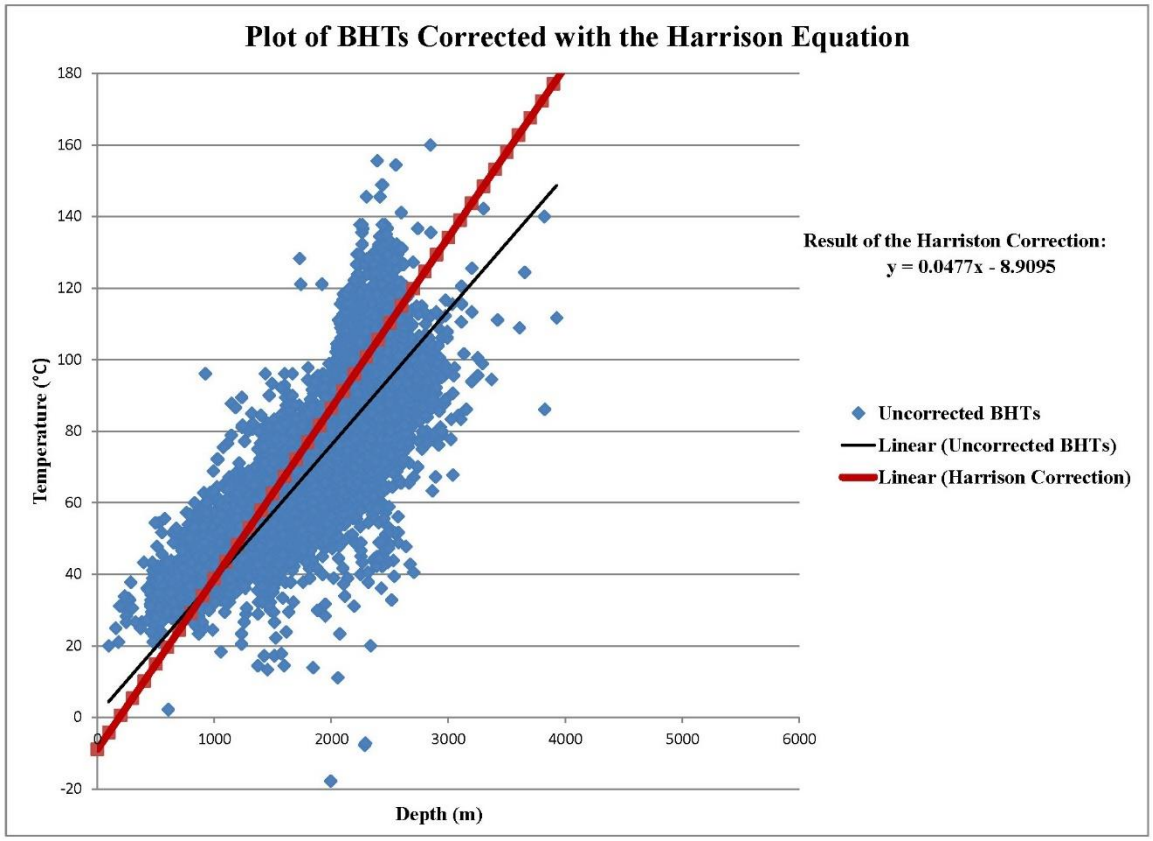

Figure 5. Plot of uncorrected bottom-hole temperatures with the equation from Harrison-corrected data.

The Kehle Correction (Figure 6) was created for the AAPG dataset (Kehle et al., 1970) to examine the process by which unreliable bottom-hole temperatures from oil and gas well header logs could be corrected. Several methods for correcting temperatures were analyzed and Gregory et al. (1980) defined the Kehle correction equation without a time variable as:

$$\boldsymbol{Tcf}\ (°\mathrm{F}) = \mathbf{-8.819\ x\ 10^{-12}\ x^3\ -\ 2.143\ x\ 10^{-8}\ x^2\ +\ 4.375\ x\ 10^{-3}\ x\ -\ 1.018}$$

where x is depth in feet.

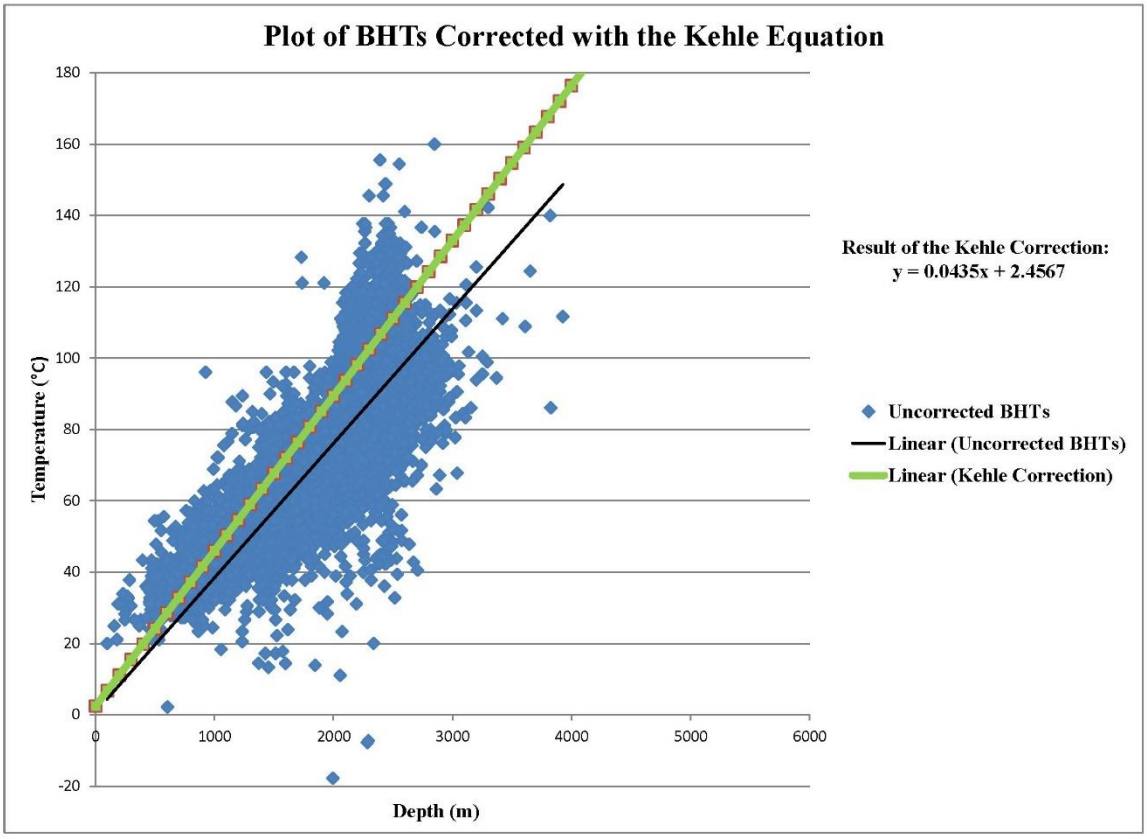

Figure 6. Plot of uncorrected bottom-hole temperatures with the equation from Kehle-corrected data.

The Förster correction (Figure 7) was created by analyzing bottom-hole temperature data in southeastern Kansas for the same reason: unreliable BHT records due to mud circulation (Förster and Merriam, 1995). Two versions of the Förster correction exist: the original Förster correction equation (Förster and Merriam, 1995), which is:

$$\boldsymbol{Tcf}\ (℃) = \mathbf{0.012}\boldsymbol{x} - \ \mathbf{3.68}$$

where x is depth in meters.

and the equation that was modified by the SMU Geothermal Laboratory (Richards 2012, personal communication):

$$\boldsymbol{Tcf}\ (℃) = \mathbf{0.017}\boldsymbol{x} - \ \mathbf{6.58}$$

where x is depth in meters.

For the purpose of uniformity, we used the equation obtained from the SMU Geothermal Laboratory.

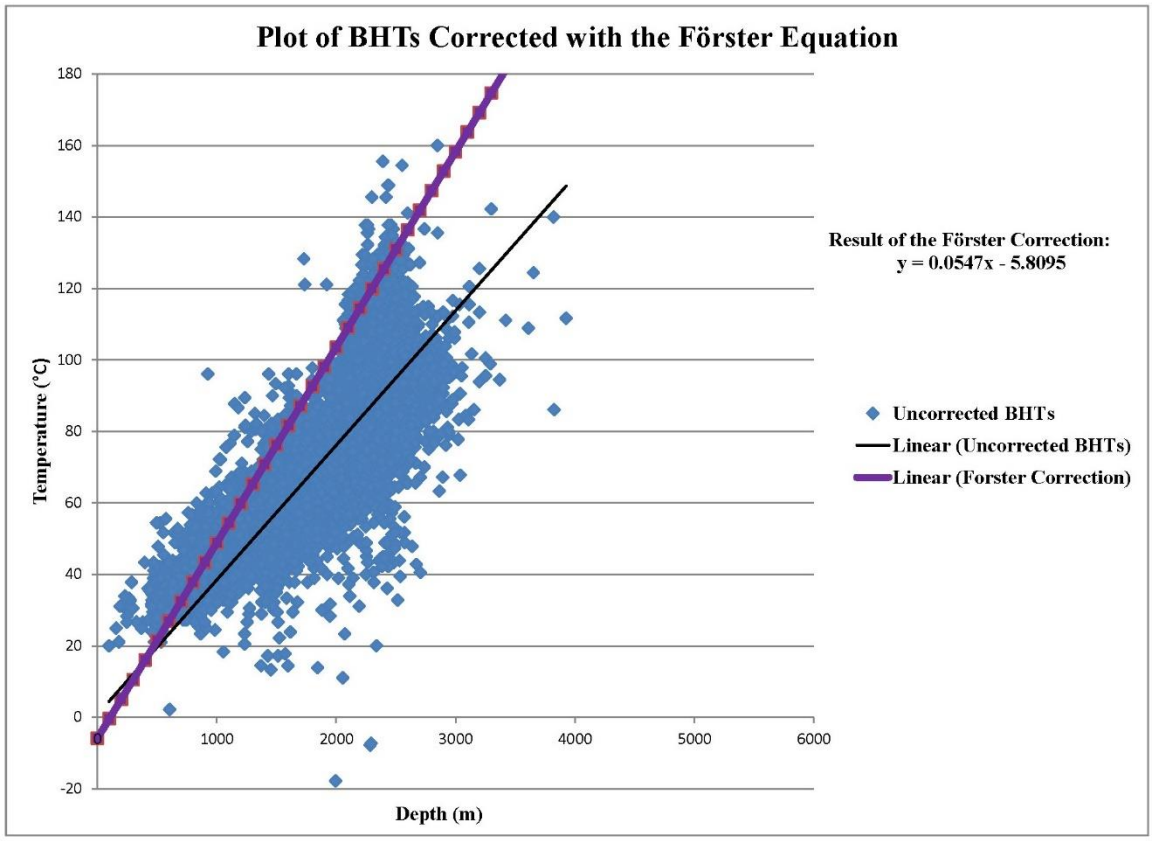

Figure 7. Plot of uncorrected bottom-hole temperatures with the equation from Förster-corrected data.

Method

Bottom-hole temperature data was obtained from the Nebraska Oil and Gas Commission and Dr. Paul Morgan of the Colorado Geological Survey. Equilibrium well data (Figure 1) was obtained from Dr. Will Gosnold at the University of North Dakota. The equilibrium dataset was entered into an Excel spreadsheet, plotted, and fitted with a linear best fit line. The equation recorded from this best fit line is referred to as the "equilibrium equation (Figure 8)."

The uncorrected bottom-hole temperatures were then corrected using the existing correction methods (Harrison, Kehle, and Förster), resulting in the creation of three new datasets. These three new datasets were then plotted in an Excel spreadsheet and fitted with a linear best fit trendline. The equations of the trendlines were recorded and integrated with the equilibrium equation (Figure 8) to obtain the area between the curves. The area between curves is interpreted to be a method by which to quantify the most accurate correction method (Figure 9). In our case, the integration yielding the smallest area between the curves is quantifiably the best of the existing corrections, the unit of which is a degree meter as defined by Crowell and Gosnold (2011).

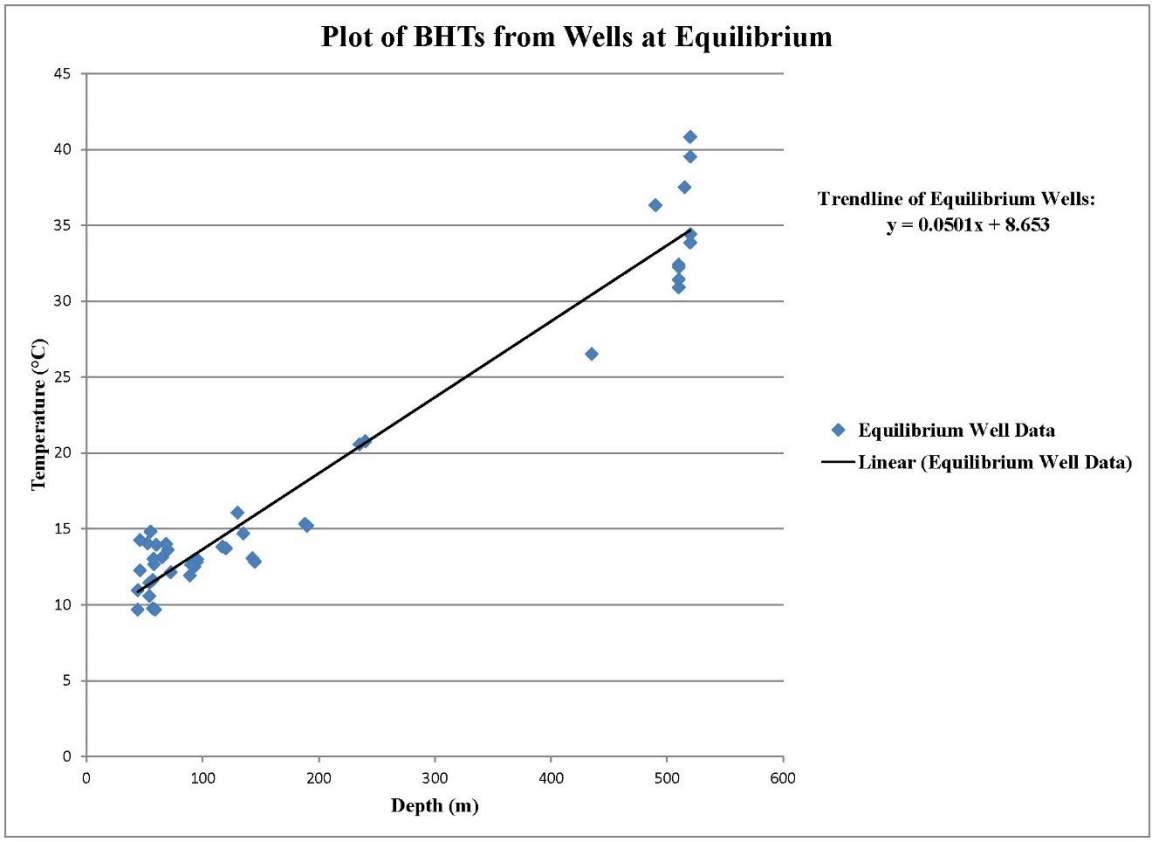

Figure 8. Plot of BHTs from wells at equilibrium.

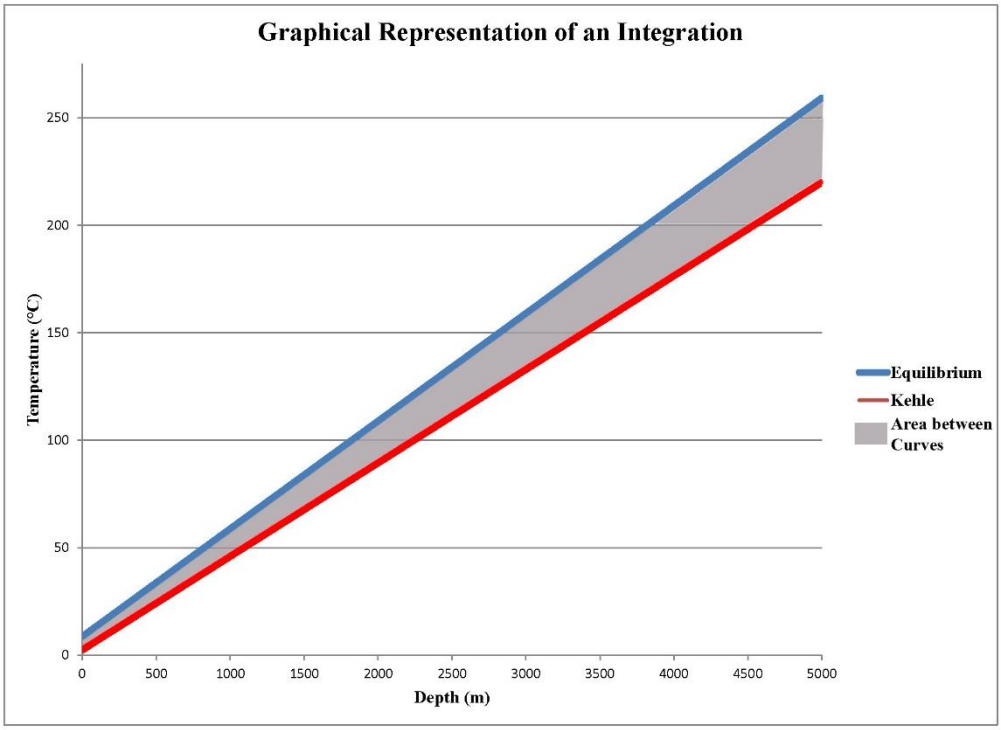

Figure 9. Graphical representation of an integration.

The results of the integrations are as follows: the Kehle correction integration yielded 188,467 degree meters, the Harrison correction integration yielded 117,812.5 degree meters, and the Förster correction had the lowest area of the existing equations, with 30,657.92 degree meters.

We then determined that we had enough data to attempt a correction scheme based on the equilibrium data equation and the equation obtained from the plot of the uncorrected temperatures. The uncorrected equation was subtracted from the equilibrium equation, giving us a new correction scheme:

$$\boldsymbol{Tcf}\ (°\mathrm{C}) = \mathbf{0.0124}\boldsymbol{x} + \mathbf{7.8825}$$

where x is depth in meters.

It should be noted that this correction equation is only appropriate for the Denver Basin, and possibly other basins with similar stratigraphy.

The bottom-hole data was then corrected using the new equilibrium correction scheme and plotted (Figure 10). The plot of the corrected data gives a best fit trendline that is the same as the original equilibrium equation. Figure 11 shows the corrected trendlines for the datasets, including how the best fit trendline of the equilibrium-corrected data superimposes on the best fit trendline for the equilibrium in situ data (the dashed orange line and thick blue line, respectively).

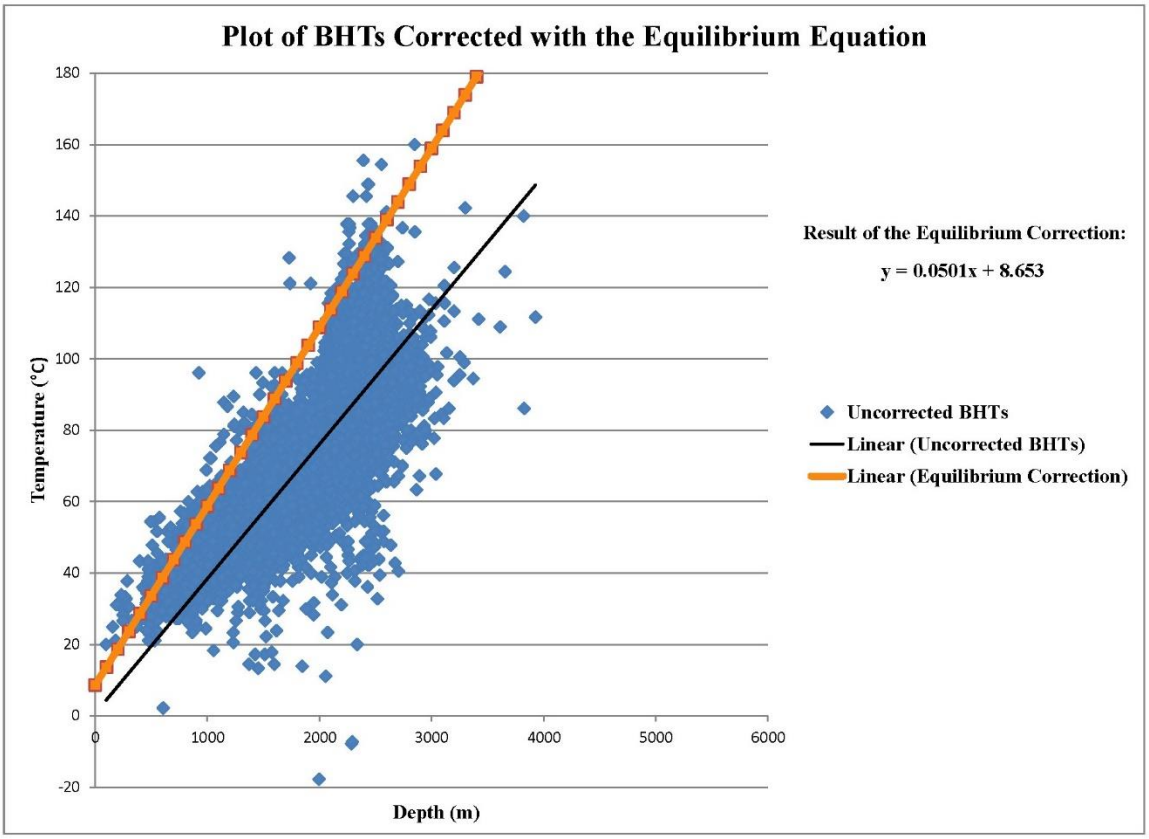

Figure 10. Plot of uncorrected bottom-hole temperatures with the equation from equilibrium-corrected data.

Conclusion

Bottom-hole temperature data are unreliable, but it remains the most abundant and readily available source for subsurface temperature information. Utilizing this method in the Denver Basin, we have determined that the Förster correction (Tcf (°C) = 0.017x -

6.58) is the most accurate of the existing corrections that do not require time of mud circulation data. We have also provided a tailored correction for the Denver Basin based on equilibrium data (Tcf (°C) = 0.0124x + 7.8825). It is important to remember that the corrected data are closer to in situ equilibrium values, but does not guarantee a correction to equilibrium in situ values.

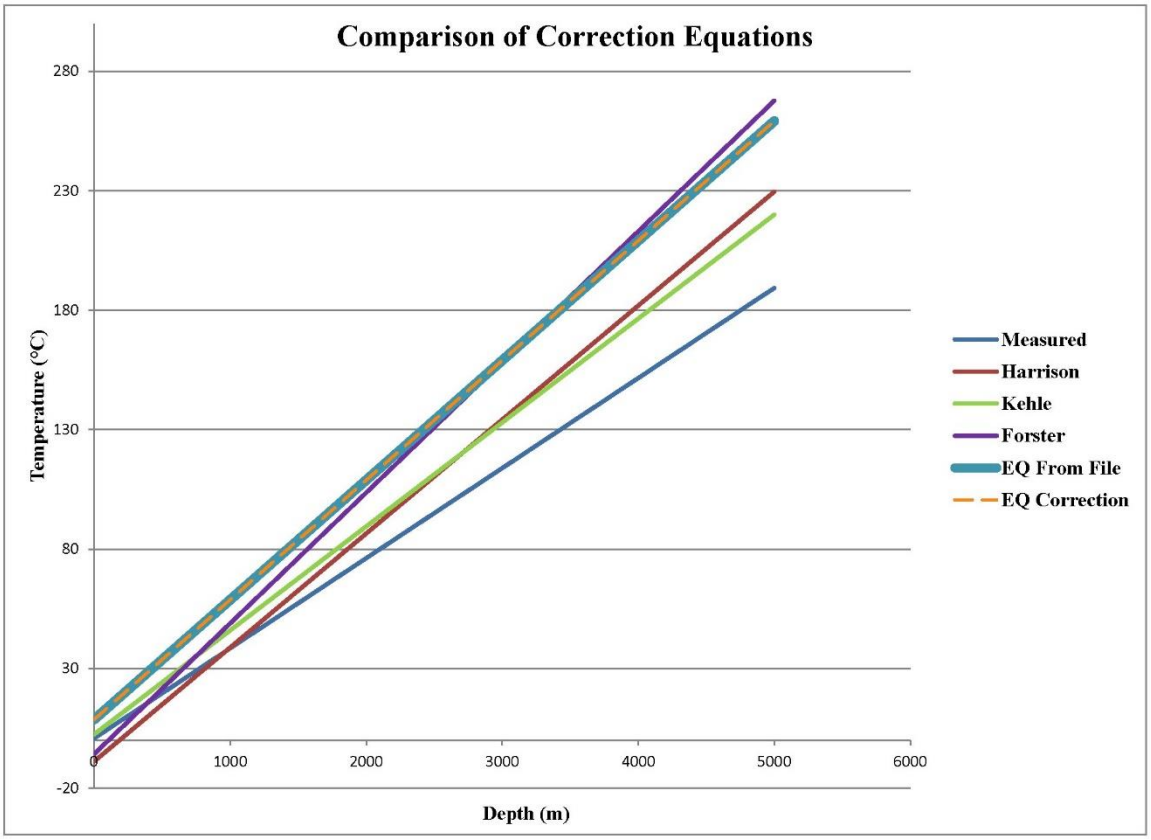

Figure 11. Comparison of correction equations.

Until now, the selection of an appropriate bottom-hole temperature correction scheme has been difficult, with few parameters to quantify level of confidence in the correction. Integrating the best fit trendline of corrected bottom-hole temperatures with the best fit trendline of equilibrium data is a method to quantifiably determine the appropriate correction. Equilibrium data can also be used to create a tailored correction

scheme. When equilibrium data are not available, it is possible that in-situ temperature information may be obtained by analyzing stratigraphic and thermal conductivity data (Gosnold et al., 2012).

Acknowledgements

The authors would like to thank Dr. Paul Morgan and the Colorado Geological Survey as well as the Nebraska Oil and Gas Commission for providing the BHT and formation data. This material is based upon work supported by the Department of Energy Geothermal Technologies Program under Award Numbers DE-EE0002854 and DE-EE0002731.

Sources Cited

Abbott, D. M., and Noe, D. C., 2002, The Consequences of Living with Geology: A Model Field Trip for the General Public, Geological Society of America, Field Guides, Vol. 3, pp. 1-16.

Blackwell, D. D., and Richards, M., 2004, Calibration of the AAPG Geothermal Survey of North America BHT Data Base: American Association of Petroleum Geologists Annual Meeting 2004, Dallas, Texas, Poster session, paper 87616.

Blackwell, D. D., Richards, M., and Stepp, P., 2010, Texas Geothermal Assessment for the I-35 Corridor East, Texas State Energy Conservation Office Contract, pp. 88.

Burchett, R. R., 1969, Geologic Bedrock Map of Nebraska: Nebraska Geological Survey, Conservation and Survey Division, Institute of Agriculture and Natural Resources.

Carlson, M. P., 1966, Configuration of Precambrian Surface in Nebraska: University of Nebraska Conservation and Survey Division, 1:250,000 scale map.

Carlson, M. P., 1993, Geology, Geologic Time and Nebraska: Conservation and Survey Division, Institute of Agriculture and Natural Resources, University of Nebraska-Lincoln, pp. 20-46.

Crowell, A. M., and Gosnold, W. D., 2011, Correcting Bottom-Hole Temperatures: A Look at the Permian Basin (Texas), Anadarko and Arkoma Basins (Oklahoma), and Williston Basin (North Dakota), Geothermal Resources Council Transactions, Vol. 35, pp. 735-738.

Curtis, B. F., 1988, Sedimentary rocks of the Denver basin: in Sloss, L.L. (editor), Sedimentary Cover—North American Craton, U.S. Geological Society of America, The Geology of North America, v. D-2, ch. 8, pp. 182-196.

Condra, G. E. and Reed, E. C., 1959, The Geological Section of Nebraska: Nebraska Geological Survey Bulletin, Number 14A, pp. 8-73.

Förster, A., Merriam, D.F., and Davis, J.C., 1996, Statistical analysis of some bottom-hole temperature (BHT) correction factors for the Cherokee Basin, southeastern Kansas: Tulsa Geol. Soc. Trans., pp. 3-9.

Gregory, A. R., Dodge, M. M., Posey, J. S., and Morton, R. A., 1980, Volume and accessibility of entrained (solution) methane in deep geopressured reservoirs-Tertiary formations of the Texas Gulf Coast, DOE Final Report DOE/ET/11397-1, pp. 361, OSTI # 5282675.

Gosnold, W. D., McDonald, M. R., and Merriam, D. F., 2012, Geothermal Resources Council Transactions, Vol. 36 (in publication).

Harrison W. E., Luza, K.V., Prater, M. L., and Chueng, P. K., 1983, Geothermal resource assessment of Oklahoma, Oklahoma Geological Survey, Special Publication 83-1.

Irwin, D., 1976, Subsurface Cross Sections of Colorado: Rocky Mountain Association of Geologists Special Publication No. 2, Plate 1.

Kehle, R.O., Schoeppel, R. J., and Deford, R. K., 1970, The AAPG Geothermal Survey of North America, Geothermics, Special Issue 2, U.N Symposium on the Development and Utilization of Geothermal Resources, Pisa 1970, Vol. 2, Part 1.

Kirkham, R. M. and Ladwig, L. R., 1979, Coal Resources of the Denver and Cheyenne Basins, Colorado: Resource Series 5: Colorado Geological Survey, pp. 10-26.

Martin, C. A., 1965, Denver Basin: Bulletin of the American Association of Petroleum Geologists, v. 49, no. 11, pp. 1908-1925.

Merewether, E.A., 1987, Oil and gas plays of the Las Animas Arch, southeastern Colorado; U.S. Geological Survey: Open-File Report 87-450D, pp. 1-6.

Morgan, P., Personal Communication, Colorado Geological Survey, February 2012, Interviewer: Anna M. Crowell.

Noe, D. C., Soule, J. M., Hynes, J. L., and Berry, K. A., 1999, Bouncing Boulders, Rising Rivers, and Sneaky Soils: A Primer of Geologic Hazards and Engineering Geology along Colorado's Front Range, *in* Lageson, D. R., Lester, A. P., and Trudgill, B. D., eds., Colorado and Adjacent Areas: Boulder, Colorado, Geological Society of America Field Guide I.

Raynolds, R. G., 2002, Upper Cretaceous and Tertiary stratigraphy of the Denver Basin, Colorado: Rocky Mountain Geology, v. 37, no. 2, pp. 111-134.

Reed, E. G. 1958, Block Diagram—-Bedrock Geology of Nebraska: Conservation and Survey Division, University of Nebraska.

Richards, M., Personal Communication, SMU Geothermal Laboratory, February 2012, Interviewer: Anna M. Crowell.

Sims, P. K. and Petermar, Z. E., 1986, Early Proterozoic Central Plains Orogen: A major buried structure in the north-central United States; in Geology, v. 14, pp. 488-491.

Sims, P. K., Day, W. C., Snyder, G. L., and Wilson, A. B., 1997, Geologic Map of Precambrian Rocks Along Part of the Hartville Uplift, Guernsey and Casebier Hill Quadrangles, Platte and Goshen Counties, Wyoming; U.S. Geological Survey: Miscellaneous Investigations Series, Map I-2567, Pamphlet, pp. 1 and 10.

CHAPTER IV

ENERGY-IN-PLACE ESTIMATE FOR THE DENVER BASIN

Table of Contents

List of Figures 42

List of Tables 43

Introduction 44

GIS-Based Geothermal Resource Assessment of the Denver Basin: Colorado and Nebraska 45

- Abstract 45
- Introduction 45
- Methods 46
- Results 50
- Conclusion 53
- References 54

List of Figures

Figure		Page
1a	Graph of Energy in Place for the Denver Basin by temperature range	44
1	Location of Denver Basin wells with BHT data.	47
2	Interpolation (kriging method) of the Lower Cretaceous wells, manually classified according to temperature range	48
3	Area polygons created from the reclassified temperature raster	49

List of Tables

Table		Page
1	Heat capacity and density of dominant rock types	46
2	Upper Cretaceous, average unit thickness 0.278 km	50
3	Lower Cretaceous, average unit thickness 0.485 km	51
4	Jurassic, average unit thickness 0.107 km	51
5	Permian, average unit thickness 0.346 km	51
6	Pennsylvanian, average unit thickness 0.560 km	52
7	Mississippian, average unit thickness 0.129 km	52
8	Ordovician, average unit thickness 0.013 km	52
9	Total thermal energy in place by temperature range, and translated to megawatts thermal and number of homes that amount of energy can theoretically power	53

Introduction

Crowell and Gosnold, 2013, was published in the Transactions of the Geothermal Resources Council, Volume 37, pages 941-943.

BHT data for the Denver Basin allows for the estimation of energy-in place using the corrected bottom-hole temperatures for geothermal evaluation. Geochronological units were used to obtain the volumes for energy estimates (Figure 1a).

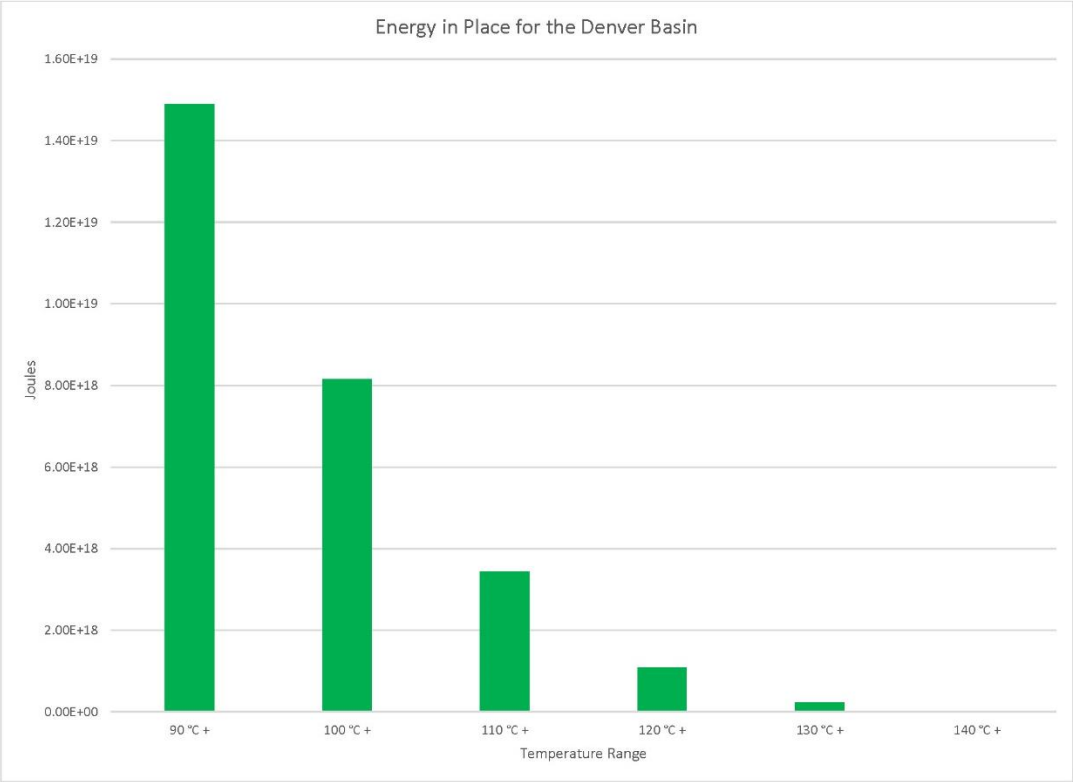

Figure 1a. Graph of Energy in Place for the Denver Basin by temperature range.

GIS-Based Geothermal Resource Assessment of the Denver Basin: Colorado and Nebraska

Anna M. Crowell and Will Gosnold

UND Geothermal Laboratory
Harold Hamm School of Geology and Geological Engineering
University of North Dakota

Keywords: Co-produced, geothermal, energy, ArcGIS, Denver Basin, Colorado, Nebraska, sedimentary basin

Abstract

We have completed a volumetric analysis of the geothermal resource potential of the Denver basin using bottom-hole temperatures (BHTs) from approximately 53,000 wells in Colorado and Nebraska. Re-evaluation of our correction scheme shows that a Harrison-type correction yields the best results for a mid-continental United States sedimentary basin. Formation names are not always constant across state boundaries, so we grouped the wells according to seven geochronological units; Lower Cretaceous, Upper Cretaceous, Jurassic, Permian, Pennsylvanian, Mississippian, and Ordovician. We utilized the recovery factor from Sorey et al., which is 0.001 for a structure the size of the Denver Basin. Our estimate of the thermal energy in place, after the recovery factor, is listed by temperature range as follows: 1.49×10^{19} Joules (J) at 90° Celsius (C) and up, 8.15×10^{18} J at 100° C and up, 3.44×10^{18} J at 110° C and up, 1.08×10^{18} J at 120° C and up, 2.35×10^{17} J at 130° C and up, and 2.09×10^{15} J at 140° C and up.

Introduction

The Denver basin is an asymmetric foreland basin with an area of approximately 156,000 square kilometers (km), underlying portions of Colorado, Nebraska, Wyoming,

and Kansas. The basin is about four kilometers deep near the Denver area, and contains sedimentary rocks ranging in age from the Cambrian to the Miocene (Martin, 1965). The structure produces both oil and gas; and, with population centers near the region of hottest temperatures, this basin is of interest for geothermal power production.

Methods

We calculate the available thermal energy in place (Q) from:

$$\mathbf{Q=\rho CpV\Delta T,}$$

where (ρ) is the density of the major rock type in the unit, and (Cp) is the heat capacity of the rock type. The values we used for each geochronological unit were the density and heat capacity of the rock found in the oil producing formations. Shale is the predominant rock type of the Upper Cretaceous unit, and Sandstone, Limestone, and Dolomite were the major rock types for the other six units (Table 1) (Touloukian et al., 1981). The density and heat capacity values for sandstone were the lowest value of the three dominating rock types; therefore, the values for sandstone were used in units that had an even mix of all three rock types.

Table 1. Heat capacity and density of dominant rock types. (Touloukian et al., 1981)

Rock Type	**Density (kg/km^3)**	**Heat Capacity (J/kg°C)**
Shale	2.35E+12	1046.03
Sandstone	2.30E+12	920.48
Limestone	2.60E+12	830
Dolomite	2.90E+12	920

We determined rock volume from oil and gas well data. About 53,000 wells (Figure 1) were compiled from the Nebraska Oil and Gas Conservation Commission and Dr. Paul Morgan of the Colorado Geological Survey. Prior work regarding a correction scheme based on equilibrium data was re-evaluated with the availability of new data (Crowell and Gosnold, 2012). A new correction scheme based on the new, deeper data that were more representative of the entire basin was found to be similar to the Harrison correction, indicating that the Harrison is the appropriate correction to use for this basin.

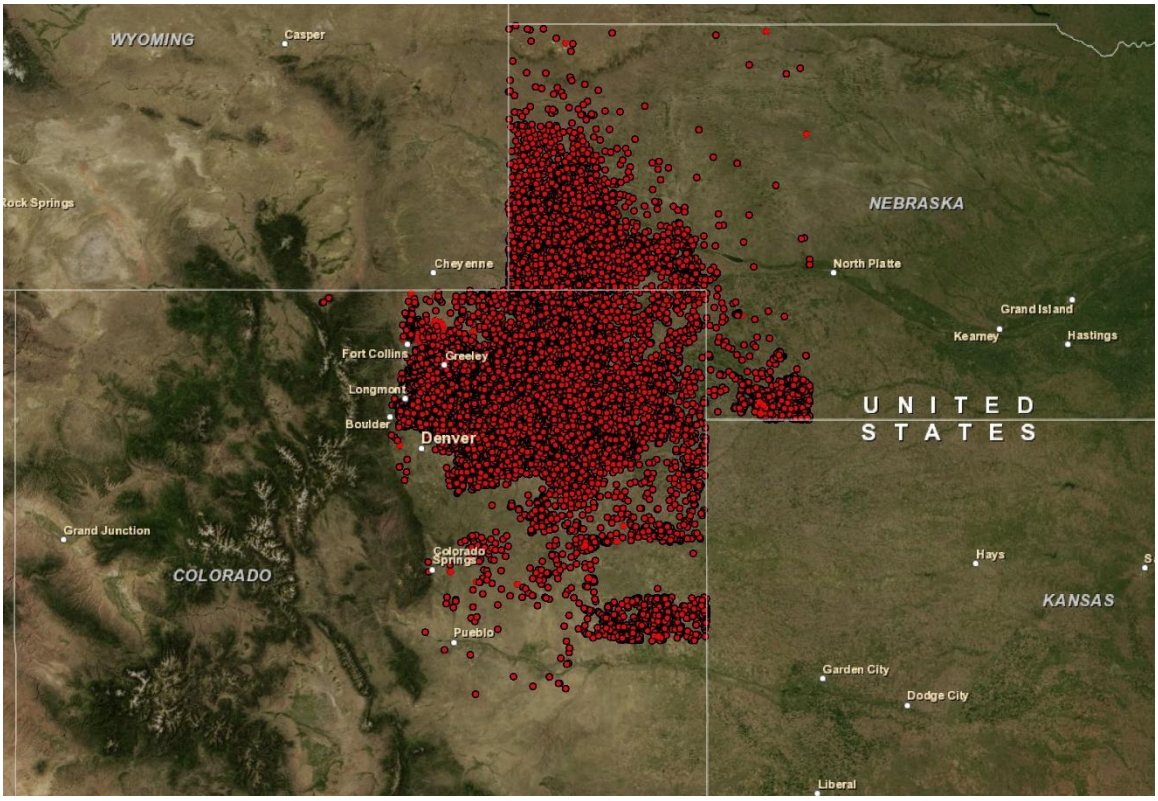

Figure 1. Location of Denver Basin wells with BHT data.

Formation names vary across state lines; therefore, formations were correlated and grouped by geochronological unit. The standard deviation was computed and values outside of two sigma were eliminated, which resulted in the deletion of approximately 2,000 wells of the 53,000 well dataset. The prepared spreadsheets were imported into a

file geodatabase within ArcGIS, each geochronological data set was interpolated with the kriging method, and the resulting raster was classified manually into ten classes representing temperature ranges of 90+, 100+, 110+, 120+, 130+, 140+, etc. up to 180 (Figure 2). The temperature rasters were reclassified into integer units and converted into polygon form to obtain surface areas of the appropriate temperatures (Figure 3). The lower limit of 90° C was determined from the MIT report, "The Future of Geothermal Energy," by Tester et al. (2006), where it is stated that with current technology, using temperatures below 90° C is infeasible for economic power production.

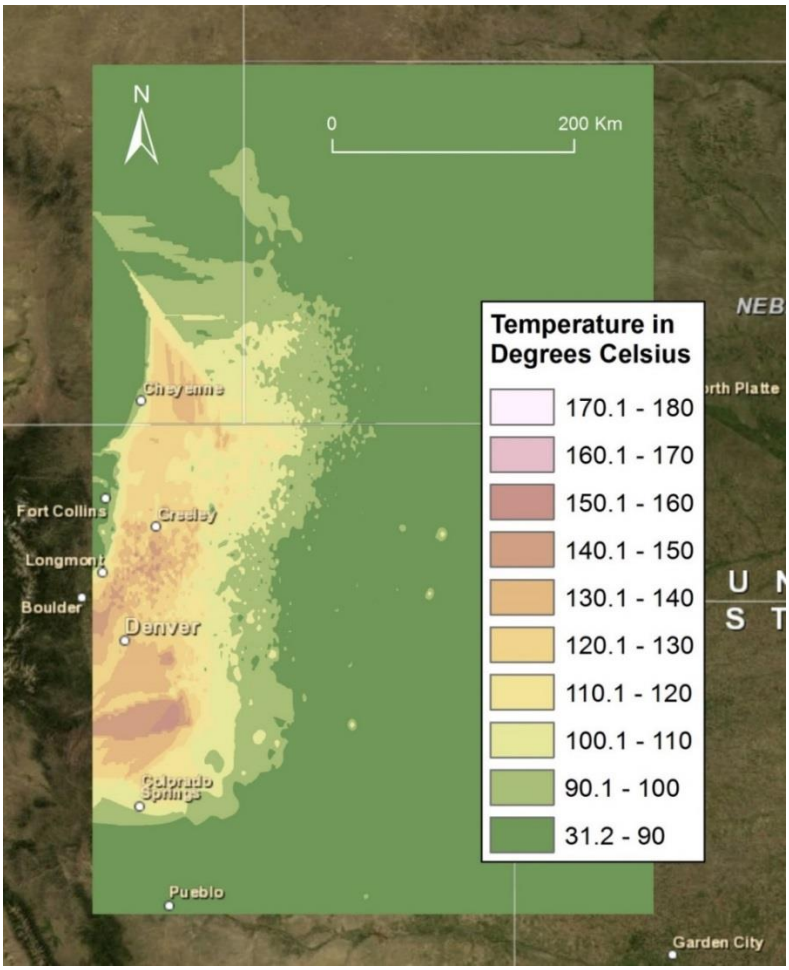

Figure 2. Interpolation (kriging method) of the Lower Cretaceous wells, manually classified according to temperature range.

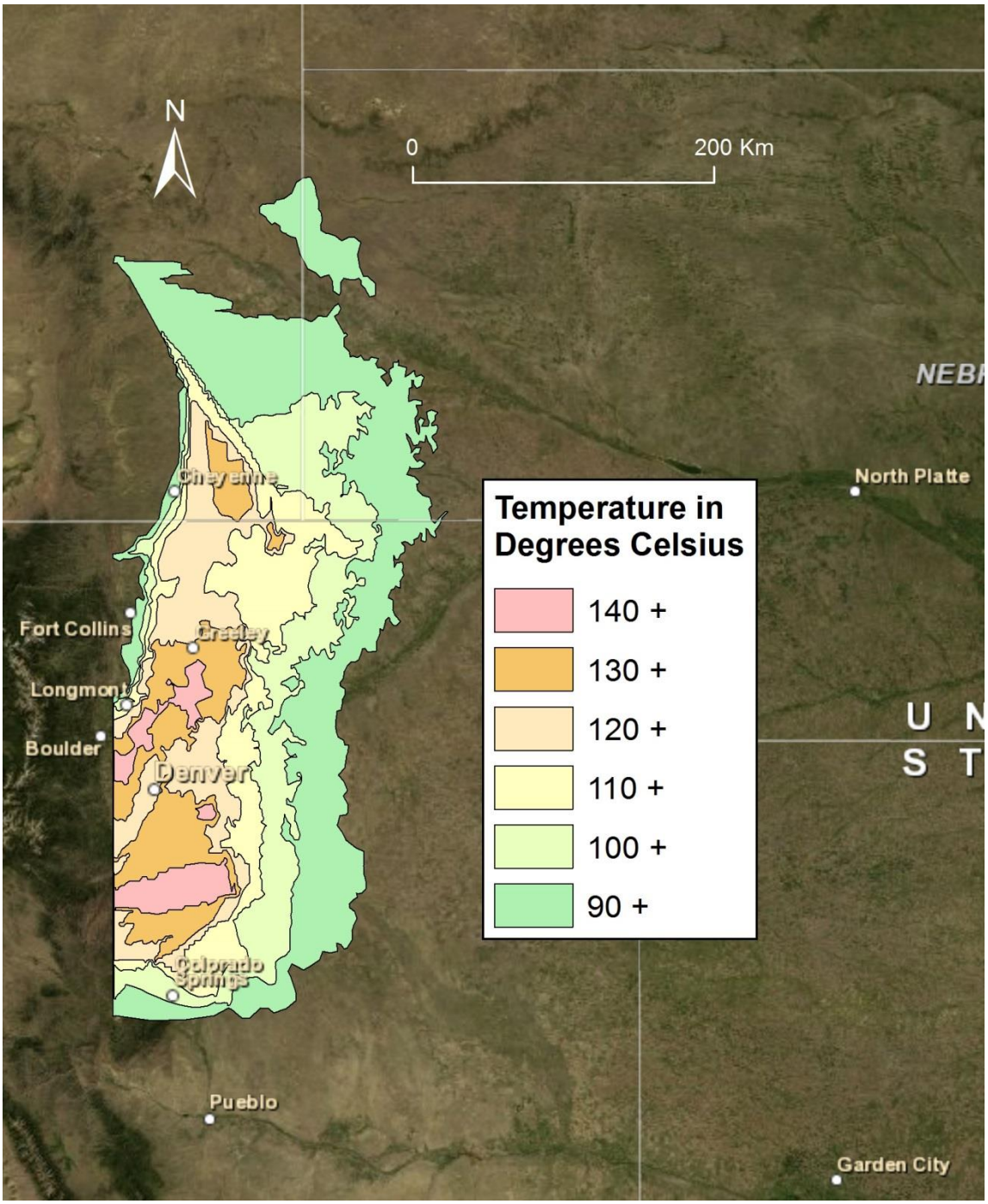

Figure 3. Area polygons created from the reclassified temperature raster.

Statistical sampling of well depth determined average geochronological unit thickness. Five percent of the wells from each unit, both top to bottom and with an even surface distribution, were analyzed point to point. The thickness at each point was

weighted and averaged. The result was multiplied by area, and volumes were calculated for each unit.

We determined the change in temperature by sorting the wells within each geochronological unit by temperature range and calculating average temperature. The mean annual temperature of Colorado is approximately 9.8° C; therefore, our ΔT was determined by subtracting 40 from each average temperature to obtain the difference. "Methods for Assessing Low-Temperature Geothermal Resources," (Sorey, 1982) analyzes appropriate well spacing, drawdown, temperature, structure, size, time, and transmissivity variables. A structure the size and type of the Denver Basin has a recovery factor of 0.001 per year.

Results

Tables 2-8 show the area, volume, average depth, average temperature, assumed ΔT, the thermal energy in place after the recovery rate is taken into consideration in Joules, and the amount that translates to in Megawatts Thermal (MWt). Values for density and heat capacity used can be found in Table 1.

Table 2 – Upper Cretaceous, average unit thickness 0.278 km.

Area (km^2)	**Volume (km^3)**	**Average Depth (km)**	**Average Temperature (°C)**	**ΔT (°C)**	**Recoverable (J)**	**in MWt**
15,773.36	4,384.99	2.12	107.71	67.71	$7.30x10^{17}$	$2.03x10^{8}$
8,190.99	2,277.10	2.13	109.39	69.39	$3.88x10^{17}$	$1.08x10^{8}$
2,312.52	642.88	2.18	115.2	75.2	$1.19x10^{17}$	$3.30x10^{7}$
273.28	75.97	2.2	126.97	86.97	$1.62x10^{16}$	$4.52x10^{6}$
3.92	1.09	2.21	137.78	97.78	$2.62x10^{14}$	$7.28x10^{4}$

Table 3. Lower Cretaceous, average unit thickness 0.485 km.

Temp (°C)	Area (km^2)	Volume (km^3)	Average Depth (km)	Average Temperature (°C)	ΔT (°C)	Recoverable (J)
90+	31,660.00	15,355.10	2.09	107.45	67.45	$2.19x10^{18}$
100+	18,113.88	8,785.23	2.27	114.43	74.43	$1.38x10^{18}$
110+	4,716.80	2,287.65	2.39	118.95	78.95	$3.82x10^{17}$
120+	1,182.80	573.66	2.43	125.85	85.85	$1.04x10^{17}$
130+	70.71	34.29	2.44	138.88	98.88	$7.18x10^{15}$

Table 4. Jurassic, average unit thickness 0.107 km.

Temp (°C)	Area (km^2)	Volume (km^3)	Average Depth (km)	Average Temperature (°C)	ΔT (°C)	Recoverable (J)	in MWt
90+	29,413.99	3,147.30	2.27	109.65	69.65	$4.64x10^{17}$	$1.29x10^{8}$
100+	13,898.03	1,487.09	2.35	113.88	73.88	$2.33x10^{17}$	$6.47x10^{7}$
110+	7,373.59	788.97	2.41	117.9	77.9	$1.30x10^{17}$	$3.62x10^{7}$
120+	490.45	52.48	2.49	125.65	85.65	$9.52x10^{15}$	$2.65x10^{6}$

Table 5. Permian, average unit thickness 0.346 km.

Temp (°C)	Area (km^2)	Volume (km^3)	Average Depth (km)	Average Temperature (°C)	ΔT (°C)	Recoverable (J)	in MWt
90+	47,539.43	16,448.64	2.53	109.28	69.28	$2.41x10^{18}$	$6.71x10^{8}$
100+	24,871.64	8,605.59	2.62	112.06	72.06	$1.31x10^{18}$	$3.65x10^{8}$
110+	8,311.67	2,875.84	2.67	117.81	77.81	$4.74x10^{17}$	$1.32x10^{8}$
120+	731.21	253	2.74	126.4	86.4	$4.63x10^{16}$	$1.29x10^{7}$

Table 6. Pennsylvanian, average unit thickness 0.560 km.

Temp (°C)	Area (km^2)	Volume (km^3)	Average Depth (km)	Average Temperature (°C)	ΔT (°C)	Recoverable (J)	in MWt
90+	90,230.49	50,529.07	2.26	102.93	62.93	$6.73x10^{18}$	$1.87x10^{9}$
100+	44,560.55	24,953.91	2.42	109.41	69.41	$3.67x10^{18}$	$1.02x10^{9}$
110+	23,912.79	13,391.16	2.53	122.28	82.28	$2.33x10^{18}$	$6.48x10^{8}$
120+	8,229.94	4,608.77	2.65	132.65	92.65	$9.04x10^{17}$	$2.51x10^{8}$
130+	2,004.70	1,122.63	2.78	135.98	95.98	$2.28x10^{17}$	$6.34x10^{7}$
140+	17	9.52	3.09	143.49	103.5	$2.09x10^{15}$	$5.80x10^{5}$

Table 7. Mississippian, average unit thickness 0.129 km.

Temp (°C)	Area (km^2)	Volume (km^3)	Average Depth (km)	Average Temperature (°C)	ΔT (°C)	Recoverable (J)	in MWt
90+	73,509.15	9,482.68	2.15	95.91	55.9	$1.12x10^{18}$	$3.12x10^{8}$
100+	44,656.60	5,760.70	2.23	104.58	64.6	$7.88x10^{17}$	$2.19x10^{8}$
110+	76	9.8	2.42	110.41	70.4	$1.46x10^{15}$	$4.06x10^{5}$

Table 8. Ordovician, average unit thickness 0.013 km.

Temp (°C)	Area (km^2)	Volume (km^3)	Average Depth (km)	Average Temperature (°C)	ΔT (°C)	Recoverable (J)	in MWt
90+	54,476.96	9,907.82	2.09	98.96	58.96	$1.24x10^{18}$	$3.44x10^{8}$
100+	31,953.68	2,901.75	2.39	102.14	62.14	$3.82x10^{17}$	$1.06x10^{8}$

Conclusion

The area from Denver to Greeley appears to have the best geothermal potential in the Denver Basin, as indicated by the interpolated temperature rasters. This is also the location of the primary population centers in the state of Colorado, and as such has access to necessary infrastructure. The thermal energy in place for the Denver basin is listed in Table 9, below.

Table 9. Total thermal energy in place by temperature range, and translated to Megawatts Thermal and number of homes that amount of energy can theoretically power.

Temp. Range (°C)	**Recoverable (J)**	**In MWt**	**After Efficiency (12%) (MWe)**	**# Homes Powered**
90 +	$1.49x10^{19}$	$4.14x10^{9}$	$4.97x10^{8}$	$2.49x10^{11}$
100 +	$8.15x10^{18}$	$2.27x10^{9}$	$2.72x10^{8}$	$1.36x10^{11}$
110 +	$3.44x10^{18}$	$9.56x10^{8}$	$1.15x10^{8}$	$5.74x10^{10}$
120 +	$1.08x10^{18}$	$3.00x10^{8}$	$3.60x10^{7}$	$1.80x10^{10}$
130 +	$2.35x10^{17}$	$6.53x10^{7}$	$7.84x10^{6}$	$3.92x10^{9}$
140 +	$2.09x10^{15}$	$5.81x10^{5}$	$6.97x10^{4}$	$3.49x10^{7}$

References

Crowell, A. M., A.T. Ochsner, and W.D. Gosnold, 2012. "Correcting Bottom-Hole Temperatures in the Denver Basin: Colorado and Nebraska", Geothermal Resources Council Transactions, v. 36, p. 201-206.

Martin, C., 1965. "Denver Basin", Bulletin of the American Association of Petroleum Geologists, v. 49, Number 11, p. 1908-1925.

Morgan, P., February 2012. Personal Communication, Colorado Geological Survey, Interviewer: Anna M. Crowell.

Nebraska Oil and Gas Conservation Commission, http://www.nogcc.ne.gov/, Accessed 5/1/2013.

NOAA, National Oceanic and Atmospheric Association, http://www.climate.gov/#climateWatch, accessed 5/1/2013.

Sorey, M.L., M. Nathenson, and C. Smith, 1982. "Methods for Assessing Low-Temperature Geothermal Resources." ***in*** Reed, M.J., ed., Assessment of Low-temperature Geothermal Resources of the United States -1982: U.S. Geological Survey Circular 892, p. 17-29.

Tester J.W., et. al., 2006. "MIT: The Future of Geothermal Energy. Impact of Enhanced Geothermal Systems [EGS] on the United States in the 21st Century," Massachusetts Institute of Technology.

Touloukian, Y.S., W.R. Judd, and R.F. Roy, 1981. "Physical Properties of Rocks and Minerals," Mc-Graw-Hill/CINDAS data series on material properties, v. II-2, Purdue Research Foundation.

CHAPTER V

ENERGY-IN-PLACE ESTIMATES FOR THE ILLINOIS AND MICHIGAN BASINS

Table of Contents

List of Figures 56

List of Tables 57

Introduction 58

Geothermal Resource Assessment of the Michigan and Illinois Basins: How Deep is Too Deep? 59

- Abstract 59
- Introduction 59
- Methods 60
- Results 65
- Conclusions 66
- References 68

List of Figures

Figure		Page
1a	Graph of Energy in Place for the Michigan Basin	58
1	Spatial extent of bottom-hole temperatures in the Illinois basin	60
2	Spatial extent of bottom-hole temperatures in the Michigan basin	61
3	BHT interpolation for the 3000-3500 meter interval	63
4	BHT interpolation for the 3500-4000 meter interval	64

List of Tables

Table		Page
1	Heat capacity and density of dominant rock types	62
2	Parameters and available heat in place for the 3000-3500 meter depth interval in the Michigan basin	65
3	Parameters and available heat in place for the 3500-4000 meter depth interval in the Michigan basin	66
4	Final estimate of energy in place, after recovery factor and taking power plant efficiency into account, along with estimated number of homes powered	66

Introduction

Crowell and Gosnold, 2014, was published in the Transactions of the Geothermal Resources Council in Volume 38, pages 27-29.

Although the datasets for the Michigan and Illinois Basins did not contain formation information, the geostatistical analysis in Chapter III determined that using depth was an accurate way to create data subsets. Therefore, the energy-in-place for the Michigan and Illinois Basins was completed comparable to the Denver Basin estimate in Chapter 4. Because only one BHT measurement in Illinois was greater than 100 °C, insufficient data existed to give an estimate for the Illinois Basin.

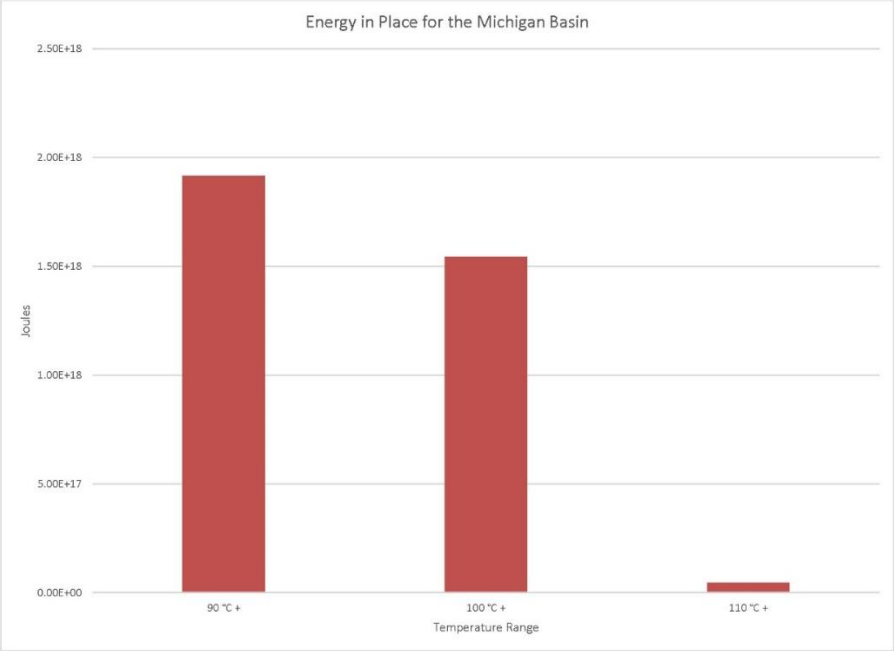

Figure 1a. Graph of Energy in Place for the Michigan Basin.

Geothermal Resource Assessment of the Michigan and Illinois Basins: How Deep is Too Deep?

Anna M. Crowell and Will Gosnold
UND Geothermal Laboratory
Harold Hamm School of Geology and Geological Engineering
University of North Dakota

Keywords: Co-produced, geothermal, energy, ArcGIS, Michigan Basin, Illinois Basin, sedimentary basin

Abstract

There is general acceptance in the geothermal community that sedimentary basins east of the Mississippi River are too cold to sustain large scale geothermal power production. The question, then, becomes, "How deep is too deep when considering feasible thermal formation waters?" The Michigan and Illinois basins have been evaluated to determine if any formation waters of sufficient temperature exist, where they may be found, and how much energy in place exists for potential power prospecting.

Introduction

Tester et al. (2006) asserted that geothermal power production can be achievable with formation waters as low as 90°C. With the current state-of-the art technology and depending on local conditions that affect the change in temperature (ΔT), this is certainly possible even with lower temperatures such as those found in Chena Hot Springs (Aneke et al., 2011). Deep sedimentary basins west of the Mississippi River have a large surface area with substantially thermal formation waters, but these conditions are lacking in basins east of the Mississippi River. Are temperatures of at least 90°C found in the Illinois and Michigan basins? How deep are these formations? How much energy is in place? Can we economically provide power from them?

Methods

Bottom-hole temperatures (spatial extent of data shown in Figures 1 and 2) were obtained from the National Geothermal Data System (NGDS) and were imported into a 'file geodatabase' with ArcGIS. These datasets include 6,184 wells within the Illinois basin and 11,833 wells within the Michigan basin. No temperature corrections were included with the datasets, thus corrections were done using the Harrison method (Harrison et al., 2006).

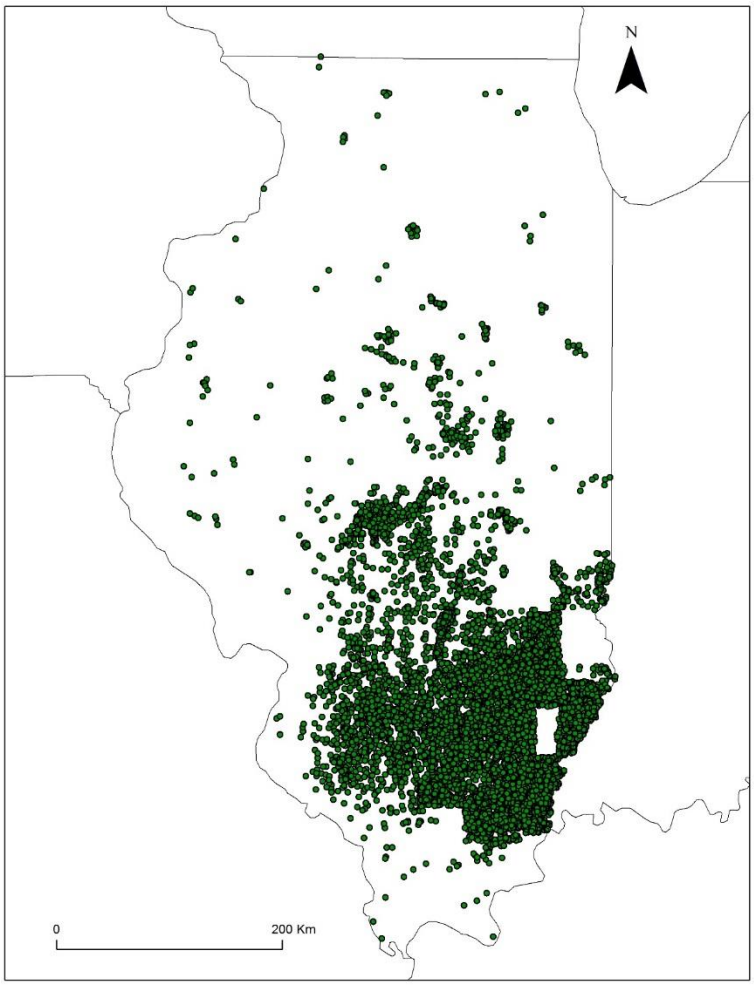

Figure 1.Spatial extent of bottom-hole temperatures in the Illinois basin.

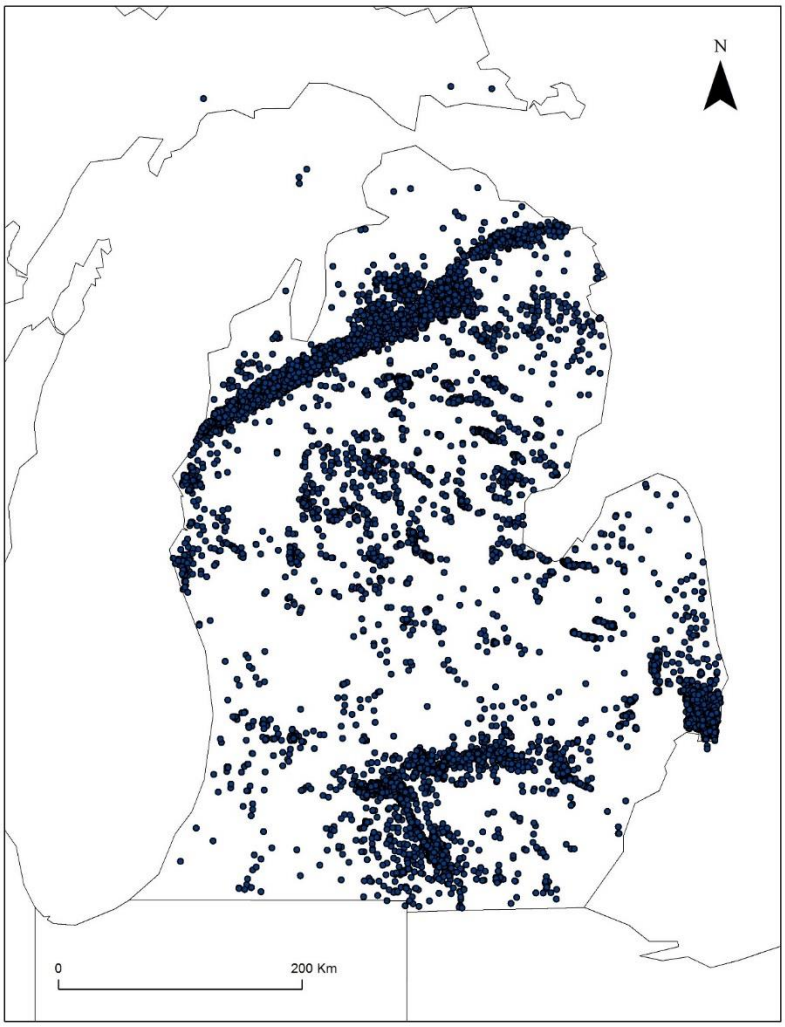

Figure 2. Spatial extent of bottom-hole temperatures in the Michigan basin.

The available heat equation, as used by Brook et al. (1978), is:

$$\boldsymbol{Q = \rho\, Cp\, V\, \Delta T}.$$

In this equation, the heat in place (Q) is equal to the density of the rock (ρ) times the heat capacity of the rock (Cp), the volume of the rock in question (V), and the change in temperature (ΔT). To determine the heat capacity and density of rocks common to sedimentary basins, we looked up the values for shale, sandstone, limestone, and

dolomite in, “Physical Properties of Rocks and Minerals,” by Touloukian et al. (1981). The values we considered are listed in Table 1.

Table 1. Heat capacity and density of dominant rock types. (Touloukian et al., 1981)

Rock Type	**Density (kg/km^3)**	**Heat Capacity (J/kg°C)**
Shale	2.35E+12	1046.03
Sandstone	2.30E+12	920.48
Limestone	2.60E+12	830
Dolomite	2.90E+12	920

Most of the records did not have formation data associated with them, so we parsed wells out based on 500 meter intervals and analyzed those wells that were 1000m to 4500m in depth. Each of these units were interpolated using the Inverse Distance Weighting (IDW) Method (Figures 3 and 4) and classified manually into 10 degree intervals, with the first break at 90°C, and going up to 150°C. This classification scheme was chosen to be comparable to work done by Crowell and Gosnold in the Denver and Williston Basins (Crowell et al., 2011; Crowell and Gosnold, 2012). We reclassified the interpolation rasters into 90°C+, 100°C+, 110°C+, and 120°C+ temperature intervals and converted the reclassified rasters into polygons, which we dissolved on reclassified values. Using the feature measurement tool in ArcGIS, we obtained polygon areas in square kilometers (km^2). The surface areas from the 90°C+, 100°C+, 110°C+, and 120°C+ intervals were multiplied with the 0.5 kilometer (km) thicknesses, and volumes calculated. The last parameter needed for the heat in place equation was the change in temperature. Michigan is a northern tier state, so it is reasonable to assume that with air cooling, a ΔT of 40°C can be used.

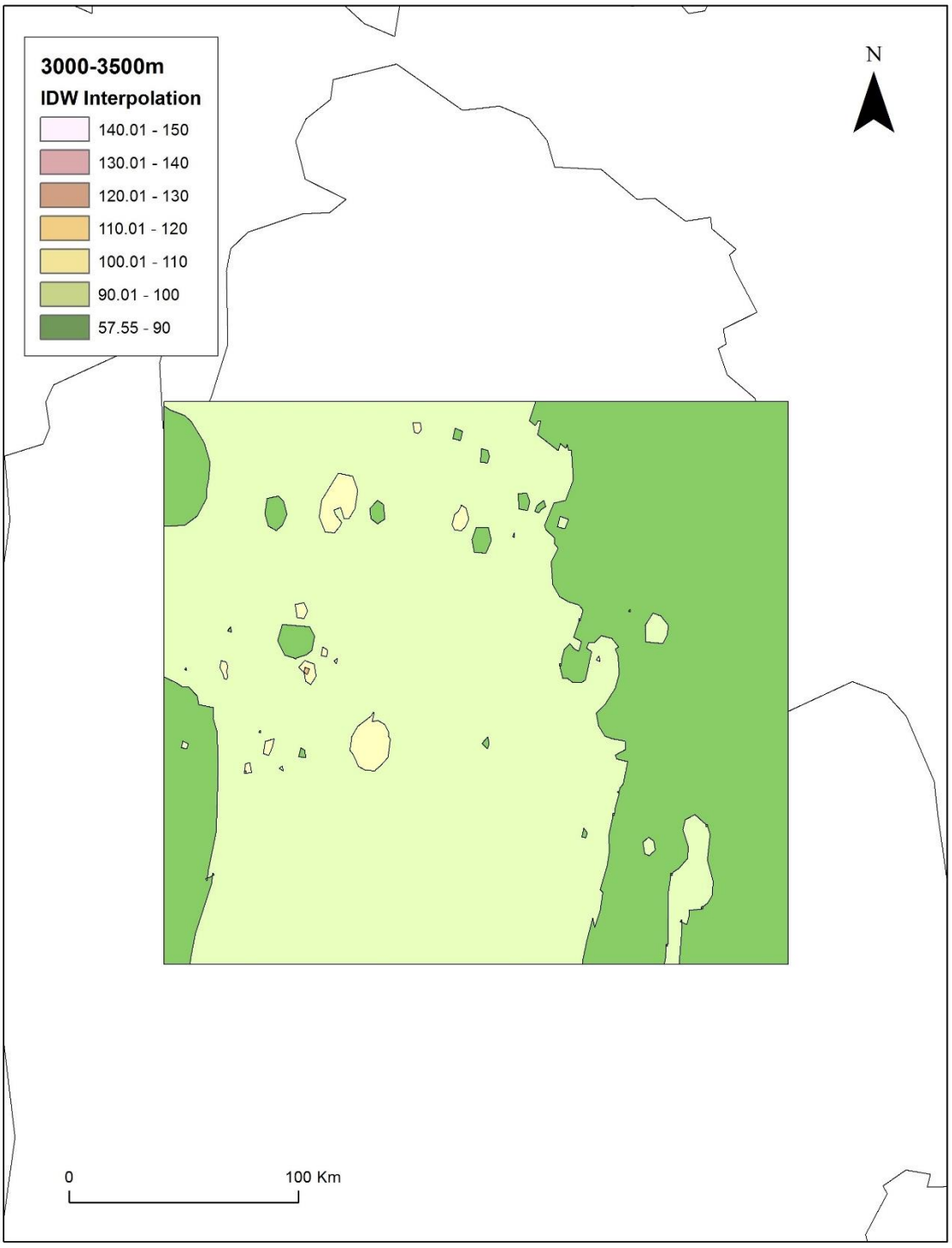

Figure 3. BHT interpolation for the 3000-3500 meter interval.

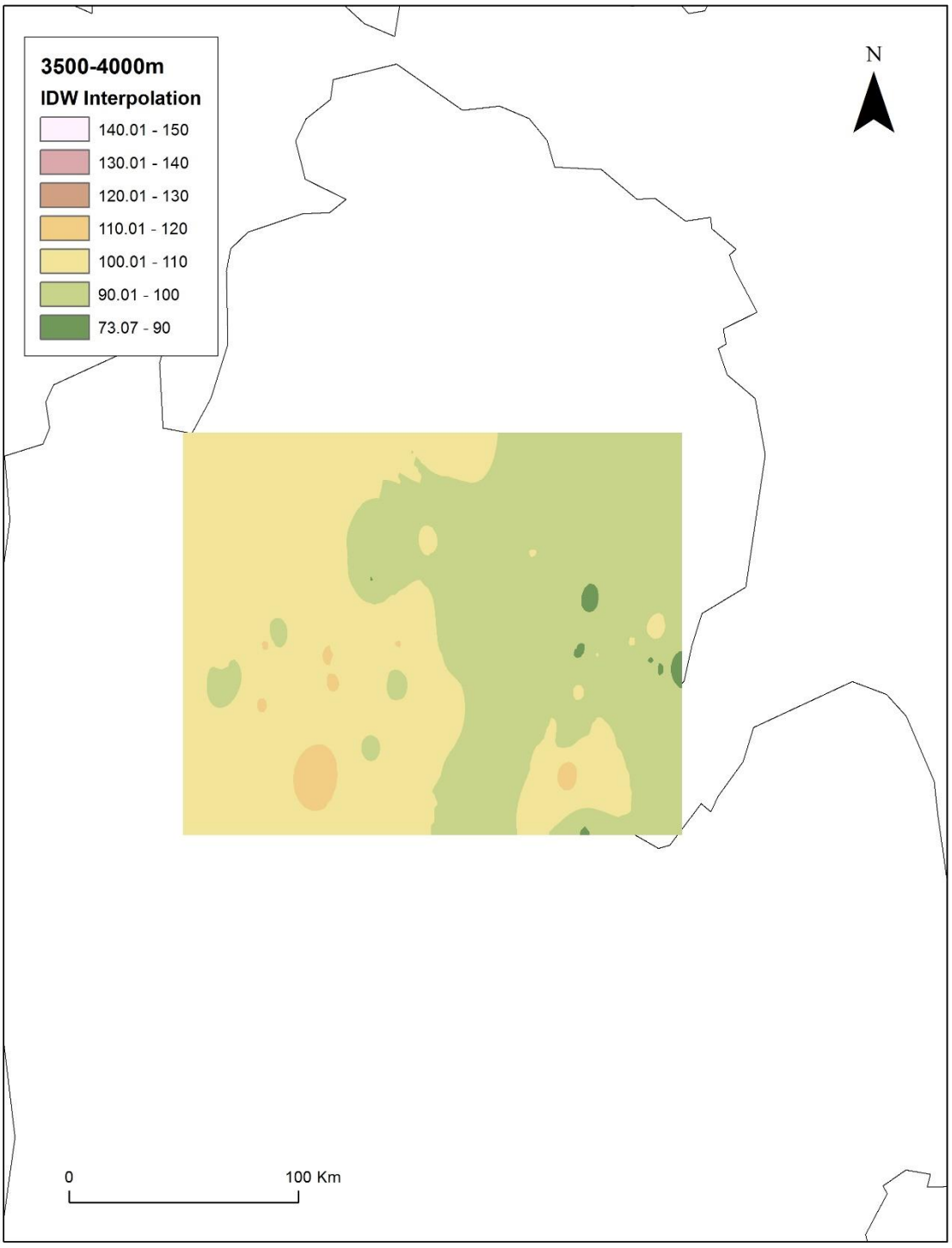

Figure 4. BHT interpolation for the 3500-4000 meter interval.

Results

The Illinois basin only has one temperature recorded over 90°C out of the 6,184 wells. The temperatures, therefore, do not fit within the scope of this study and the basin was discarded as a candidate for large-scale geothermal power production.

The Michigan basin has temperatures over 90°C below a depth of 3000 meters. A total of 172 wells were analyzed in the 3000-4000 meter depth interval. The 3000-3500 meter interval has a minimum temperature of 57.5°C, a maximum temperature of 115.3°C, and a mean temperature of 92.6°C with a standard deviation of ±7°C. The 3500-4000 meter interval has a minimum temperature of 90.3°C, a maximum temperature of 117.4°C, and a mean temperature of 109.9°C with a standard deviation of 10.1°C. The available energy in place for each depth interval is listed in Tables 2 and 3. The recovery factor of 0.001 was determined by Sorey et al., (1982) when they looked at well spacing, well drawdown, and how much water and energy could be extracted without depleting the resource over a thirty-year period. It is important to remember that the recovery rate as defined by Sorey et al. (1982) is not a guarantee of energy extraction, but is more accurately described as a ***sustainable*** extraction rate.

Table 2. Parameters and available heat in place for the 3000-3500 meter depth interval in the Michigan basin.

Temp. Interval	**Area (km^2)**	**Volume (km^3)**	**Average Temp. (°C)**	**ΔT**	**Q (J)**	**Recoverable (J)**	**MWt**
90°C +	41,323.39	20,661.70	92.6	52.6	$23{,}000 \times 10^{17}$	$23{,}000 \times 10^{14}$	$64{,}000 \times 10^{4}$
100°C +	770.09	385.05	92.6	52.6	430×10^{17}	430×10^{14}	$1{,}200 \times 10^{4}$
110°C +	4.46	2.23	92.6	52.6	2.5×10^{17}	2.5×10^{14}	6.9×10^{4}

Table 3. Parameters and available heat in place for the 3500-4000 meter depth interval in the Michigan basin.

Temp. Interval	Area (km^2)	Volume (km^3)	Average Temp. (°C)	ΔT	Q (J)	Recoverable (J)	MWt
90°C +	18,090.85	9,045.43	109.9	69.9	130×10^{19}	130×10^{16}	37×10^{7}
100°C +	19,239.72	9,619.86	109.9	69.9	140×10^{19}	140×10^{16}	39×10^{7}
110°C +	605.46	302.73	109.9	69.9	4.5×10^{19}	4.5×10^{16}	1.3×10^{7}

Conclusions

Although no temperatures suitable for large-scale power production have been found in the Illinois basin, future work for other geothermal uses, such as district heating and direct use, may be worthwhile. The calculation of heat flow points and projection to isotherms would be especially valuable to determine how deep formations of interest would be.

The Michigan basin has limited potential for large-scale power production. The 90° C isotherm only begins to appear at a depth of 3000 meters, which is infeasible for economic power production with current technology. The energy summary, along with the estimate after passing the fluid through a binary Organic Rankin Cycle with an efficiency of 12% and the number of homes possibly powered can be found in Table 4.

Table 4. Final estimate of energy in place, after recovery factor and taking power plant efficiency into account, along with estimated number of homes powered.

Temp. Range (°C)	Recoverable (J)	In MWt	After Efficiency (12%) (MWt)	# Homes Powered
90°C	370×10^{16}	110×10^{7}	123×10^{6}	61,716,000,000
100°C	150×10^{16}	42×10^{7}	50×10^{6}	25,020,000,000
110°C	4.5×10^{16}	1.3×10^{7}	1.5×10^{6}	750,600,000

Even though the appropriate isotherm is too deep to produce economically with current technology, and taking into account that the available energy in place is approximately $1/5^{th}$ that of a large, deep, hot basin such as the Denver-Julesberg (Crowell and Gosnold, 2013), an estimated 61 trillion homes can potentially be powered if technology evolves to that level. An estimate by the US Census bureau states that the number of homes in the United States as of 2010 is 80 million (U.S. Census Bureau, 2010). If only a fraction of the energy can be produced, we can still greatly offset fossil fuel usage

References

Aneke, M., Agnew, B., and C. Underwood, 2011. "Performance Analysis of the Chena Binary Geothermal Power Plant", Applied Thermal Engineering, v. 3, p. 1825-1832.

Brook, C. A., Mariner, R. H., Mabey, D. R., Swanson, J. R., Guffanti, M., and L. J. P. Muffler, 1978. "Hydrothermal Convection Systems with Reservoir Temperatures ≥ 90°C," *in* Assessment of Geothermal Resources of the United States – 1978, United States Geological Survey Circular 790, p. 18-43.

Crowell, A. M., and W.D. Gosnold, 2013. "GIS-Based Geothermal Resource Assessment of the Denver Basin: Colorado and Nebraska," Geothermal Resources Council Transactions, v. 37, p. 941-943.

Crowell, A. M., Klenner, R., and W.D. Gosnold, 2011. "GIS Analysis for the Volumes, and Available Energy of Selected Reservoirs: Williston Basin, North Dakota," Geothermal Resources Council Transactions, v. 35, p. 1557-1561.

Harrison W. E., Luza, K.V., Prater, M. L., and Chueng, P. K., 1983. "Geothermal resource assessment of Oklahoma," Oklahoma Geological Survey, Special Publication 83-1.

Sorey, M.L., Nathenson, M., and C. Smith, 1982. "Methods for Assessing Low-Temperature Geothermal Resources." ***in*** Reed, M.J., ed., Assessment of Low-temperature Geothermal Resources of the United States -1982: U.S. Geological Survey Circular 892, p. 17-29.

Tester J.W., et. al., 2006. "MIT: The Future of Geothermal Energy. Impact of Enhanced Geothermal Systems [EGS] on the United States in the 21st Century," Massachusetts Institute of Technology.

Touloukian, Y.S., Judd, W. R., and R.F. Roy, 1981. "Physical Properties of Rocks and Minerals," Mc-Graw-Hill/CINDAS data series on material properties, v. II-2, Purdue Research Foundation.

U.S. Census Bureau, 2010. Current Population Reports: Projections of the Number of Households and Families in the United States: 1995 to 2010, P25-1129.

CHAPTER VI

PLAY FAIRWAY ANALYSIS

Table of Contents

List of Figures 70

List of Tables 72

Introduction 73

Integrating Geophysical Data in GIS for Geothermal Power Prospecting 74

- Abstract 74
- Introduction 75
- Methods 76
- Discussion 84
  - The Denver Basin 84
  - The Illinois Basin 87
  - The Michigan Basin 89
  - The Williston Basin 91
- Results 94
- Conclusions 95
- Sources Cited 102

List of Figures

Figure		Page
1	Spatial extent of temperature data in the Denver-Julesberg basin, obtained from the NDGS	78
2	Example of one of the interpolation layers in the Denver-Julesberg Basin.	79
3	Example of the geothermal gradient interpolation layer for the Denver basin against the DEM backdrop	80
4	An example of a magnetic intensity interpolation for the state of Colorado	81
5	An example of a Bouger gravity anomaly interpolation for the state of Colorado.	82
6	Slope calculated from the Digital Elevation Model (DEM) for the State of Colorado	83
7	The areas of high geothermal gradient in the Denver basin are plotted against a surface geology map of Colorado	85
8	Areas of high geothermal gradient in the Denver Basin against the DEM for the state of Colorado	86
9	The magnetic intensity interpolation with areas of high geothermal gradient	86
10	A lower gravity anomaly running along the base of the Front Range correlates to the high geothermal gradient just west of the city of Denver	87
11	The areas of high geothermal gradient in the Illinois basin are plotted against a surface geology map of Illinois	88
12	Areas of high geothermal gradient in the Illinois Basin against the DEM for the state of Illinois	89
13	The magnetic intensity interpolation in the Illinois Basin with areas of high geothermal gradient	90
14	Three of the five areas of interest in the Illinois Basin have high gravity anomalies, indicating possible intrusive ferromagnesian bodies or dense crystalline rocks	91

15 The areas of high geothermal gradient in the Michigan basin are plotted against a surface geology map of Michigan 92

16 Comparing the DEM to the areas of interest in the Michigan Basin shows area of possibly higher slope and quite a few rivers, which is, again, an environmental concern for geothermal development 93

17 Magnetic intensity for areas of interest in the Michigan Basin appear to be average, which would be expected for a cratonic basin with no recent sedimentation 93

18 The Keweenawan rift is clearly visible in the gravity anomaly interpolation of the Michigan Basin 94

19 The areas of high geothermal gradient in the Williston basin are plotted against a surface geology map of North Dakota.....95

20 The DEMs for North Dakota and the Williston Basin show very little, as in the Illinois Basin, except where major rivers are present 96

21 Analysis of the Magnetic Intensity interpolation for the Williston Basin and North Dakota indicates nearly no magnetite, and therefore thick sediments with few mafic intrusions 96

22 Both the Magnetic and Gravity interpolations show the mafic tube-shaped intrusion in the North Central part of the state 97

23 Final Play Fairway Map for Colorado 98

24 Final Play Fairway Map for Illinois.....99

25 Final Play Fairway Map for Michigan.....100

26 Final Play Fairway Map for North Dakota 101

List of Tables

Table Page

1 Table of reclassification breaks used for each layer to normalize the four study locations, based on how desirable the layer value is 83

2 Weighting matrix used in raster algebra 84

Introduction

Crowell and Gosnold, 2015, has been accepted for publication in October 2015 in the Geological Society of America Journal GEOSPHERE. The publication is presented as it was accepted.

Results presented in Chapters II-V were combined to create a *favorability map*, also known in the petroleum industry as a *play fairway analysis*. Using corrected bottom-hole temperatures with calculated geothermal gradient, and ground slope calculated from Digital Elevation Models (DEMs), magnetic intensity, and the size of the Bouger gravity anomaly for the basis of our *play fairway analysis* using *raster algebra*. We combined this raster with an overlay of the other data for each basin to find optimal locations for new geothermal power production projects.

Integrating Geophysical Data in GIS for Geothermal Power Prospecting

Anna Crowell and Will Gosnold

University of North Dakota

Abstract

GIS-based resource assessment is an important and relatively inexpensive tool for identifying areas that are of interest for geothermal power production. Of particular interest is the under-exploited industry of co-produced fluids and low temperature formation waters in oil and gas producing basins. Obtaining bottom-hole temperature (BHT) data is now free and easily accessible due to the efforts of the National Geothermal Data System (NGDS). Oil and gas producing sedimentary basins in Colorado, Illinois, Michigan, and North Dakota contain formation waters of a temperature that is adequate for geothermal power production (90°-150° C) using existing binary power plant technology. While resource assessment gives a broad picture of the energy available in a basin, the problem remains of knowing where a power plant must go, and if it is economically feasible to do so in any given area. The Denver, Illinois, Michigan, and Williston sedimentary basins were evaluated using a Play Fairway Analysis methodology to identify optimum locations for Geothermal Power Production. These regions have been previously assessed for thermal energy in place, and geothermal gradients from that study, along with gravity anomaly information, magnetic intensity, and Digital Elevation Models (DEMs) for slope analysis were incorporated into a geodatabase for map generation. Raster layers were created and then reclassified into nine classes each, with high geothermal gradient, low magnetic intensity, low Bouger

anomaly, and low slope receiving the highest values. The layers were then weighted using a matrix weight assignment similar to that used in the Environmental Protection Agency's DRASTIC water pollution model, and combined with the 'Raster Algebra' tool in ArcGIS. Areas of greatest potential were identified and overlaid on a DEM layer. This shows locations where temperature will be highest at the shallowest depths in regions of soft sediments, refining the map creation process.

Introduction

With increasing public awareness of our reliance on foreign fuels, it has become clear that energy independence is an issue of national security. We also face devastating climate change effects due, in part, to increased greenhouse gas emissions. Fossil fuels also pose other threats to the environment, such as pipeline leaks and oil spills. Geothermal energy, therefore, has the potential to be an important part of our nation's energy portfolio.

Co-produced fluids, the hot water brought to the surface along with oil during the pumping phase, are of special interest as this water is hot enough to flash a secondary working fluid in an Organic Rankine Cycle (ORC) binary power plant. Geothermal power plants built on Enhanced Geothermal System (EGS) reservoirs and using "closed-loop" cycles will produce near-zero carbon dioxide (CO_2) emissions, one of the principal greenhouse gases (GHGs) implicated in global warming (Clark et al., 2012;Tester et al., 2006). In comparison with fossil-fueled, nuclear, or solar electric power plants, EGS plants require much less land area per megawatt (MW) installed or per megawatt hour (MWh) delivered (Tester et al., 2006). The benefits of EGS also apply to low temperature geothermal and co-produced power production where existing wells are

used, mitigating any potential environmental impacts from drilling. Geothermal energy production also has the advantage over other methods of renewable/sustainable sources in that it can be modulated to be either intermittent or base load, according to demand. Base load power production means that energy is being provided to the infrastructure constantly, as the power-producing energy is always available.

Understanding sedimentary basin structure and the thermal energy contained within is an important first step to producing energy from co-produced and low temperature resources; however, these analyses do little to show a potential producer or investor where appropriate well or plant locations exist. Other considerations that must be taken into account are: how deep is the appropriate reservoir, and how hot are those temperatures expected to be? Are these identified areas crystalline or softer sedimentary rocks, which affect potential drilling costs or extent of the reservoir? Are the sediments dense, which can be related to pore space, possible permeability, or lithology indicators? We propose using geothermal gradient calculated from corrected bottom-hole temperatures in conjunction with, magnetic and gravity data, and digital elevation models as a tool for assessment of heat distribution and to constrain locations where optimal conditions for heat extraction exist.

Methods

Resource assessments have been completed on four sedimentary basins in the mid-continent region: The Michigan and Illinois basins (Crowell and Gosnold, 2014), The Denver-Julesberg Basin (Crowell et al., 2013), and the Williston Basin (Crowell et al., 2011). These previous works have shown that with current technology, geothermal

production in the Michigan and Illinois basins is marginally feasible at best, but with the advent of future technology, power production may become economic.

Bottom-hole temperature data were obtained from the National Geothermal Data System (NGDS), corrected using the Harrison method (Harrison et al., 1983), and imported into ArcGIS. Included in the analysis were 36,861 wells for the Denver-Julesberg basin (some well locations shown in Figure 1), 6,269 wells for the Illinois basin, 9,298 wells for the Michigan basin, and 9,332 wells for the Williston basin. The wells were then sorted according to depth, and interpolation surfaces generated for every 500 meters down the stratigraphic column (Figure 2). This was used for assessment of energy in place, and was kept in the geodatabase for future reference. Geothermal gradients were then calculated using the following formula:

$$\frac{\partial T}{\partial Z} = \frac{(BHT - Surface\ Temperature)}{depth}$$

The average surface temperatures used for each state were obtained from the National Climate Data center, listed as: Colorado at 7.3° C, Illinois at 10.97° C, Michigan at 6.89° C, and North Dakota at 4.68° C. Once calculated, geothermal gradient values for each basin were interpolated using the Kriging method and analyzed for areas in which hotter temperatures could be found at relatively shallow depths (Figure 3).

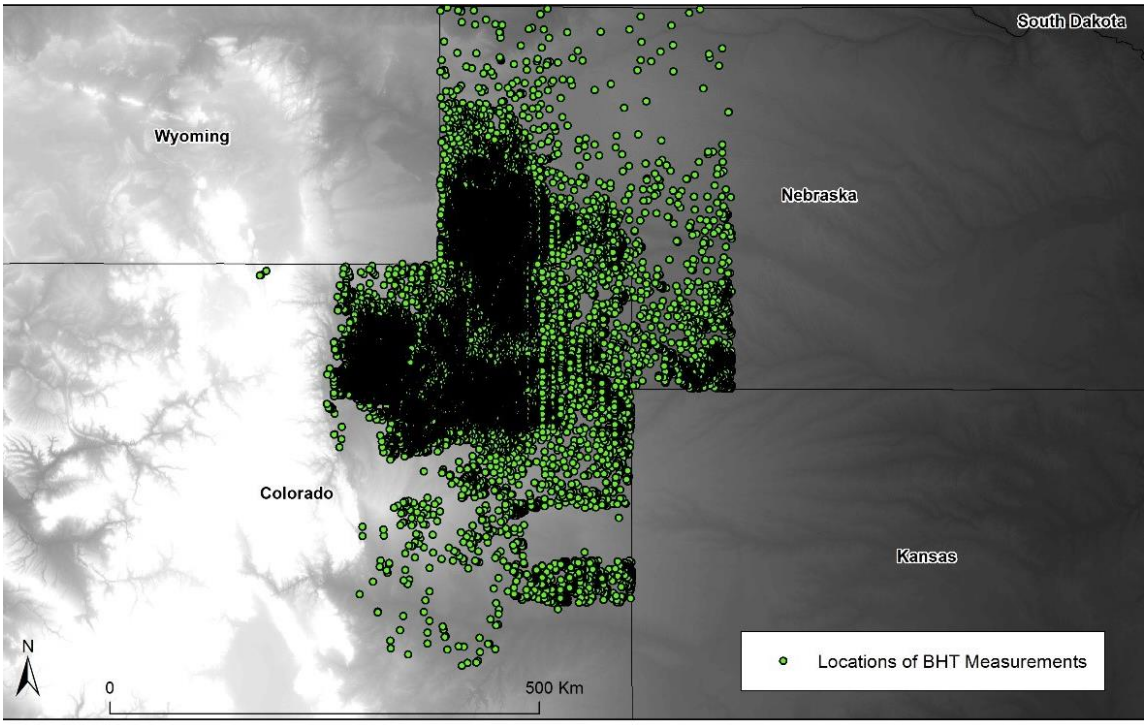

Figure 1. Spatial extent of temperature data in the Denver-Julesberg basin, obtained from the NDGS. The points represent the locations of the 36,861 wells used for bottom-hole temperature and geothermal gradient calculations.

Gravity and magnetic data were obtained from the Gravity and Magnetic Database of the U.S. hosted by the University of Texas, El Paso (University of Texas at El Paso, 2014). The robust dataset included 232,129 magnetic and 46,535 gravity data points for Colorado, 191,079 magnetic and 106,420 gravity data points for Illinois, 376,256 magnetic and 68,092 gravity data points for Michigan, and 172,604 magnetic and 20,933 gravity points for North Dakota. In a gravity survey, low gravity values indicate likely areas of thick sediments, whereas areas of high gravity values indicate denser igneous or metamorphic rocks. High magnetic intensity values indicate rocks containing magnetite, indicating dense mafic rock, whereas low values indicate sediments or granite. Sediments have the lowest magnetic intensity values because little to no mafic

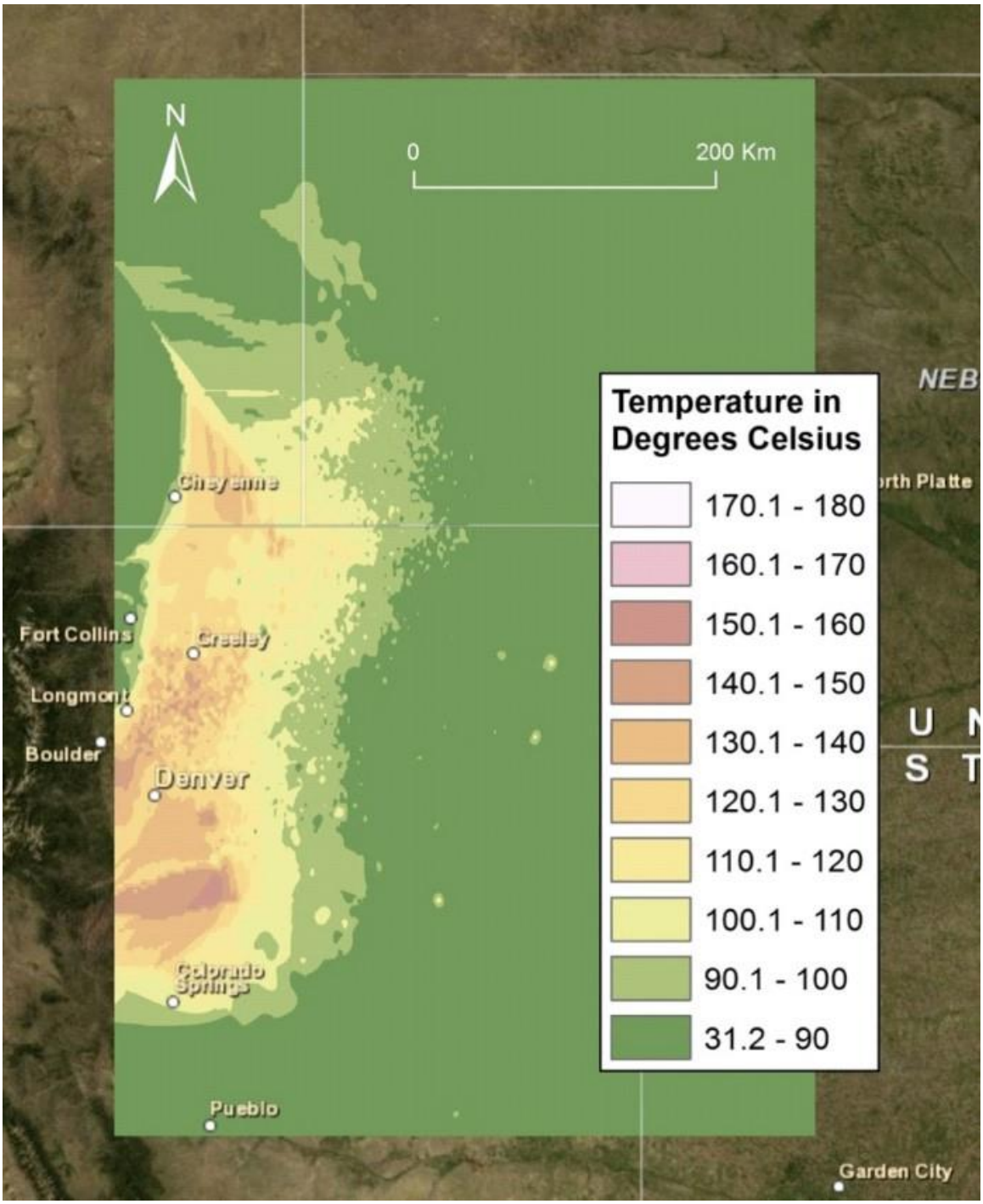

Figure 2. Example of one of the interpolation layers in the Denver-Julesberg Basin. Bottom-hole temperatures at a depth of 2000-2500 meters were interpolated using the kriging method.

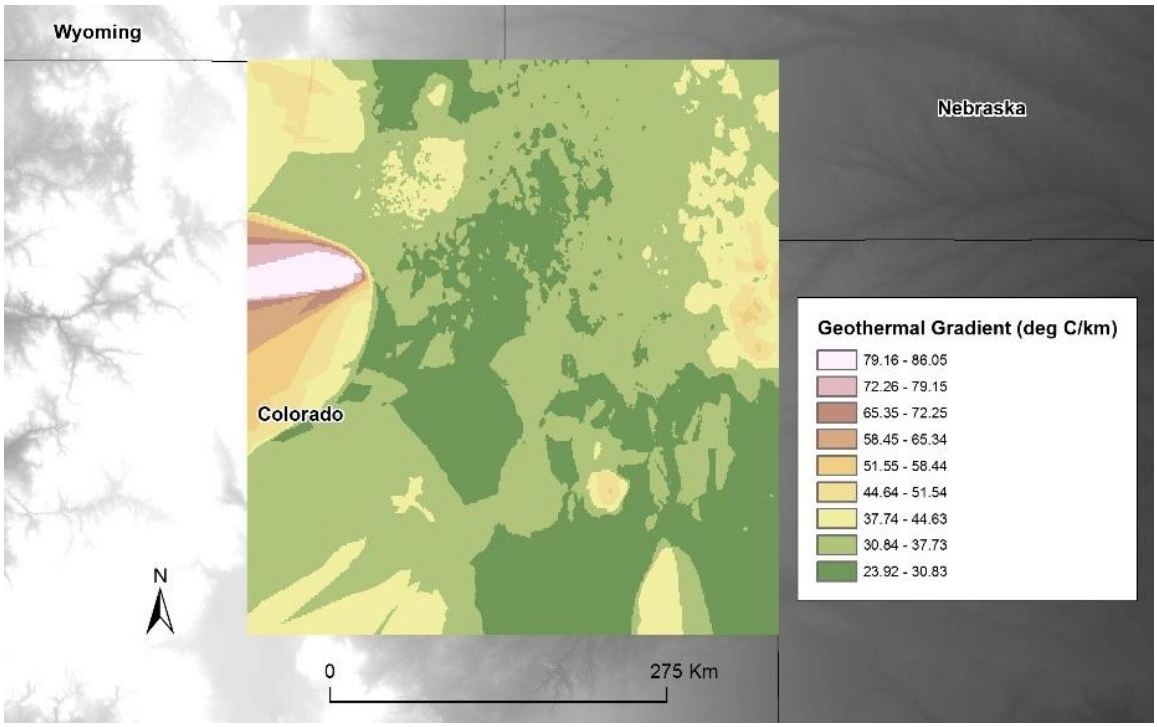

Figure 3. Example of the geothermal gradient interpolation layer for the Denver basin against the DEM backdrop. The geothermal gradients were calculated for each well in the 36,861 point dataset and interpolated using the kriging method.

grains are present. The datasets were added as layers into the ArcGIS geodatabase and interpolated using the Kriging method (Figures 4 and 5). Slope was calculated from Digital Elevation Model (DEM) layers (Figure 6), comprising another geodatabase layer. Slope was considered because while geothermal power plants have a small footprint, attempting to construct a power plant on an area with any significant slope means increased construction costs for levelling the area.

The geothermal gradient, gravity, magnetic, and slope layers were reclassified using the ranges for all four basins on a scale of 1-9, with 9 being most desirable, to ensure compatibility between the basins and to prepare for raster algebra. Reclassification values are shown in Table 1. A weighting matrix, similar to that proposed by the

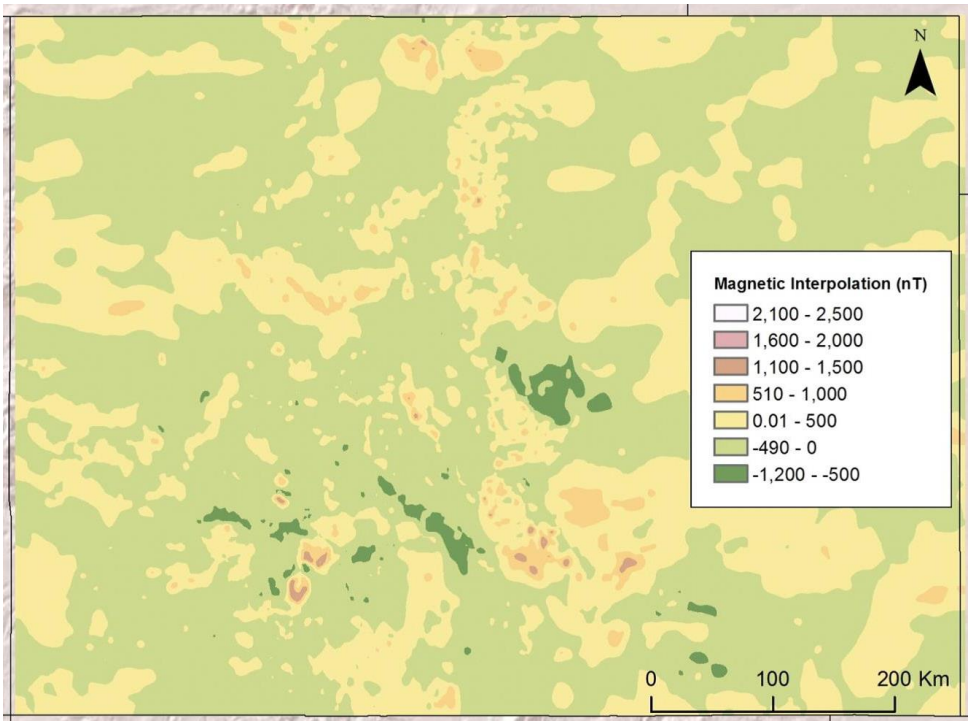

Figure 4. An example of a magnetic intensity interpolation for the state of Colorado. This layer was created with the kriging interpolation method from 232,129 data points downloaded off of the University of Texas, El Paso Gravity and Magnetics database of the U.S. Areas of low magnetic intensity are of interest since they indicate areas with little to no mafic rocks.

Environmental Protection Agency's DRASTIC model for evaluating water pollution (Babicker et al., 2005), was then calculated to determine what values to use within the raster algebra tool (Table 2). The raster algebra tool was run, and overall desirability values were calculated. The combination of weighted attributes, as shown in Table 2, results in raster cells indicating where slope, magnetic intensity, and gravity are lowest, and geothermal gradient is highest. The warmer colors in the resulting raster indicate areas where geothermal power plant placement would be optimal given these four variables. Once the desirability value, a unitless number, was calculated, the clip tool was

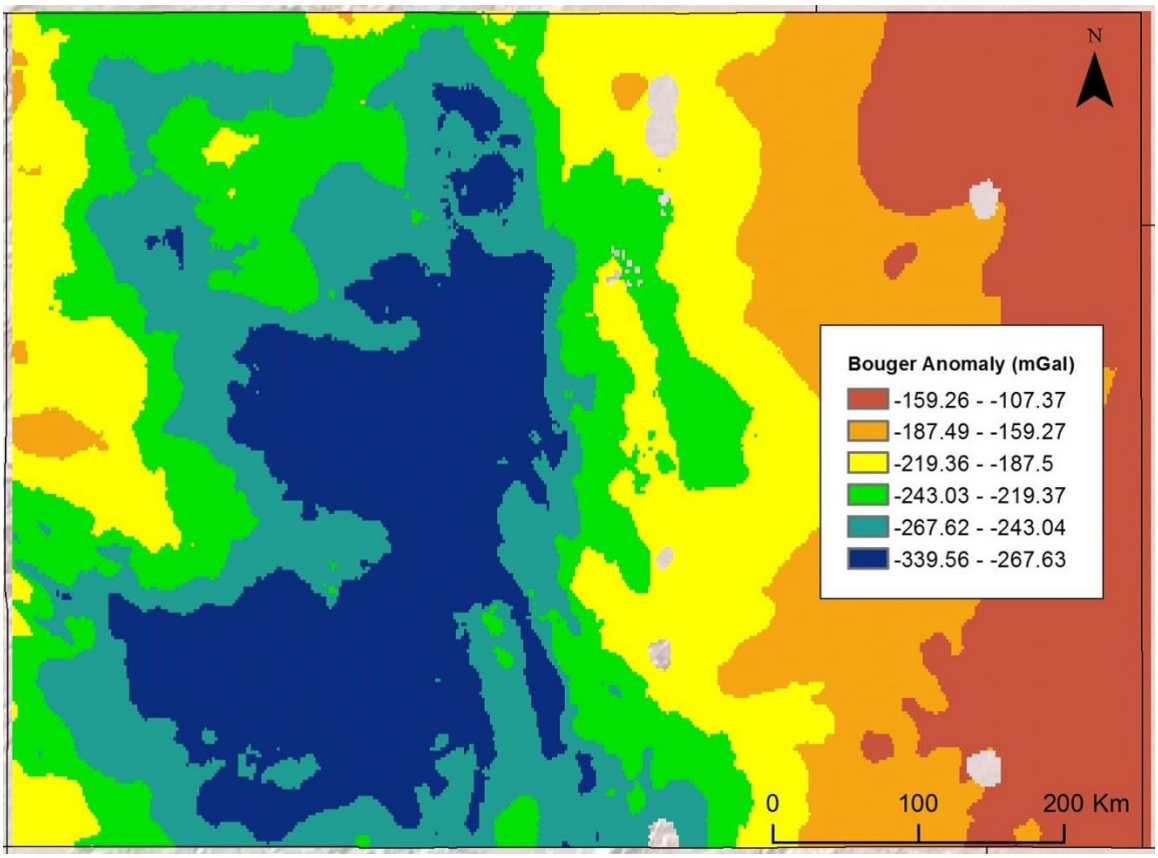

Figure 5. An example of a Bouger gravity anomaly interpolation for the state of Colorado. This layer was created with the kriging interpolation method from 46,535 data points downloaded off of the University of Texas, El Paso Gravity and Magnetics database of the U.S. Areas with a low Bouger gravity anomaly value are of interest since they indicate areas that are less dense, usually thick sediments.

used to remove areas with values below 3 on a scale of 1-9. The desirability cutoff of 3 was chosen because although geothermal gradient is not extremely high, it indicates where a temperature of 110°C can be found within the first two kilometers of sediment in addition to favorable values for the other three attributes.

Table 1. Table of reclassification breaks used for each layer to normalize the four study locations, based on how desirable the layer value is. Higher geothermal gradient indicates higher temperature at a shallower depth, low magnetic intensity indicates a lack of mafic rocks, low gravity indicates rocks that are less dense such as thick sedimentary layers, and low slope is desirable to keep construction costs lower.

		Breaks			
Desirability	Reclassified Value	Geothermal Gradient (deg C/meter)	Magnetic Intensity (nT)	Gravity Anomaly (mGal)	Slope (no unit)
High	9	144	-1112	-306	611,111.00
	8	128	-224	-262	1,222,222.00
	7	112	664	-218	1,833,333.00
	6	96	1552	-174	2,444,444.00
	5	80	2440	-130	3,055,555.00
	4	64	3328	-86	3,666,666.00
	3	48	4216	-42	4,277,777.00
	2	32	5104	2	4,888,888.00
Low	1	16	5992	46	5,499,999.00

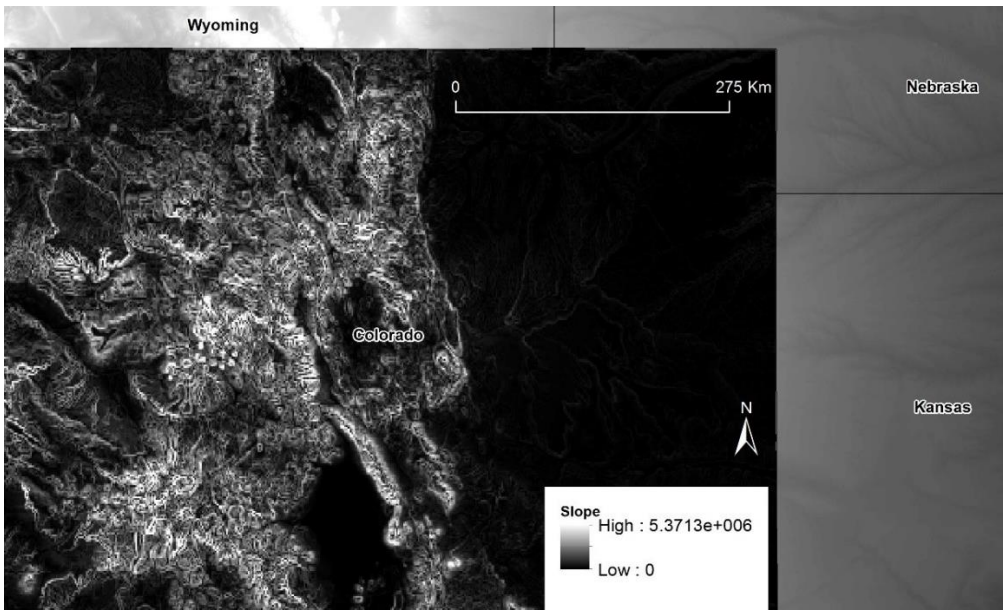

Figure 6. Slope calculated from the Digital Elevation Model (DEM), State of Colorado. The DEM used in the calculation was projected in Universal Transverse Mercator (UTM); therefore, the number is unitless and was reclassified for use in raster calculation to values of 1-9, with 9 being at or near zero slope.

Table 2. Weighting matrix used in raster algebra. Cost is one of the greatest barriers to geothermal exploration, so desirability was determined by what variables influence the lowest cost. Geothermal gradient was determined to be of greatest importance, followed by gravity anomaly, magnetic intensity, and finally slope. The values in the table are a range of importance, so no units are associated with them.

	Geothermal Gradient	Gravity Anomaly	Magnetic Intensity	Slope	Weight
Geothermal Gradient	***	2	3	4	9
Gravity Anomaly	1/2	***	2	3	5.5
Magnetic Intensity	1/3	1/2	***	2	2.83
Slope	1/4	1/3	1/2	***	1.08

Discussion

The Denver Basin

The Denver Basin is an asymmetric foreland basin that trends north-south, parallel to the Rocky Mountains. The entire basin, which spans Wyoming, Nebraska, and Colorado, has a surface area of approximately 155,000 km^2 (Curtis, 1988; Martin, 1965). The areas of high geothermal gradient appear to be fault controlled and lithologically controlled (Figures 7 and 8), and these regions are surrounded by basement faults and outcrops of crystalline rock. Comparing the geothermal gradient to the magnetic intensity map (Figure 9) reveals that the locations of interest are located above regions of relatively lower magnetic intensity for the region, however, the magnetite content in the nearby crystalline rock exposures is obvious. Examination of the regional gravity anomaly (Figure 10) indicates less dense rock than the surrounding area, especially in the pink "hot spot." The areas west of Denver are of interest because they are located near high

population centers, and costly infrastructure is already in place. These high population areas are near the depocenter of the basin and the Golden Fault along the Front Range of the Rocky Mountains, where the hottest temperatures in the basin are located. Colorado is required to provide thirteen percent of its energy from renewable energy by the year 2020, and although it is currently providing fourteen percent from renewable sources, none of the existing sources are base-load (U.S. EIA, 2014). Geothermal power production is therefore of considerable interest in this state.

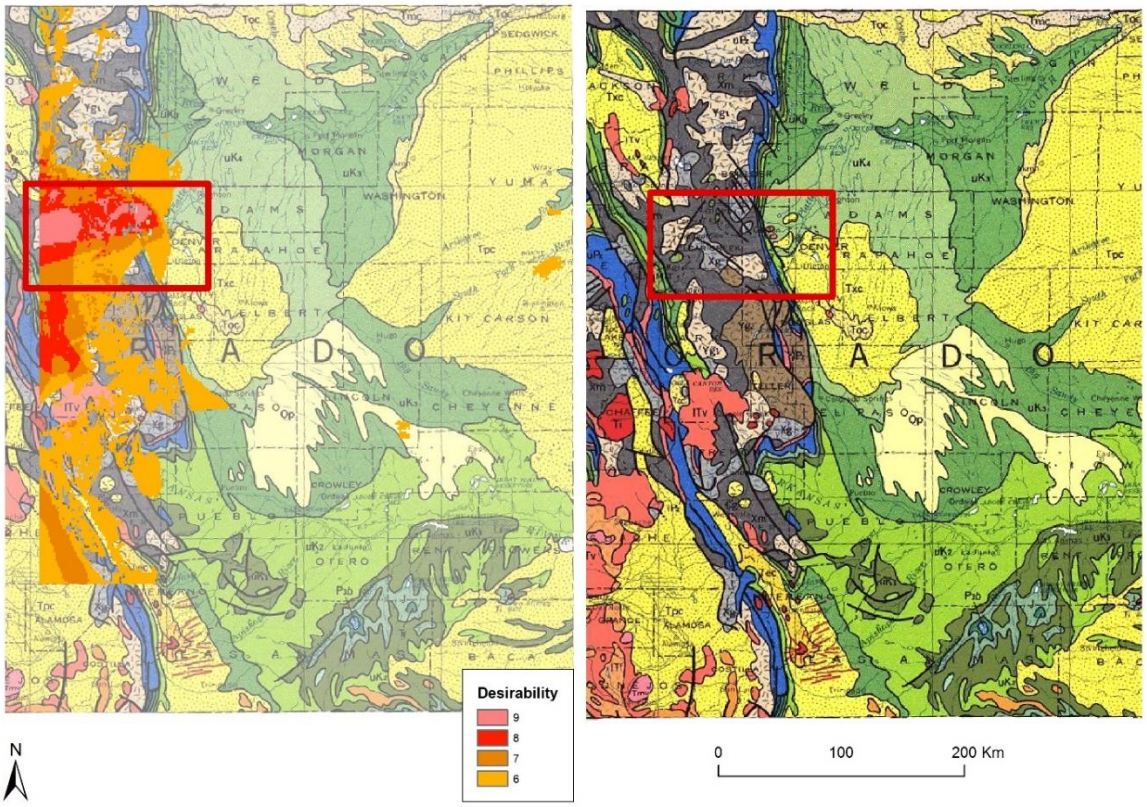

Figure 7. The areas of high geothermal gradient in the Denver basin are plotted against a surface geology map of Colorado. The red square indicates a major area of interest just west of the city of Denver. The temperature regime for the Denver Basin does appear to be fault controlled.

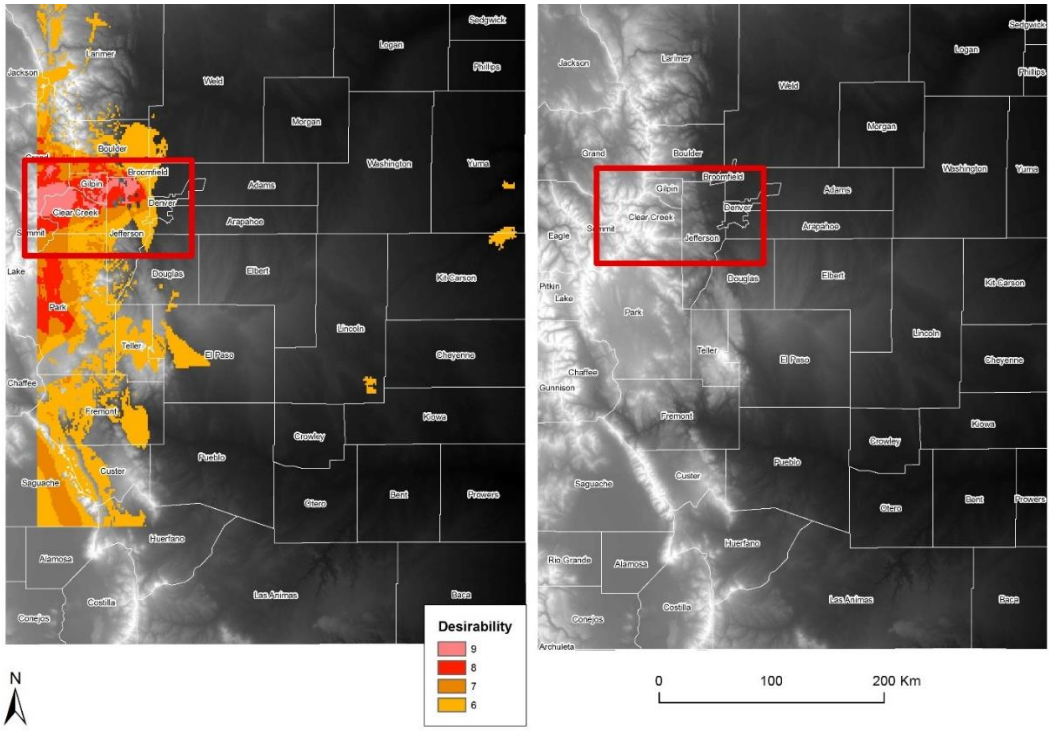

Figure 8. Areas of high geothermal gradient in the Denver Basin against the DEM for the state of Colorado. The Front Range is clearly visible, and many rivers are present. Water regulations need to be taken into account when developing this area for geothermal use.

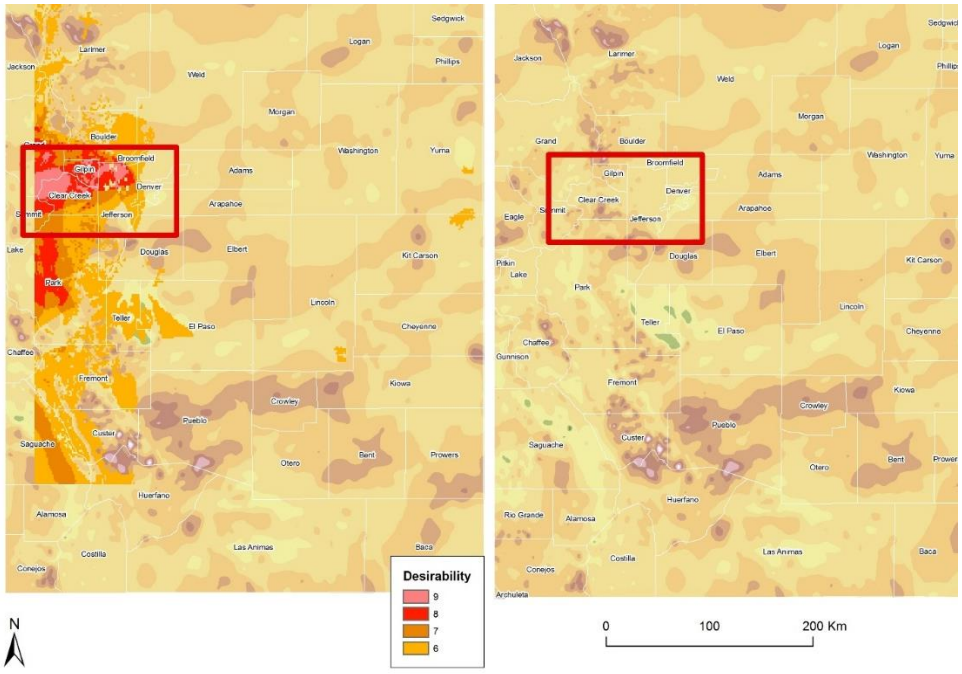

Figure 9. The magnetic intensity interpolation with areas of high geothermal gradient. Sediments from the Front Range are present in this basin, which may explain the presence of sediments with a higher ferromagnesian content.

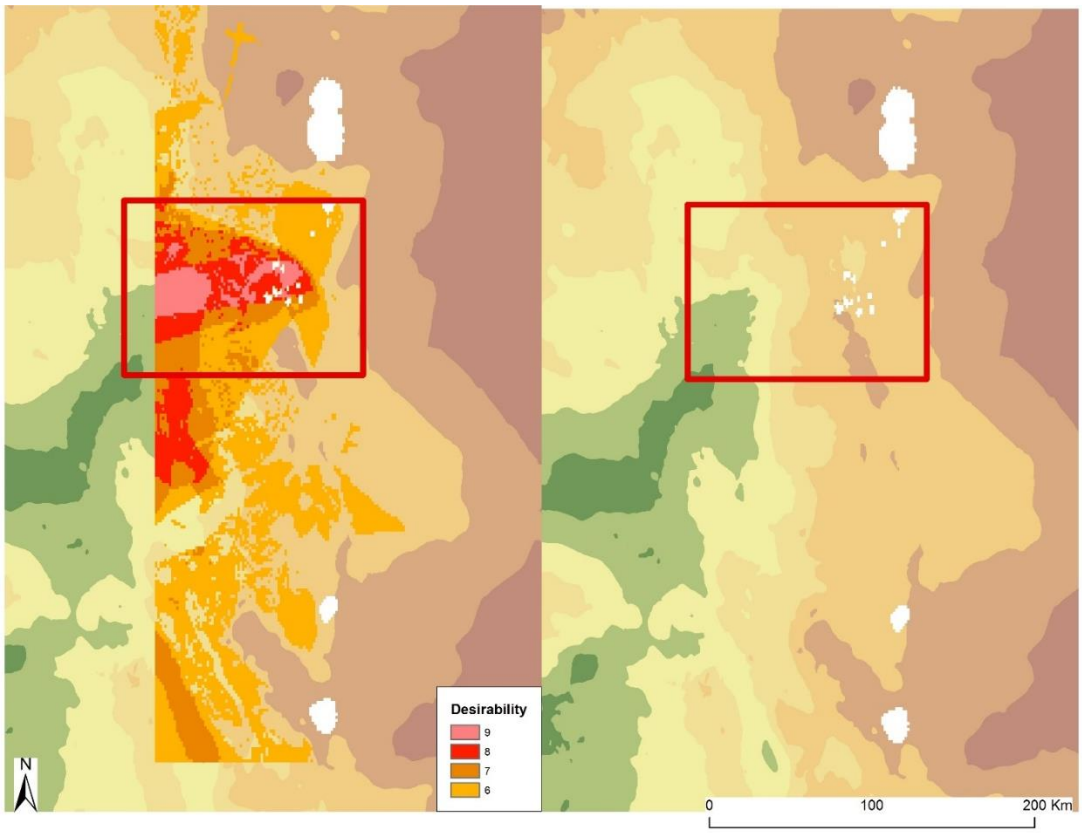

Figure 10. A lower gravity anomaly running along the base of the Front Range correlates to the high geothermal gradient just west of the city of Denver. The gravity anomaly then increases away from the range as sediments thin.

The Illinois Basin

The Illinois Basin is an asymmetrical cratonic basin, with a Northeast to Southwest trending axis. Located primarily within the state of Illinois, it has margins in Kentucky and Indiana, spanning a surface area of 155,400 km^2 (Macke, 1995). Areas of high geothermal gradient appear in predominantly Cambrian to Pennsylvanian aged surface rock, and do not appear to be fault controlled (Figures 11 and 12). Relatively low magnetic intensity is found in the areas of interest indicating little to no magnetite and therefore little crystalline rock (Figure 13). In three of the five areas, the gravity anomaly is higher, indicating denser rocks at depth (Figure 14) and perhaps shallower sediments in

these areas. The depth required to reach temperatures useable with current power generating technologies in Illinois is too great to make geothermal power production feasible; however, temperatures are sufficient for district heating and greenhouse applications. Even though the state has a desirability rating that reaches 8, these areas are small and isolated, possibly the result of localized fracturing. The state of Illinois has an average energy usage that is forty-four percent higher than the U.S. average (U.S. EIA, 2014). Using geothermal reserves can provide considerable contributions to offset current energy needs.

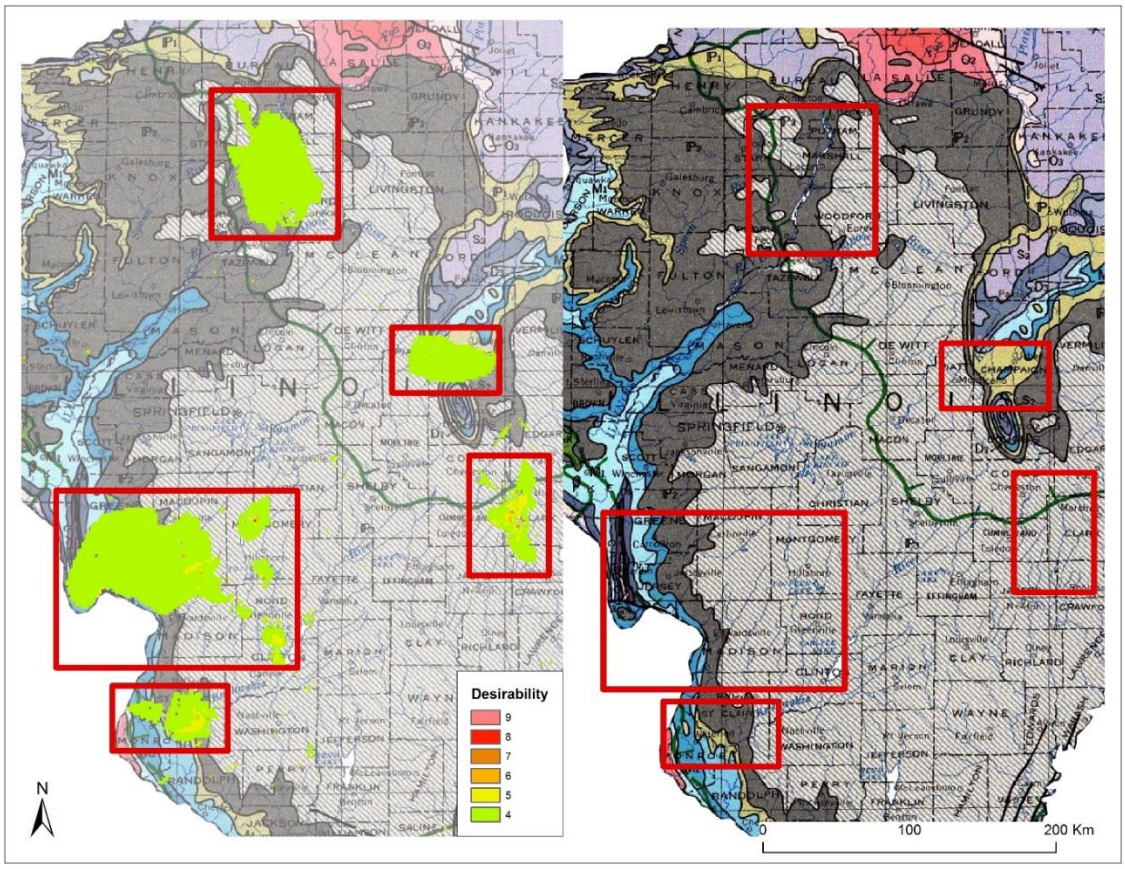

Figure 11. The areas of high geothermal gradient in the Illinois basin are plotted against a surface geology map of Illinois. The red squares indicates major areas of interest, in predominantly Cambrian to Pennsylvanian aged rock. The temperature regime for the Illinois Basin does not appear to be fault controlled.

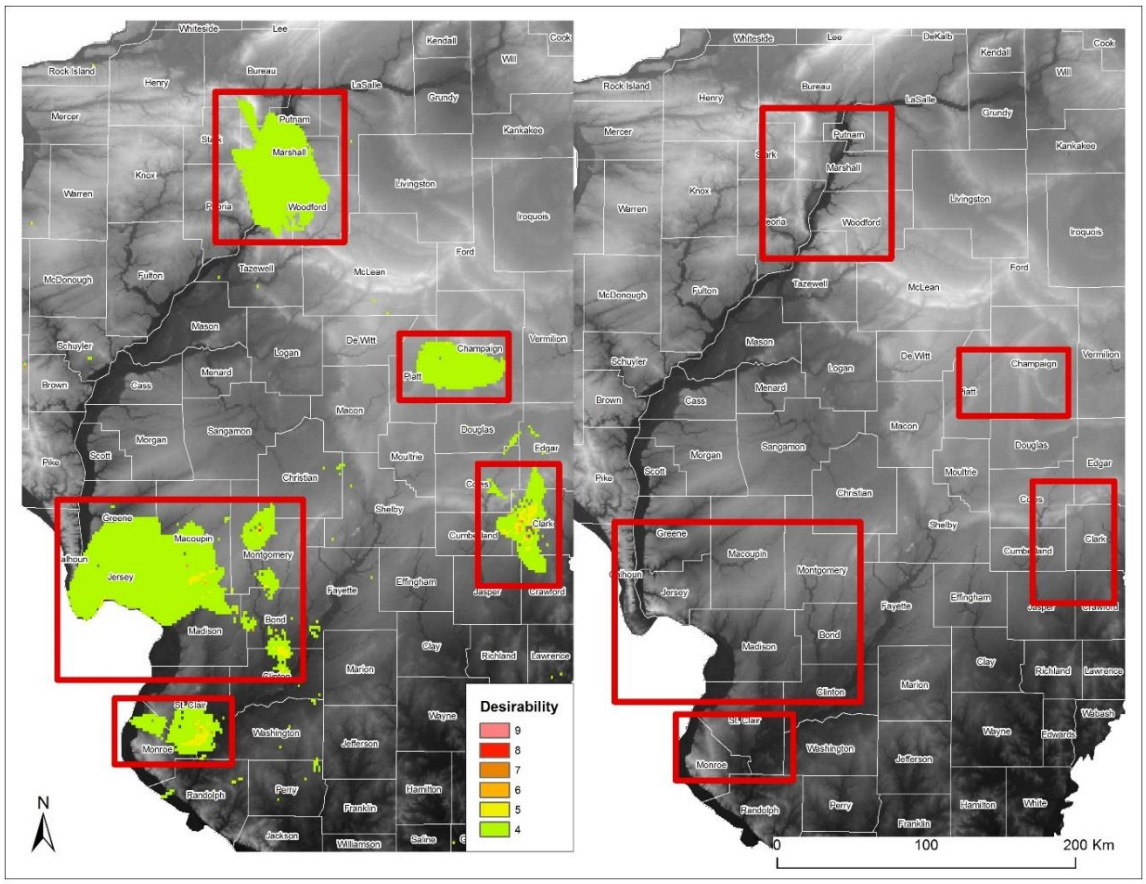

Figure 12. Areas of high geothermal gradient in the Illinois Basin against the DEM for the state of Illinois. In the three cratonic basins, the DEM and resulting slope calculations were useful mostly for location of possible water and environmental impacts.

The Michigan Basin

The Michigan Basin is a roughly symmetrical cratonic basin. The surface area includes the entire state of Michigan, Indiana, Ohio, and parts of Canada, over 308,210 km^2 (Dolton, 1995). Areas with high geothermal gradient are around the rim of the basin, in predominantly Devonian and Mississippian age rocks, and does not appear to be fault controlled (Figures 15 and 16). The magnetic intensity of the study areas appears to be average, which would be expected in areas with thick sediment and little to no magnetite (Figure 17). Analysis of the gravity anomaly map clearly shows the rift that runs through

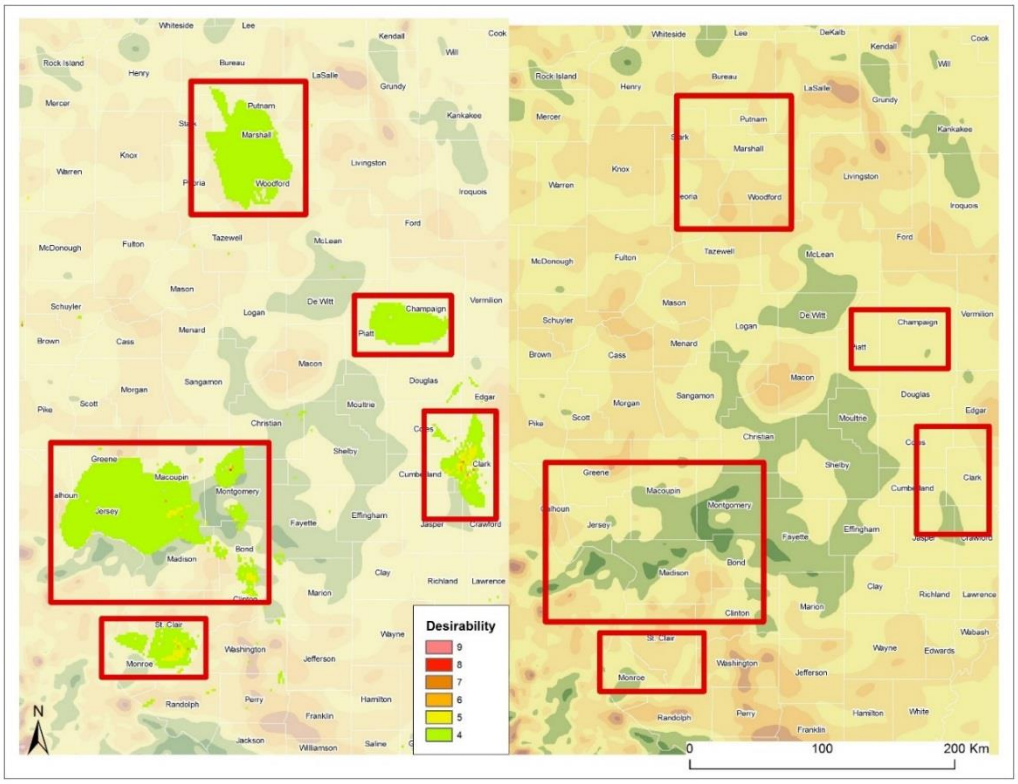

Figure 13. The magnetic intensity interpolation in the Illinois Basin with areas of high geothermal gradient. The areas of interest appear to have sediments with little to no magnetite present.

the middle of the state, and therefore the high ferromagnesian mineral content in the area (Figure 18). On either side of the rift, the gravity anomaly drops off in intensity. In Michigan, much like in Illinois, the depth at which temperatures can be found that are adequate for geothermal power production are too great to be feasible with current technology, but the potential for district heating and direct use is adequate. The Mid-continental Rift System, which runs through the center of the state, appears to be the major control of geothermal gradient. The weather is cooler in Michigan than most parts of the country (U.S. EIA, 2014), so energy savings with district heating, in particular, are beneficial.

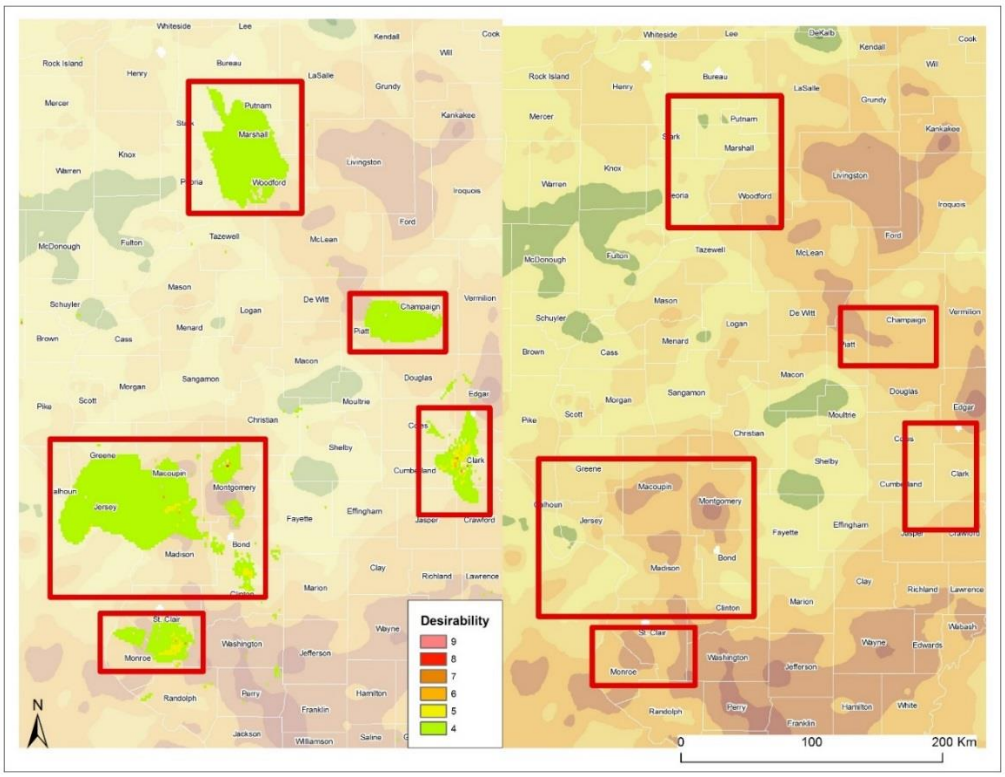

Figure 14. Three of the five areas of interest in the Illinois Basin have high gravity anomalies, indicating possible intrusive ferromagnesian bodies or dense crystalline rocks.

The Williston Basin

The Williston Basin is an asymmetric cratonic basin that trends roughly North-South (Heck 2002). The surface area includes primarily North Dakota, and to a lesser degree in Montana, Saskatchewan, and Manitoba, for a total of 133,644 km2 (Carlson and Anderson, 1965). Not much is revealed when comparing the geothermal gradient to the geology and surface expression of the basin (Figures 19 and 20), indicating that the "hot spots" are most likely not fault controlled. The magnetic intensity map (Figure 21) does show the areas of interest in soft sediments with little to no magnetite presence, showing a lack of near surface crystalline rock. The gravity map (Figure 22) is much

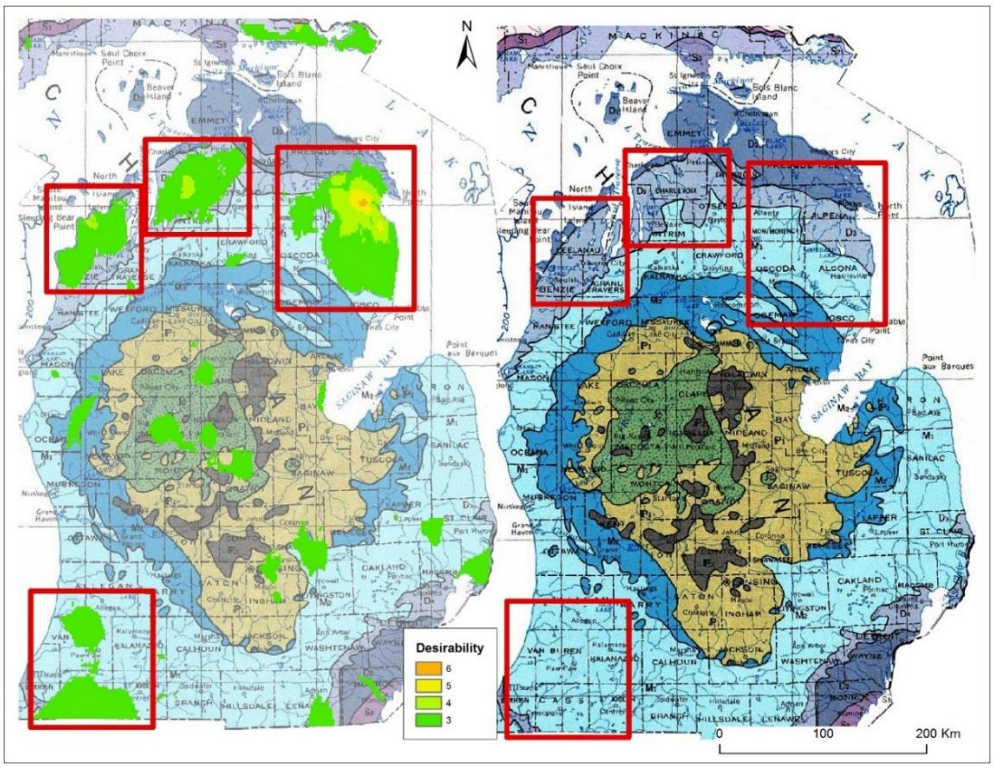

Figure 15. The areas of high geothermal gradient in the Michigan basin are plotted against a surface geology map of Michigan. The red squares indicates major areas of interest, in Devonian and Mississippian rocks. The temperature regime for the Michigan Basin does not appear to be fault controlled.

more informative, as it shows the presence of the mafic pipe-shaped intrusion in the northcentral part of the state, as well as the north-south trend of the granite greenstone terrain in the large area of interest. The oil boom in the North Dakota portion of the Williston Basin is straining the infrastructure, and with the energy needed to pump the oil wells increasing rapidly, the need for more produced power exists. The Nesson, Billings, and Little Knife Anticlines appear to be the most significant structural controls on the geothermal gradient. North Dakota is also among the coldest states in the country (U.S. EIA, 2014), so significant energy requirements exist before accounting for the excess need for oil drilling and pumping. The geothermal gradient is conveniently highest in the

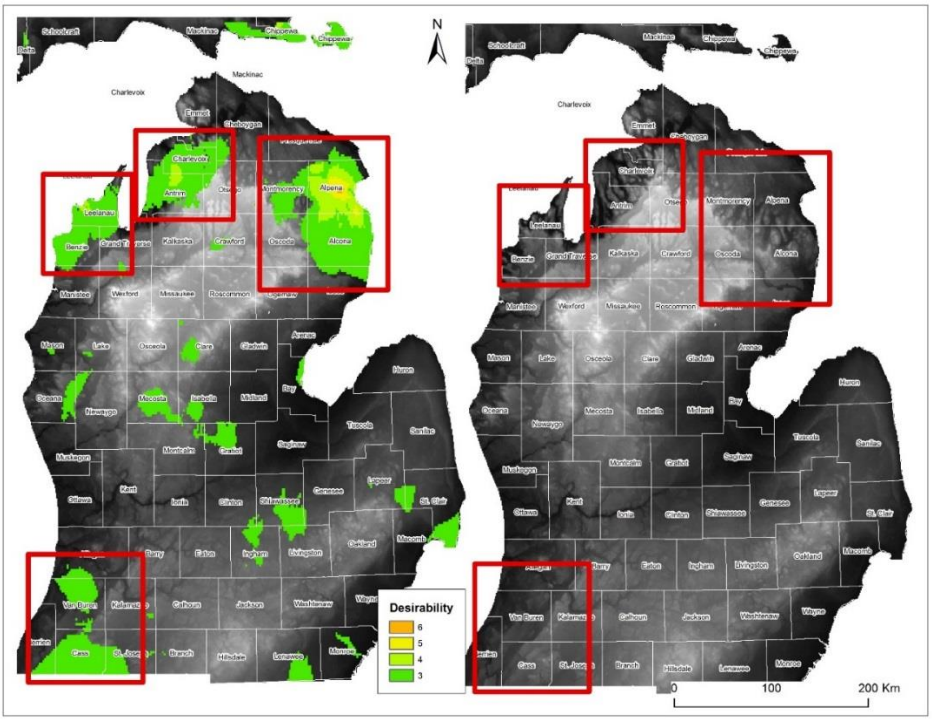

Figure 16. Comparing the DEM to the areas of interest in the Michigan Basin shows area of possibly higher slope and quite a few rivers, which is, again, an environmental concern for geothermal development.

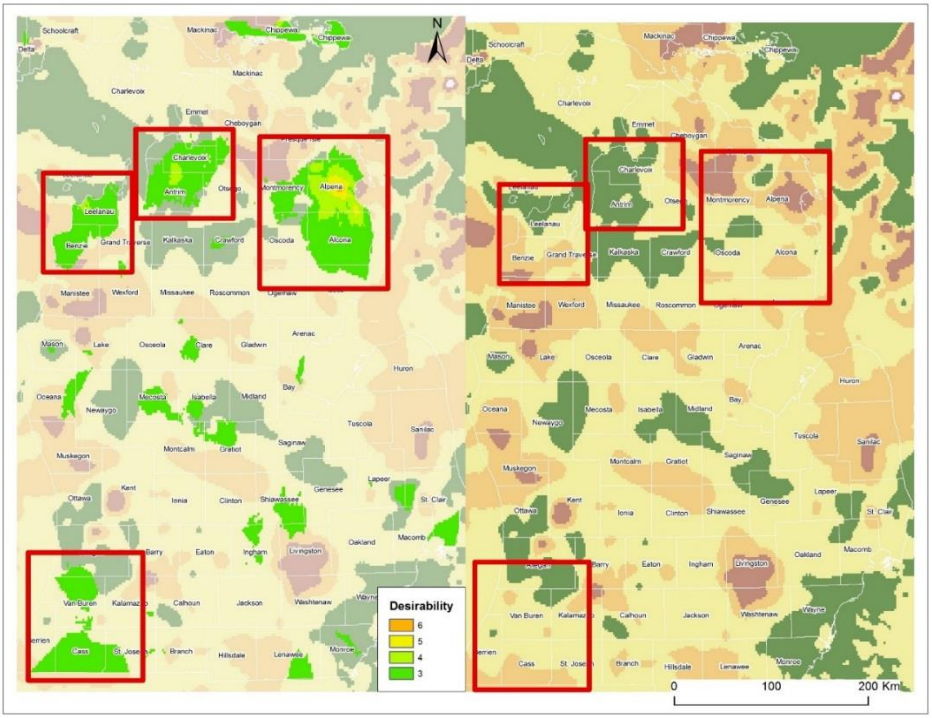

Figure 17. Magnetic intensity for areas of interest in the Michigan Basin appear to be average, which would be expected for a cratonic basin with no recent sedimentation.

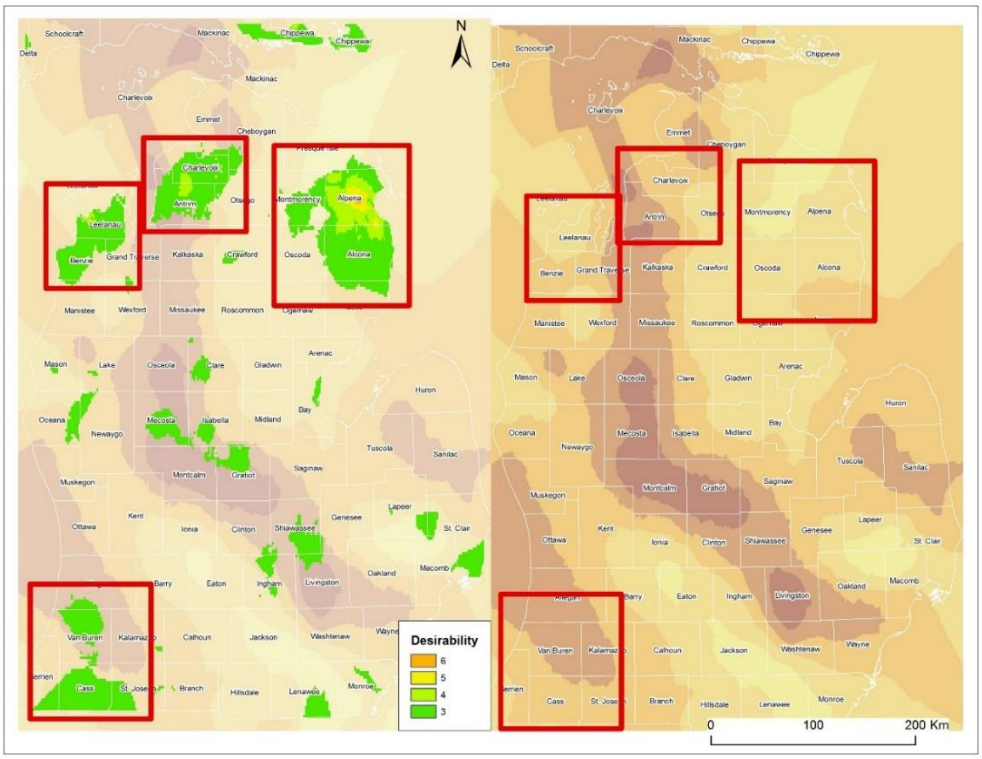

Figure 18. The Keweenawan rift is clearly visible in the gravity anomaly interpolation of the Michigan Basin. The presence of a thinner crust in this area may be responsible for some of the higher geothermal gradients in the areas of interest.

region where geothermal power production would be most needed. While the gradient points to low temperature resources, these are sufficient for supplying smaller, portable ORC binary plants as talked about by Gosnold et al., 2013.

The Williston and Denver-Julesberg basins not only show promise for further feasibility studies, but appear to have excellent potential. These reports and the following research assume an adequate, sustainable water flow is available.

Results

Using the desirability value to help select optimal power plant locations is known as a Play Fairway analysis. Cost is one of the greatest barriers to geothermal exploration, so desirability was determined by what variables influence the lowest cost. The state of

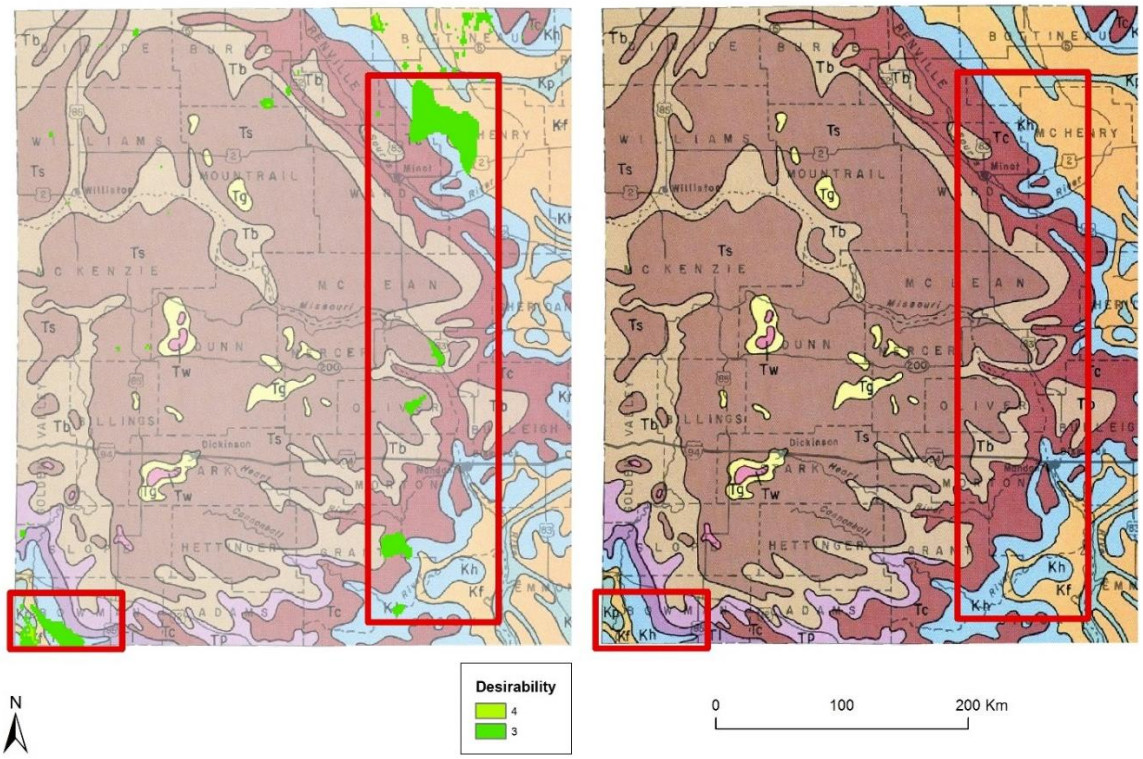

Figure 19. The areas of high geothermal gradient in the Williston basin are plotted against a surface geology map of North Dakota. The red squares indicate major areas of interest. The temperature regime for the Williston Basin does not appear to be fault controlled.

Colorado clip using a desirability value cutoff of 3 included most of the state, which isn't useful in determining power plant placement. In this case, a new clip using only values of 6 and above were included in the Colorado map (Figure 23), which ranges from 6-9. Illinois has a desirability range from 4-8 (Figure 24), Michigan has a desirability range from 3-6 (Figure 25), and North Dakota has a desirability range from 3-4 (Figure 26).

Conclusions

Assuming an adequate, sustainable water supply, the Denver-Julesberg basin has the highest capacity for large scale geothermal power production near population centers where infrastructure currently exists. While not all oil-producing basins have the

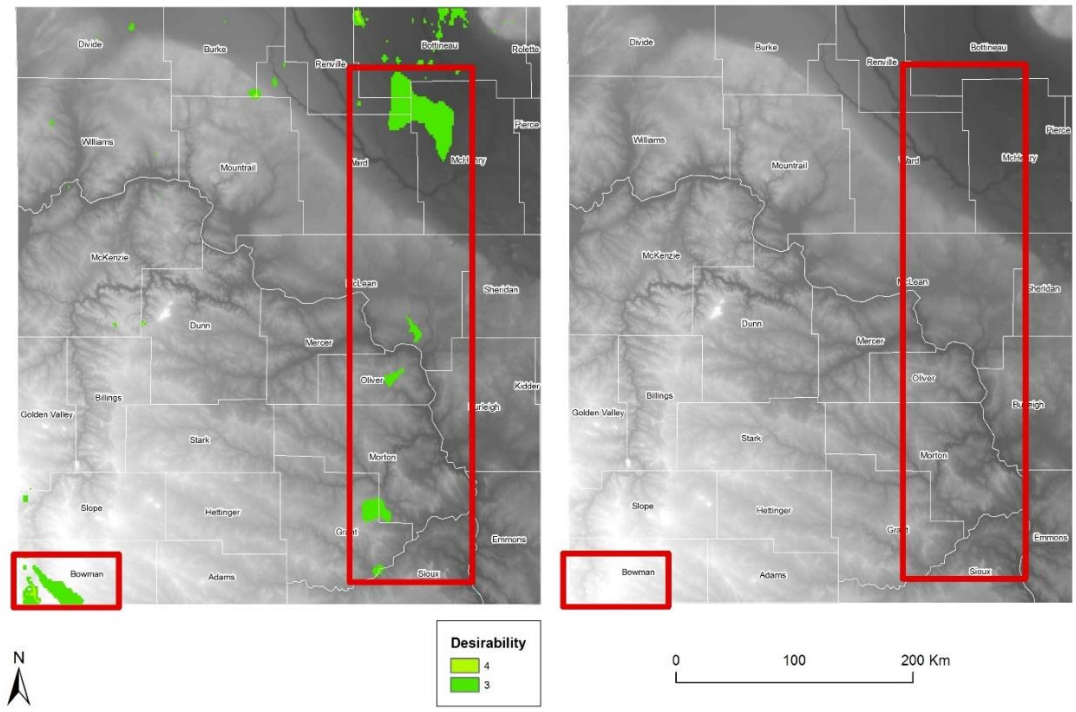

Figure 20. The DEMs for North Dakota and the Williston Basin show very little, as in the Illinois Basin, except where major rivers are present. Very little change in slope is experienced in this area.

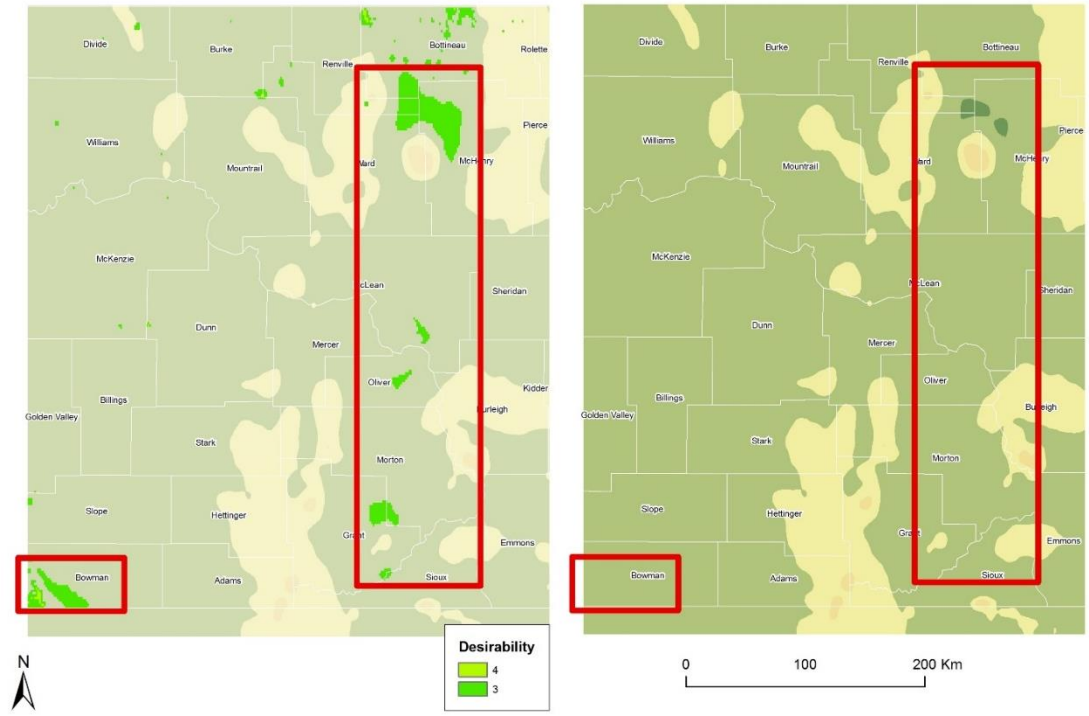

Figure 21. Analysis of the Magnetic Intensity interpolation for the Williston Basin and North Dakota indicates nearly no magnetite, and therefore thick sediments with few mafic intrusions.

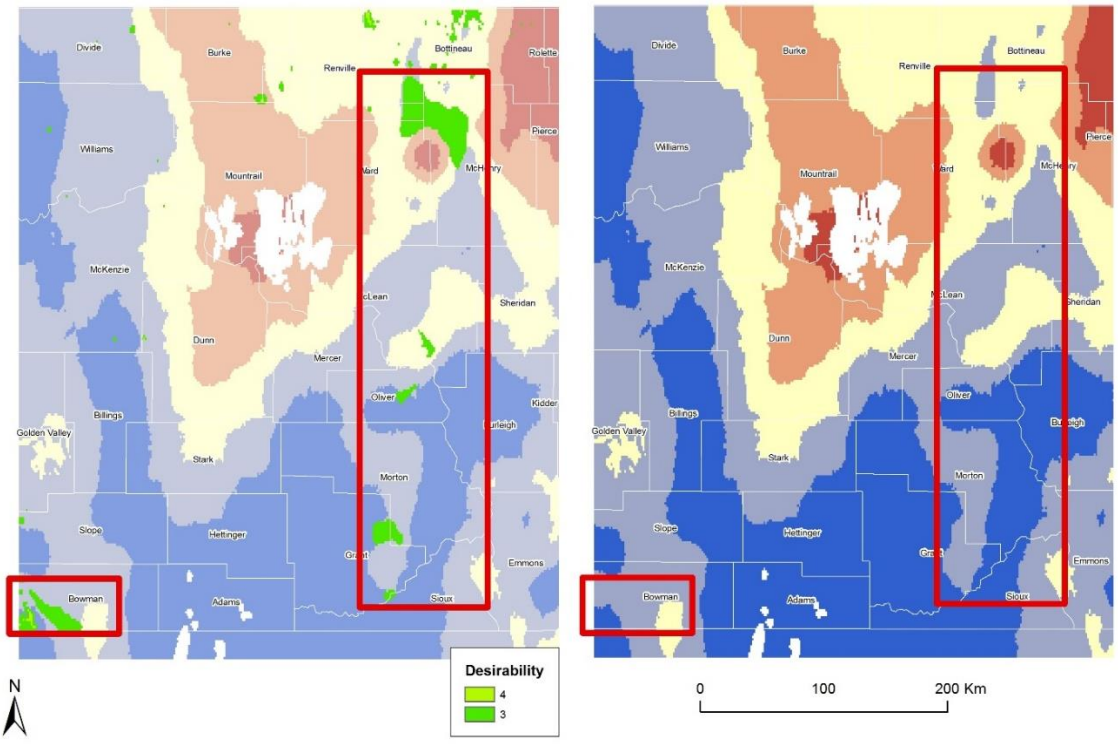

Figure 22. Both the Magnetic and Gravity interpolations show the mafic tube-shaped intrusion in the North Central part of the state. This gravity interpolation, however, also shows the north to south trending granite/greenstone terrains present in the subsurface of the basin.

capability to produce electricity from geothermal brines with current technology, such as Illinois and Michigan, the need exists for offsetting energy production from power plants, many of which run on coal. Other forms of energy use, such as district heating and direct use, have the capacity to offset present power production and should not be ignored. Low temperature power production, such as that found in North Dakota, is also of use with smaller binary power plants that can generate power locally for use in drilling and pumping oil.

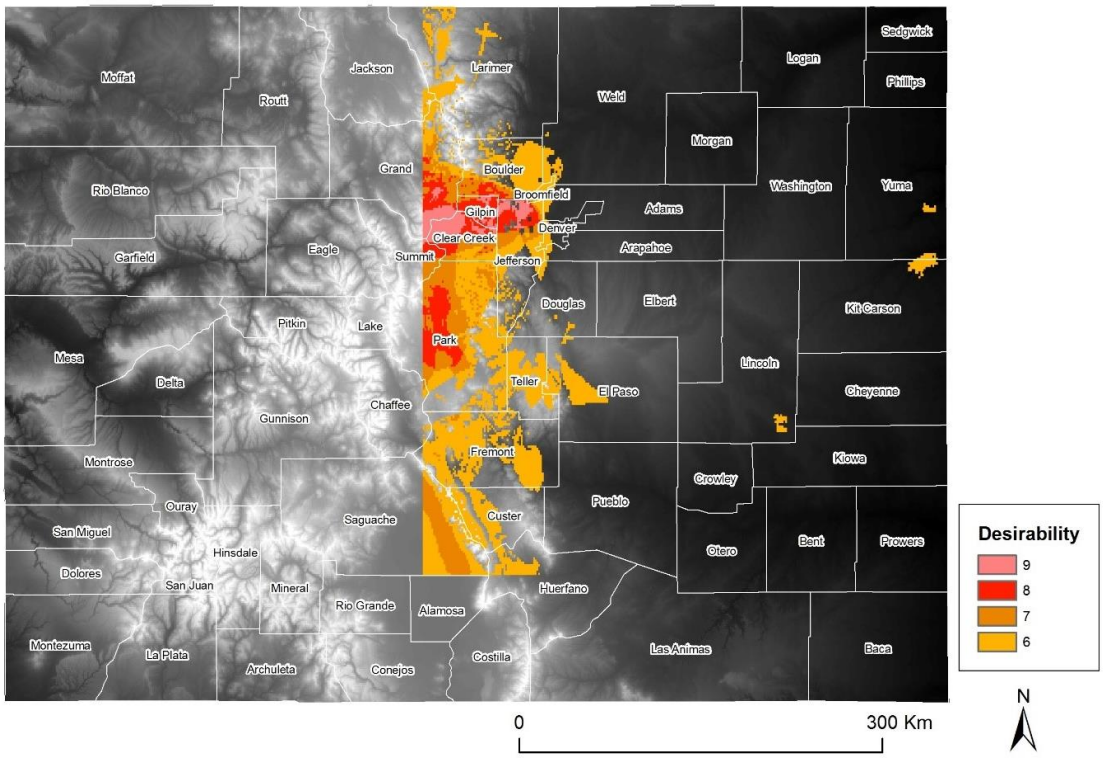

Figure 23. Final Play Fairway Map for Colorado. The counties with the greatest potential are Boulder (6-8), Broomfield (6-9), Clear Creek (6-9), Fremont (6, 7), Gilpin (7-9), Park (6-8), Saguache (6, 7), and Teller (6).

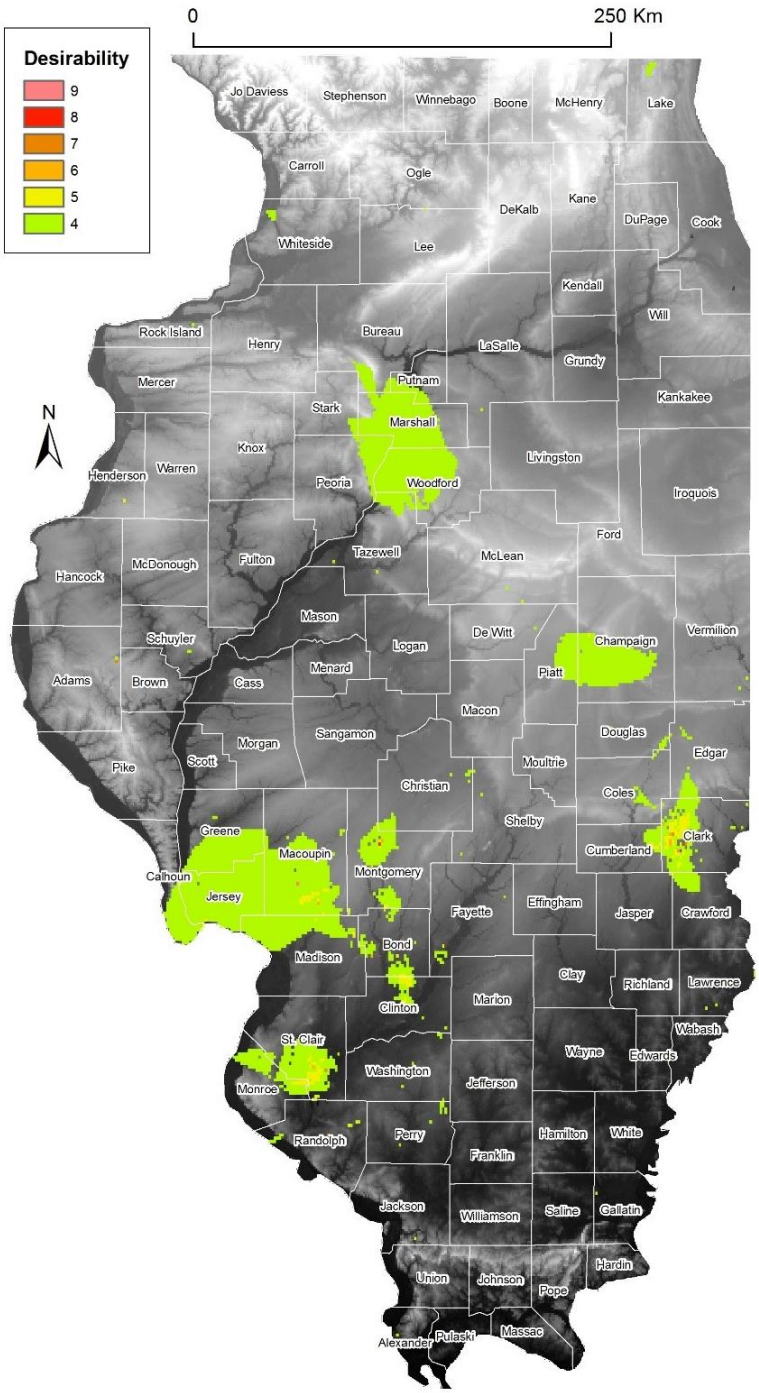

Figure 24. Final Play Fairway Map for Illinois. The counties with the greatest potential are Calhoun (4), Champaign (4), Clark (4-6), Clinton (4, 5), Greene (4), Jersey (4), Macoupin (4-6), Marshall (4), Montgomery (4-8), St. Clair (4-6), and Woodford (4).

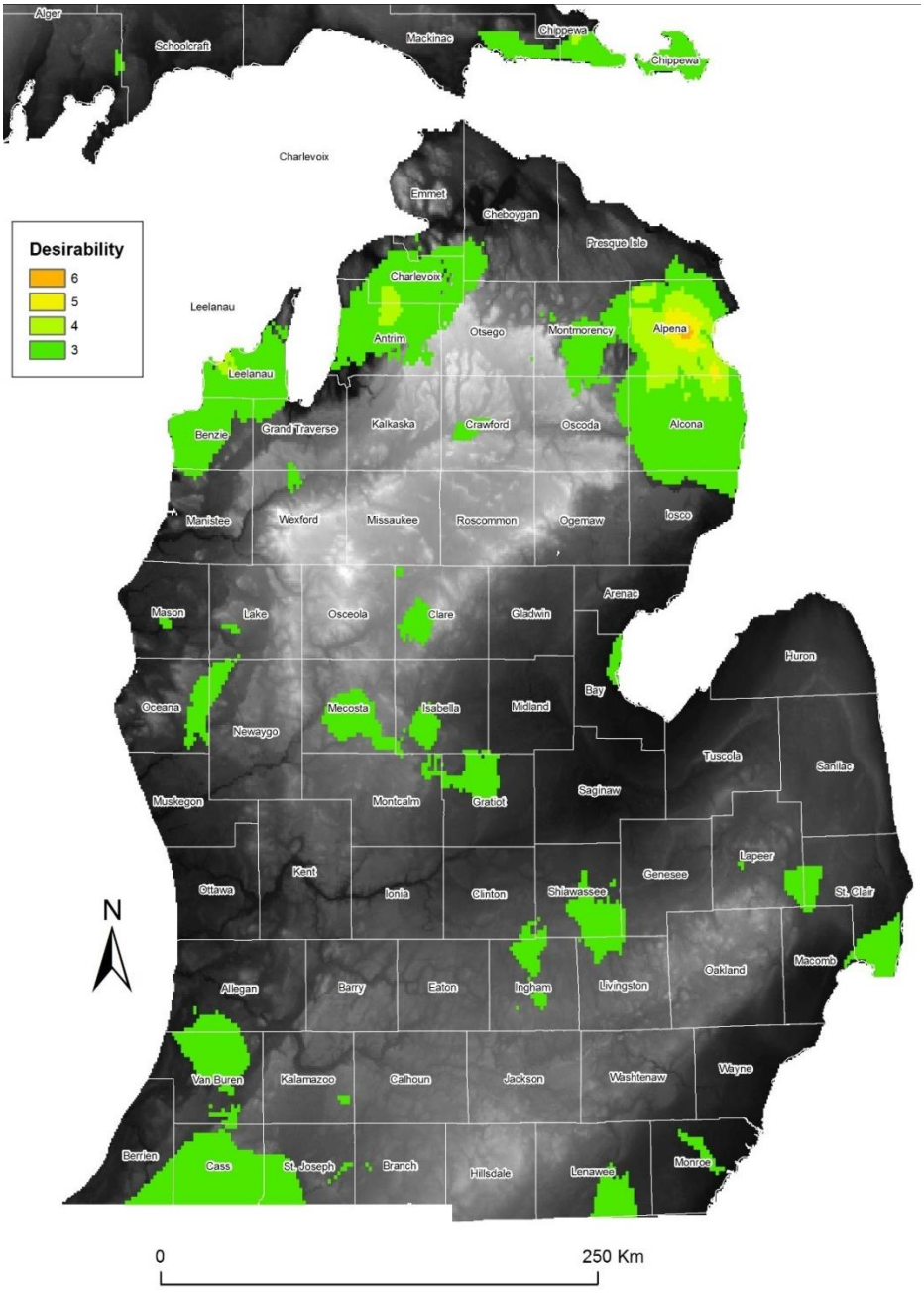

Figure 25. Final Play Fairway Map for Michigan. The counties with the greatest potential are Alcona (3), Alpena (3-6), Antrim (3, 4), Benzie (3), Cass (3), Charlevoix (3, 4), Chippewa (3, 4), Crawford (3), Gratiot (3), Ingham (3), Isabella (3), Leelenaw (3, 4), Lenawee (3), Mackinaw (3), Mecosta (3), Montmorency (3), Shiawasee (3), St. Clair (3), and Van Buren (3).

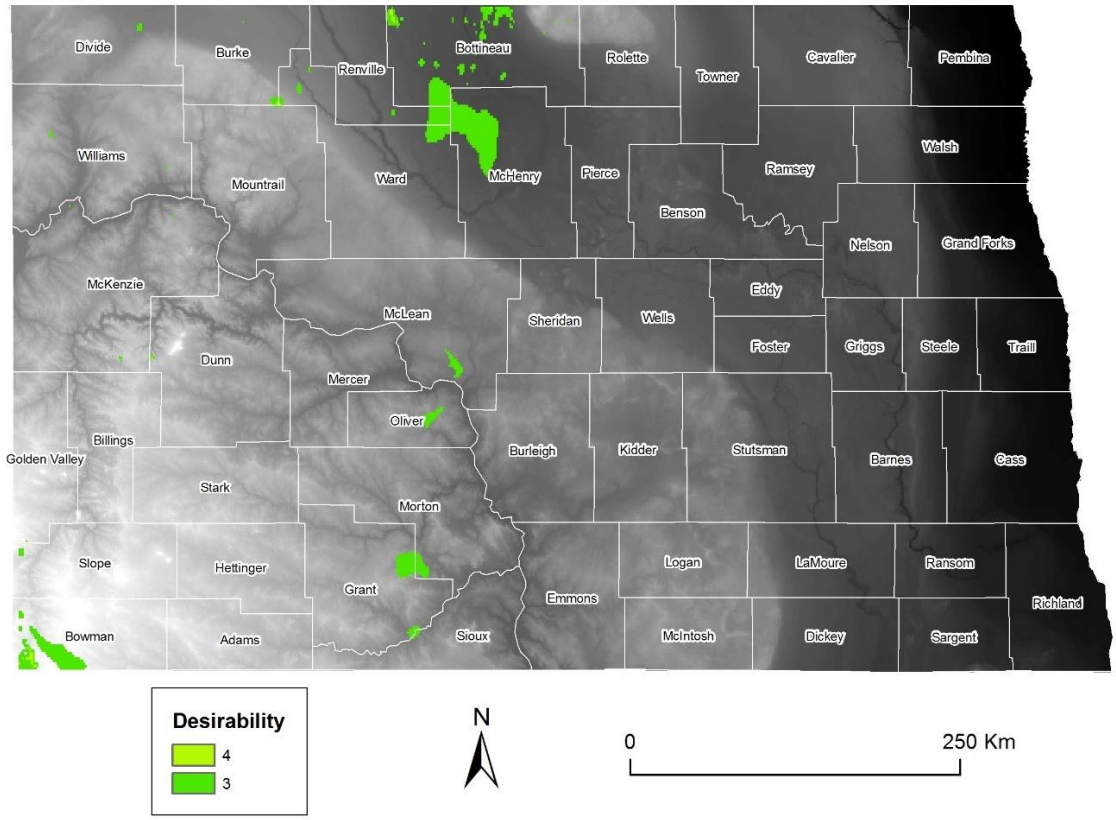

Figure 26. Final Play Fairway Map for North Dakota. The counties with the greatest geothermal potential are Bottineau (3, 4), Bowman (3, 4), Grant (3), McHenry (3), Mclean (3), Morton (3), Oliver (3), and Renville (3).

Sources Cited

Babiker, I.; Mohamed, M.; Hiyama, T.; and K. Kato, 2005. A GIS-based DRASTIC model for assessing aquifer vulnerability in Kakamigahara Heights, Gifu Prefecture, Central Japan. Science of the Total Environment, vol. 345 p. 127-140.

Carlson C.G., and S.B. Anderson, 1965. Sedimentary and Tectonic History of North Dakota Part of Williston Basin. Bulletin of the American Association of Petroleum Geologists, v. 49, no. 11, P. 1833-1849.

Clark, C.; Sullivan, J.; Harto, C.; Han, J.; and M. Wang, 2012. Life Cycle Environmental Impacts of Geothermal Systems. Proceedings, 37th Workshop on Geothermal Reservoir Engineering, Stanford, CA.

Crowell, A. M. and W. Gosnold, 2014. GIS/Volumetric Geothermal Resource Assessment of the Michigan and Illinois Basins. Transactions of the Geothermal Resources Council, vol. 38. P. 947-950.

Crowell, A. M.; Ochsner, A. T.; and W. Gosnold, 2013. GIS-Based Geothermal Resource Assessment of the Denver Basin: Colorado and Nebraska. Transactions: Geothermal Resources Council vol. 37. P. 201-206.

Crowell, A. M.; Klenner, R.; and W. Gosnold, 2011. GIS Analysis for the Volume and Available Energy of Selected Reservoirs: Williston Basin, North Dakota," Transactions: Geothermal Resources Council vol.35. P. 1557-1561.

Curtis, B. F., 1988. Sedimentary rocks of the Denver basin: in Sloss, L.L. (editor), Sedimentary Cover—North American Craton, U.S. Geological Society of America, The Geology of North America, v. D-2, ch. 8, P. 182-196.

Dolton, G.L., 1995. Michigan Basin Province (063). In: Gautier, D.L., Dolton, G.L., Takahashi, K.I., Varnes, K.L. (Eds.), 1995 National assessment of United States oil and gas resources: results, methodology, and supporting data. U.S. Geological Survey, pp. GS–30.

Geology.com, 2014. U.S. Map Collections for all 50 States. http://geology.com/state-map/. Accessed 3/14/2014.

Gosnold, W.; Barse, K.; Bubach, B; Crowell, A.; Crowell, J.; Jabbari, H.; Sarnoski, A; and D. Wang, 2013. Co-Produced Geothermal Resources and EGS in the Williston Basin, Transactions of the Geothermal Resources Council, vol. 37, p. 721-726.

Harrison W.E., K.V. Luza, M.L Prater, and P.K. Chueng, 1983. Geothermal resource assessment of Oklahoma, Oklahoma Geological Survey, Special Publication 83-1.

Heck T.J., LeFever, R.D., Fischer, D.W., and J. LeFever, 2010. Overview of the Petroleum Geology of the North Dakota Williston Basin. <https://www.dmr.nd.gov/ndgs/Resources/ WBPetroleumnew.asp> Accessed 12/30, 2010.

Macke, D.L., 1995. Illinois Basin Province (064). In: Gautier, D.L., Dolton, G.L., Takahashi, K.I., Varnes, K.L. (Eds.), 1995 National assessment of United States oil and gas resources: results, methodology, and supporting data. U.S. Geological Survey, pp. GS–35.

Martin, C. A., 1965. Denver Basin: Bulletin of the American Association of Petroleum Geologists, v. 49, no. 11, P. 1908-1925.

NGDS, 2014. National Geothermal Data System. www.geothermaldata.org. Accessed 12-2-2014.

NOAA, 2014. National Climate Data Center Data Access. http://www.ncdc.noaa.gov/data-access. Accessed 3/27/2014.

Tester J.W., et. al., 2006. MIT: The Future of Geothermal Energy. Impact of Enhanced Geothermal Systems [EGS] on the United States in the 21st Century. Massachusetts Institute of Technology.

University of Texas at El Paso, 2014. Gravity and Magnetic Database of the U.S., http://irpsrvgis08.utep.edu/viewers/Flex/GravityMagnetic/GravityMagnetic_CyberShare/. Accessed 3/14/2014.

U.S. EIA, 2014. U.S. Energy Administration Association: State Profile Energy Estimates. http://www.eia.gov/state/. Accessed 3/14/2014.

CHAPTER VII

CONCLUSIONS

The Moran's I and Getis-Ord tests, Chapter II, determined that separating the data into subsets using measurement depth intervals was more statistically accurate than using formation information. The exercise in quantifying the accuracy of correction schemes in Chapter 3 was useful to learn which of the existing correction schemes was the best, and up to what depth each equation was accurate. The Harrison correction is the best correction to use for basins up to 4,500 meters deep, and the Kehle correction works well for deeper basins, from 4,500 meters up to 8,000 meters deep.

The lack of freely available data and a lack of quality data hampered the energy in place investigation, especially for the Illinois and Williston Basins. The Williston Basin Energy in place (Crowell et al., 2011) is shown in Figure 7. The Denver Basin (Chapter IV) is hot enough to produce geothermal energy on a large scale economically, the Illinois and Michigan Basins (Chapter V) are only economic with current technology for direct use and district heating. The Williston Basin has potential for small scale energy production and district heating.

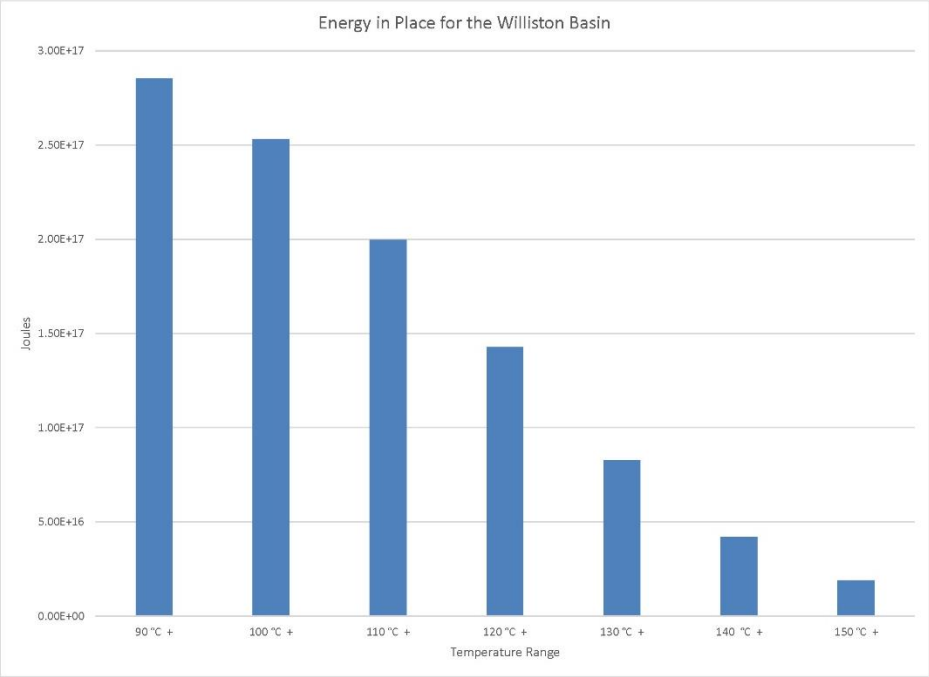

Figure 7. Graph of Energy in Place for the Williston Basin.

The Play Fairway Analysis generated results that identified low risk exploration sites and quantified energy resources in place; however, the results can be improved if a separate play fairway analysis is generated using suitable parameters for the manner in which the resource is to be developed (i.e., large and small scale power production, direct use, and district heating).

Future work is required to refine the play fairway analysis process. Including infrastructure, population centers, roadways, land use, water permitting information, and climate will increase the robustness of the model.

APPENDICES

Appendix A
List of Acronyms

AAPG	American Association of Petroleum Geologists
API	American Petroleum Institute
BHT	Bottom-hole temperature
C	Celsius
DEM	Digital Elevation Model
DOE	Department of Energy
EIA	Energy Institute of America
GIS	Geographical Information System
GRC	Geothermal Resources Council
GSNA	Geothermal Survey of North America
J	Joules
K	Kelvin
km	kilometer
kWe	killiwatts electric
L/s	Liters per second
m	Meters
Mt/yr	Megatons per year
MW	Megawatt
MWe	Megawatts electric
MWt	Megawatts thermal
mW/m^2	milliwatts per meter squared

NAD83	North America Datum, 1983
OCR	Optical Character Recognition
OECD	Organization for Economic Co-operation and Development
PSCWi	Public Service Commission of Wisconsin
SMU	Southern Methodist University
Tcf	Temperature correction factor
TD	Total Depth
TPES	Total Percentage Energy by Source

SOURCES CITED

Abbott, D. M., and D. C. Noe, 2002. The Consequences of Living with Geology: A Model Field Trip for the General Public, Geological Society of America, Field Guides, vol. 3, p. 1-16.

Anselin, L., 1999. Spatial Econometrics. https://csiss.ncgia.ucsb.edu/aboutus/presentations/files/baltchap.pdf. Accessed 7/12/2015.

Aller, L., Bennet, T., Lehr, J. H., Petty, R. J., and G. Hacket, 1987. DRASTIC: A standardized system for evaluating groundwater pollution using hydrological settings. Preparado por National water well association para US EPA Office of Research and Development, Ada, USA.

Aneke, M., Agnew, B., and C. Underwood, 2011. Performance Analysis of the Chena Binary Geothermal Power Plant, Applied Thermal Engineering, vol. 3, p. 1825-1832.

AWS/NREL, 2012. United States – Land-based and Offshore Annual Average Wind Speed at 80m. AWS Truepower and the National Renewable Energy Laboratory. http://www.nrel.gov/gis/wind.html. Accessed 6/16/2015.

Babiker, I., Mohamed, M., Hiyama, T., and K. Kato, 2005. A GIS-based DRASTIC model for assessing aquifer vulnerability in Kakamigahara Heights, Gifu Prefecture, Central Japan. Science of the Total Environment, vol. 345 p. 127-140.

Beardsmore, G. R., and J. P. Cull, 2001. Crustal Heat Flow: A Guide to Measurement and Modelling. Cambridge University Press, New York, New York, United States.

Blackwell, D. D., and M. Richards, 2004. Calibration of the AAPG Geothermal Survey of North America BHT Data Base: American Association of Petroleum Geologists Annual Meeting 2004, Dallas, Texas, Poster session, paper 87616.

Blackwell, D. D., Richards, M., and P. Stepp, 2010. Texas Geothermal Assessment for the I-35 Corridor East, Texas State Energy Conservation Office Contract, pp. 88.

Brook, C. A., Mariner, R. H., Mabey, D. R., Swanson, J. R., Guffanti, M., and L. J. P. Muffler, 1978. Hydrothermal Convection Systems with Reservoir Temperatures ≥ 90°C, in Assessment of Geothermal Resources of the United States – 1978, United States Geological Survey Circular 790, p. 18-43.

Carlson C.G., and S.B. Anderson, 1965. Sedimentary and Tectonic History of North Dakota Part of Williston Basin. Bulletin of the American Association of Petroleum Geologists, vol. 49, no. 11, p. 1833-1849.

Clark, C., Sullivan, J., Harto, C., Han, J., and M. Wang, 2012. Life Cycle Environmental Impacts of Geothermal Systems. Proceedings, 37th Workshop on Geothermal Reservoir Engineering, Stanford, CA.

Crowell, A. M., Klenner, R., and W.D. Gosnold, 2011. GIS Analysis for the Volumes, and Available Energy of Selected Reservoirs: Williston Basin, North Dakota, Geothermal Resources Council Transactions, vol. 35, p. 1557-1561.

Crowell, A. M., and W.D. Gosnold, 2011. Correcting Bottom-Hole Temperatures: A Look at the Permian Basin (Texas), Anadarko and Arkoma Basins (Oklahoma), and Williston Basin (North Dakota), Geothermal Resources Council Transactions, vol. 35, p. 735-738.

Crowell, A. M., Ochsner, A.T., and W.D. Gosnold, 2012. Correcting Bottom-Hole Temperatures in the Denver Basin: Colorado and Nebraska, Geothermal Resources Council Transactions, vol. 36, p. 201-206.

Crowell, A. M., and W.D. Gosnold, 2013. GIS-Based Geothermal Resource Assessment of the Denver Basin: Colorado and Nebraska, Geothermal Resources Council Transactions, vol. 37, p. 941-943.

Crowell, A. M. and W. Gosnold, 2014. GIS/Volumetric Geothermal Resource Assessment of the Michigan and Illinois Basins. Transactions of the Geothermal Resources Council, vol. 38. p. 947-950.

Curtis, B. F., 1988. Sedimentary rocks of the Denver basin: in Sloss, L.L. (editor), Sedimentary Cover—North American Craton, U.S. Geological Society of America, The Geology of North America, vol. D-2, ch. 8, p. 182-196.

DOE, 2014. Geothermal Heat Flow and Existing Plants. Department of Energy. http://www.energy.gov/maps/geothermal-heat-flow-and-existing-geothermal-plants. Accessed 6/16/2015.

Dolton, G.L., 1995. Michigan Basin Province (063). In: Gautier, D.L., Dolton, G.L., Takahashi, K.I., Varnes, K.L. (Eds.), 1995 National assessment of United States oil and gas resources: results, methodology, and supporting data. U.S. Geological Survey, p. GS–30.

Esri, Inc., 2013. ArcGIS 10.2 Helpfiles. Environmental Systems Research Institute, Redmond, CA. www.esri.com. Accessed 6/1/2015.

Förster, A., Merriam, D.F., and J. C. Davis, 1996. Statistical analysis of some bottom-hole temperature (BHT) correction factors for the Cherokee Basin, southeastern Kansas: Tulsa Geological Society Transactions, p. 3-9.

Geology.com, 2014. U.S. Map Collections for all 50 States. http://geology.com/state-map/. Accessed 3/14/2014.

Gosnold, W. D., Personal Communication, University of North Dakota, February 2012, Interviewer: Anna M. Crowell.

Gosnold, W., Barse, K., Bubach, B, Crowell, A., Crowell, J., Jabbari, H., Sarnoski, A, and D. Wang, 2013. Co-Produced Geothermal Resources and EGS in the Williston Basin, Transactions of the Geothermal Resources Council, vol. 37, p. 721-726.

Gosnold, W., MacDonald, M., Klenner, R, and D. Merriam, 2012. Thermostratigraphy of the Williston Basin, Transactions of the Geothermal Resources Council, vol. 36, p. 663-670.

Gregory, A. R., Dodge, M. M., Posey, J. S., and R. A. Morton, 1980. Volume and accessibility of entrained (solution) methane in deep geopressured reservoirs-Tertiary formations of the Texas Gulf Coast, DOE Final Report DOE/ET/11397-1, pp. 361, OSTI # 5282675.

GRC, 2014. What is Geothermal? Geothermal Resources Council. http://www.geothermal.org/what.html. Accessed 6/1/2015.

Harrison W.E., Luza, K.V., Prater, M.L, and P.K. Chueng, 1983. Geothermal resource assessment of Oklahoma, Oklahoma Geological Survey, Special Publication 83-1.

Heck, T.J., LeFever, R.D., Fischer, D.W., and J. LeFever, 2010. Overview of the Petroleum Geology of the North Dakota Williston Basin. https://www.dmr.nd.gov/ndgs/Resources/WBPetroleumnew.asp. Accessed 12/30/2010.

Herzog, H.J. and D. Golomb, 2004. Carbon Capture and Storage from Fossil Fuel Use, in C.J. Cleveland (ed.), Encyclopedia of Energy, Elsevier Science Inc., New York, p. 277-287.

IEA, 2014. IEA's 2014 Key World Energy Statistics Report. International Energy Agency. http://www.iea.org/publications/freepublications/publication/key-world-energy-statistics-2014.html. Accessed 6/16/2015.

Kehle, R.O., Schoeppel, R. J., and R. K. Deford, 1970. The AAPG Geothermal Survey of North America, Geothermics, Special Issue 2, U.N Symposium on the Development and Utilization of Geothermal Resources, Pisa 1970, vol. 2, Part 1.

Macke, D.L., 1995. Illinois Basin Province (064). In: Gautier, D.L., Dolton, G.L., Takahashi, K.I., Varnes, K.L. (Eds.), 1995 National assessment of United States oil and gas resources: results, methodology, and supporting data. U.S. Geological Survey, p. GS–35.
Martin, C., 1965. Denver Basin, Bulletin of the American Association of Petroleum Geologists, vol. 49, no. 11, p. 1908-1925.

Morgan, P., Personal Communication, Colorado Geological Survey, February 2012, Interviewer: Anna M. Crowell.

Nebraska Oil and Gas Conservation Commission, http://www.nogcc.ne.gov/, Accessed 5/1/2013.

NGDS, 2014. National Geothermal Data System. www.geothermaldata.org. Accessed 12/2/2014.

NOAA, 2014. National Climate Data Center Data Access. http://www.ncdc.noaa.gov/data-access. Accessed 3/27/2014.

Noe, D. C., Soule, J. M., Hynes, J. L., and K. A. Berry, 1999. Bouncing Boulders, Rising Rivers, and Sneaky Soils: A Primer of Geologic Hazards and Engineering Geology along Colorado's Front Range, in Lageson, D. R., Lester, A. P., and Trudgill, B. D., eds., Colorado and Adjacent Areas: Boulder, Colorado, Geological Society of America Field Guide I.

Paradis, E., 2009. Moran's Autocorrelation Coefficient in Comparative Methods. R Foundation for Statistical Computing, Vienna.

PetroStrategies, 2015. Drilling Operations. PetroStrategies, Inc. http://www.petrostrategies.org/Learning_Center/drilling_operations.htm#Drilling%20Costs. Accessed 6/16/2015.

Roberts, B. J., 2012. Concentrating Solar Resource of the United States. National Renewable Energy Laboratory. http://www.nrel.gov/gis/solar.html. Accessed 6/16/2015.

Sorey, M.L., Nathenson, M., and C. Smith, 1982. Methods for Assessing Low-Temperature Geothermal Resources, in Reed, M.J., ed., Assessment of Low-temperature Geothermal Resources of the United States -1982: U.S. Geological Survey Circular 892, p. 17-29.

Tester J.W., et. al., 2006. MIT: The Future of Geothermal Energy. Impact of Enhanced Geothermal Systems [EGS] on the United States in the 21st Century, Massachusetts Institute of Technology.

Touloukian, Y.S., Judd, W.R., and R.F. Roy, 1981. Physical Properties of Rocks and Minerals, Mc-Graw-Hill/CINDAS data series on material properties, vol. II-2, Purdue Research Foundation.

University of Texas at El Paso, 2014. Gravity and Magnetic Database of the U.S., http://irpsrvgis08.utep.edu/viewers/Flex/GravityMagnetic/GravityMagnetic_CyberShare/. Accessed 3/14/2014.

U.S. Census Bureau, 2010. Current Population Reports: Projections of the Number of Households and Families in the United States: 1995 to 2010, p. 25-1129.

U.S. Climate Data, 2015. U.S. Climate Data: Temperature – Precipitation – Sunshine – Snowfall. www.usclimatedata.com/climate/. Accessed 6/16/2015.

U.S. EIA, 2014. U.S. Energy Administration Association: State Profile Energy Estimates. http://www.eia.gov/state/. Accessed 3/14/2014.

USGS, 1975. Assessment of Geothermal Resources of the United States - 1975. US Geological Survey Circular, no. 726.

USGS, 1978. Assessment of Geothermal Resources of the United States - 1978. US Geological Survey Circular, no. 790.

USGS, 1982. Assessment of Geothermal Resources of the United States - 1980. US Geological Survey Circular, no. 892.

Yang Z., and C. Zu, 2010. Methods of the Volume Measurement of Reservoir Using GIS: Research and Practice. Second International Conference on Technology, p. 237-240.